Essays in Energy Economics: Incentives and Consumer Response

Inauguraldissertation

zur

Erlangung des Doktorgrades

der

Wirtschafts- und Sozialwissenschaftlichen Fakultät

der

Universität zu Köln

2023

vorgelegt

von

M. Sc. Fabian Arnold

aus

Aachen

Referent:	Prof. Dr. Marc Oliver Bettzüge
Korreferent:	Jun.-Prof. Dr. Oliver Ruhnau
Tag der Promotion:	20.12.2023

Acknowledgements

I would like to express my gratitude to Prof. Dr. Marc Oliver Bettzüge for supervising my thesis. His ideas and feedback have played a pivotal role in developing my research interests and have improved my research over the years. I also want to thank Jun.-Prof. Dr. Oliver Ruhnau for co-refereeing my thesis. Furthermore, my gratitude goes to Prof. Dr. Oliver Gürtler for chairing the examination committee.

I am very grateful for the opportunity to work at the Institute of Energy Economics at the University of Cologne (EWI). This includes not only financial support and an encouraging environment for working on my research but also the opportunity to immerse myself in diverse and exciting topics within the energy sector through various projects. Moreover, I am thankful for the support from the institute's administration and IT department.

I am thankful for my excellent colleagues at the institute. Beyond the enjoyable times together, joint project work and discussions widened my professional and personal horizons. My special thanks go to my excellent co-authors Amir Ashour Novirdoust, Philipp Theile, Amelie Sitzmann, Samir Jeddi, Arne Lilienkamp, and Nils Namockel, as well as Dominic Lencz, Berit Hanna Czock and Cordelia Frings for the great teamwork and all the cheerful memories made.

I gratefully acknowledge financial support from the German Federal Ministry of Education and Research (BMBF) within the Kopernikus-project 'New ENergy grid StructURes for the German Energiewende' (ENSURE) (grant number 03SFK1L0-2), as well as from the 'Förderinitiative Wärmewende' of the Gesellschaft zur Förderung des Energiewirtschaftlichen Instituts an der Universität zu Köln e.V.

Finally, I am truly fortunate to be surrounded by wonderful friends and, most importantly, my family. Special thanks go to my parents, who provided me with constant support and encouragement. Foremost, I want to express my deepest gratitude to Patricia and Fiete for having my back, believing in me and giving me the joy and confidence to complete this journey.

Fabian Arnold Cologne, December 2023

Contents

List of Figures

List of Tables

1 Introduction

The field of energy economics explores energy markets and the relationship between the production, distribution, and consumption of energy resources. Within this framework, research is concerned, for example, with the design of markets, prices, and policy interventions and the associated effects on economies, societies, welfare, and the environment.

In the last decade, governments worldwide have pledged to reduce the amount of greenhouse gases emitted within their territories over the medium and long term to mitigate anthropogenic climate change. Major greenhouse gas emitters like China, the United States of America, and the European Union have set themselves net-zero targets for their greenhouse gas or CO_2 emissions. This means that by the specified target dates, no more respective emissions are to be emitted in these countries than are removed through carbon sinks. The goal of achieving near-complete decarbonization necessitates a comprehensive transformation across all sectors of energy generation, conversion, and consumption. Energy economic research can play a central role in understanding this transformation and the challenges it poses.

In energy end-use sectors, it is individual consumers of energy and energy dependent services, in particular, who implement this transformation. The decisions and actions consumers undertake while investing in, utilizing, and eventually discarding a product or service play a pivotal role in driving the decarbonization efforts within specific sectors. In the sectors such as heating or transport, consumers make investment choices, such as selecting heating technologies or vehicles. In the course of the decentralization of electricity generation, electricity consumers are also engaging in investments in decentralized systems like photovoltaic (PV) and storage systems. Apart from investment decisions, consumers also decide on the utilization of their assets. Besides emissions, these decisions affect the energy system as a whole: The flexibility of electricity procurement and the decisions consumers make about when and where to consume electricity play a central role in questions of the necessary grid and generation capacity expansion.

One approach to encourage desired consumer investment and decisions is the utilization of economic incentives. Consumers can be incentivized, for example, to lower their greenhouse gas emissions or to make decisions in a way that is beneficial to the energy system by creating new or utilizing existing markets. These incentives include tradable quotas or certificates, subsidies, as well as taxes, fees, or other price signals (Coria & Sterner, 2011). The design of such policies is a challenging task. Prior to implementation, conducting theoretical as well as

quantitative analysis of the effects and effectiveness of price signals and economic incentives requires an understanding of real-world consumer responses.

The individual chapters of this thesis, therefore, deal with concrete examples of economic incentives and consumer response. While Chapter 2 is centered around the theoretical analysis of different environmental policy options for investments in zero emission backstop technologies under present bias, Chapter 3 and Chapter 4 provide empirical insights into real-world consumer response to price signals. In Chapter 3, the impact of regionally differing electricity prices on PV investments is investigated, and Chapter 4 analyzes the functional form and magnitude of short-term electricity demand response at the wholesale level. Furthermore, Chapter 5 explores the implications of varying incentives in electric vehicle charging on regional residual load curves. The four essays are self-contained and may be read in any order. Each chapter is based on a paper to which all the authors contributed equally:

1. Environmental policy instruments for investments in backstop technologies under present bias - an application to the building sector. Joint work with Amir Ashour Novirdoust and Philipp Theile, *EWI Working Paper 23/05* (Arnold, Ashour Novirdoust, & Theile, 2023).
2. How prices guide investment decisions under net purchasing - An empirical analysis on the impact of network tariffs on residential PV. Joint work with Amelie Sitzmann and Samir Jeddi, initially presented as *EWI Working Paper 21/07* (Arnold et al., 2021) and subsequently published in *Energy Economics* (Arnold et al., 2022). The chapter is based on the latter version.
3. On the functional form of short-term electricity demand response - insights from high-price years. *EWI Working Paper 23/06* (Arnold, 2023).
4. Diffusion of electric vehicles and their flexibility potential for smoothing residual demand - A spatio-temporal analysis for Germany. Joint work with Arne Lilienkamp and Nils Namockel, *EWI Working Paper 23/04* (Arnold, Lilienkamp, & Namockel, 2023).

The remainder of the introduction is divided into two sections: Section 1.1 provides an outline of the content of the four essays. Section 1.2 discusses the methodological approaches of the essays, as well as limitations and potential areas of further research.

1.1 Outline

1.1.1 Environmental policy instruments for investments in backstop technologies under present bias - an application to the building sector

Worldwide, policy instruments, including incentives like carbon pricing or subsidies, are being discussed and implemented as ways to achieve greenhouse gas emission reductions. If individuals exhibit present bias, Heutel (2015) has shown that optimal policies targeting investments in the efficiency state of externality-producing durable goods and their usage consist of two components, one aimed at the externality and one aimed at the present bias. Chapter 2 generalizes Heutel's theoretical model by defining a larger technology set. This allows to represent the dependence of fuel prices and emission intensities on technologies used in the building sector and to include a zero emission backstop technology. First the effect of this model generalization on Heutel's main propositions is examined, assuming still that the backstop technology is not optimal. Second, this examination is extended to the case when the backstop technology is optimal. In a stylized case study for a representative building in Germany, magnitudes of the present bias effect on investment and utilization decisions on heating systems, emissions, policies, and deadweight loss are estimated. The chapter shows that as long as social costs of carbon and the corresponding CO_2 price are not high enough to make the backstop technology optimal, Heutel's proposition holds that optimal policies must consist of two components. Contrary to Heutel's proposition, if the social costs of carbon and the CO_2 price are high enough, a single instrument can address both the externality and present bias. While the level of this single instrument, i.e., a tax or subsidy, depends on the level of present bias, the chapter finds that there exists a tax-subsidy combination that is optimal regardless of the level of present bias.

1.1.2 How prices guide investment decisions under net purchasing - An empirical analysis on the impact of network tariffs on residential PV

Within the regulation of net purchasing, investment incentives for residential PV depend on the remuneration for grid feed-in and the consumption costs that households can save by self-consumption. Network tariffs constitute a substantial part of these consumption costs. Chapter 3 uses postcode-level data for Germany between 2009 and 2017 and exploits the regional heterogeneity of network tariffs to investigate whether they encourage to invest in PV installations and evaluate how the nonlinear tariff structure impacts residential PV adoption. The results show that network tariffs do impact PV adoption. The effect has increased in recent years when self-consumption has become financially more attractive, and the results confirm the expectation that PV investments are driven by the volumetric

tariff. Policy reforms that alter the share between the price components are, thus, likely to affect residential PV adoption. Further, with self-consumption becoming a key incentive, price signals can effectively support the coordination of electricity demand and supply in Germany.

1.1.3 On the functional form of short-term electricity demand response - insights from high-price years

Demand response is crucial for balancing supply and demand in the presence of intermittent electricity generation. In 2021/2022, wholesale power prices in Germany have been dramatically higher than ever before, which offers the opportunity to investigate the demand response in high-price situations. Chapter 4, thus, discusses the applicability of the two common functional forms of demand response under these circumstances, namely linear and log-log. Using a two-stage least squares approach, the short-term own-price elasticity of electricity demand in Germany is estimated for the period from 2015 to 2022. The day-ahead forecast of wind power generation serves as an instrumental variable for the day-ahead price. The analysis shows that for low prices, the linear assumption tends to yield similar average elasticities to the constant elasticity obtained from the log-log specification. However, estimators based on linear functions exhibit significant variations depending on whether low or high prices are considered. This discrepancy arises from the observation that remaining demand at high prices tends to have limited flexibility. In contrast, the log-log approach provides smaller differences between estimates based on low and high prices. The exponential nature of the log-log function captures the decrease in absolute demand response at high prices, resulting in more consistent estimations across the price range.

1.1.4 Diffusion of electric vehicles and their flexibility potential for smoothing residual demand - A spatio-temporal analysis for Germany

The transformation of the energy system causes increasing stress on distribution grid components. However, flexible electric vehicle (EV) charging, if incentivized adequately, can help mitigate this impact by reducing peaks in loads and feed-in. To understand the potential of EV charging flexibility for reducing peaks on regional and national levels, Chapter 5 estimates regional residual demand time series for Germany for the years 2019, 2030 and 2045. The chapter focuses on modelling private EV diffusion via sigmoid functions and deriving driving and charging profiles based on micro mobility data. Further, two deployment schemes for EV flexibility are distinguished: (1) all EVs contribute to flattening the national residual load curve; (2) local EVs contribute to flattening regional residual load curves. The chapter finds that the residual load curves change structurally as positive and negative peaks in residual demand increase over the years on the regional and national levels. Although the absolute flexibility potential of EV

home charging increases with the number of vehicles, its marginal utility to reduce load peaks declines. Especially in load-dominated regions, the national deployment of flexibility can result in higher regional demand peaks compared to a scenario without charging flexibility. The two approaches of flexibility activation can be contradictory in their effects: While regional incentivization is less efficient in reaching the smoothing in the national residual demand curve, national incentivization can even lead to increased strain on the local level.

1.2 Methodology, Limitations and Further Research

Each chapter of this thesis discusses a particular aspect in energy economic research. Therefore, tailored to the distinct research question of each chapter, suitable and differing methodological approaches are applied.

Chapter 2 deals with environmental policy instruments for investments in durable goods, assuming consumers are present biased. For this purpose, an analytical model for investment decisions from Heutel (2015) is generalized to represent a larger technology set and allow for the existence of zero emission backstop technologies. In a stylized case study for a representative building in Germany, magnitudes of the present bias effect on investment and heating decisions, emissions, policies, and deadweight loss are numerically estimated.

In order to determine the welfare-optimal decisions of households, the "long-run criterion" is utilized. Applying this criterion is based on the paternalistic assumption that the household's choices, due to present bias, might not align with their welfare optimization. This premise is central to the validity of the results but certainly open to critical examination. Moreover, applying the "long-run criterion" as a welfare measure constitutes only one of several alternative welfare criteria applicable in the case of time-inconsistent discounting. Testing the validity of the chapter's findings using alternative criteria is a potential avenue for future research. Similarly, discussing the effect of heterogeneous households or varying ages of heating systems on policy forms another promising research trajectory.

In **Chapter 3**, postcode-level data for Germany from 2009 to 2017 is utilized to exploit the regional heterogeneity of network tariffs to investigate whether they encourage investment in PV installations. To this end, a Poisson quasi-maximum likelihood estimator (PQMLE) with fixed effects is applied.

The fixed effects approach allows the capture of unobserved heterogeneity across both temporal and regional dimensions. The approach, thus, absorbs a substantial portion of the variance inherent within the model. While the within-variance of the central explanatory variable, the network tariffs, remains large enough to show statistically significant effects after controlling for the fixed effects, the within-variance of the covariates does not. Consequently, the model can not be applied to analyze the effect of covariates such as income, housetype, age, or

number of buildings on PV investments. To conduct such analyses, alternative model frameworks are necessary, introducing further research opportunities.

Chapter 4, akin to Chapter 3, carries out an empirical investigation. Here, the short-term own-price elasticity of electricity demand in Germany is estimated for the period of 2015-2022, employing a two-stage least squares (2SLS) methodology.

By utilizing aggregated electricity demand data and wholesale-level day-ahead electricity prices, the estimated price responses encapsulate the cumulative reaction of all consumers, inclusive of those who exhibit inelastic behavior. Additionally, the chosen estimation model estimates not only the demand response to the price in a specific hour but also implicitly includes intertemporal cross-price elasticities with the preceding and subsequent hour. This potential influence of autocorrelation on estimation results, thus, emerges as a critical consideration and presents a path for further research.

Throughout the analysis, the applicability of the two most commonly used functional forms of demand response, namely linear and log-log, is discussed and investigated. Subsequent research could introduce other functional forms, such as piece-wise linear models, or delve into quantile regression models to further investigate demand response's dependence on price levels.

In **Chapter 5**, the analysis aims at understanding the potential of EV charging flexibility for reducing peaks on regional and national levels. To this end, regional residual demand time series for Germany in 2019, 2030, and 2045 are estimated. The regional diffusion of electric vehicles is estimated using sigmoid functions, while charging patterns are derived from micro mobility data. Subsequently, two distinct EV charging behaviors are translated into optimization problems, enabling a comparative analysis of the resultant residual demand time series.

The estimation of developments far into the future is naturally subject to great uncertainty. Assumptions regarding electricity demand, for example, stem from a study that assumes the achievement of the climate and technology targets set by the German government (dena, 2021), while electricity generation projections are derived directly from the government's targets. Hence, this study presents a specific vision of the future against which the results should be contextualized. Furthermore, the optimization of household charging assumes perfect foresight and information. Consequently, the results stand as an upper bound, depicting the effects of the charging strategies under perfect execution.

While the effects of flexibility deployment on regional and national residual load curves are estimated, concrete grid expansion and electricity generation costs remain unquantified. Moreover, while the chapter deals with the effects of different charging behaviors, it does not delve into the specific policy schemes that could facilitate implementation. Thus, possibilities for further research persist.

Beyond this discussion, the respective chapters provide comprehensive descriptions of the methodological approaches and limitations.

2 Environmental policy instruments for investments in backstop technologies under present bias - an application to the building sector

2.1 Introduction

2.1.1 Background and motivation

Governments of many countries have set themselves climate targets, i.e., emission reduction targets. These targets no longer aim at a mere partial reduction of greenhouse gas (GHG) emissions but rather at a reduction of GHG emissions to zero or close to zero. More than 70 countries pledged to reach net-zero emissions, including the countries of the European Union, China, and the USA (United Nations, 2023). Investments must be stimulated and carried out beyond efficiency improvements to achieve these climate neutrality goals. Therefore, in all sectors investments in zero emission technologies, i.e., backstop technologies, must be made.

An example is the residential building sector: Global GHG emissions from building operations, i.e., heating and hot water provision, have increased in recent years. In 2021 global direct CO_2 emissions from building operations accounted for around 8 % of global energy-related CO_2 emissions (IEA, 2022). In the residential building sector, decarbonization needs to be carried out by private households investing in new technologies (e.g., heating systems and refurbishment) and choosing their indoor temperature level. In this paper, the analysis is applied to the residential building sector, although the results are generalizable.

The prominent policy from classic economics to reach the first-best outcome in the presence of an environmental externality (i.e., the emitted emissions) is to introduce a price on said externality (i.e., a carbon or CO_2 price), internalizing the externality into the decision-making rationale of the households, like the Pigouvian tax (Pigou, 1920). Empirical literature suggests that individuals do not always behave according to classic rational choice theory. Behavioral issues, such as time-inconsistent discounting (e.g., present bias), could prevent individuals from investing optimally in time. Heutel (2015) has shown that if consumers experience present bias, a Pigouvian tax does not lead to welfare optimal investment decisions for externality-producing durable goods. Instead, the optimal policy mix consists of an instrument to correct the externality and

another one aiming at the present bias, constituting an internality. Besides carbon taxation or pricing, these instruments can include subsidies, taxes based on efficiency, or mandates.

In his analysis, Heutel (2015) assumes that consumers can invest in technologies with different efficiencies. Sheer improvement of efficiencies in externality-producing durable goods, however, cannot reduce externalities to zero. Thus, by assumption, no backstop technology exists. In his analysis, the author finds that there exists a welfare-optimal amount of externalities (i.e., GHG emissions) resulting from the Pigouvian tax rate, representing the monetary damage of the externality and the utility drawn from the externality-producing good. In contrast, in many countries, climate neutrality is the declared political target. The implicit assumption is thus, that the damage from GHG emissions is higher than corresponding abatement costs, and correspondingly, the optimal amount of GHG emissions is zero. Put differently, the policy maker is interested in target-consistent CO_2 pricing and policy measures rather than taxing the externality at the rate of social costs of carbon (Aldy et al., 2021).

Building on the work of Heutel (2015), this raises the following questions. First: How can Heutel's model be generalized to account for the existence of zero emission backstop technologies with finite costs? Second: What does this generalization imply for the main propositions of the model? Third: What are optimal policies under present bias for externality-producing durable goods if the optimal investment decision is the investment in the backstop technology?

We generalize the analytical model of Heutel (2015) for investments in externality-producing durable goods under present bias by allowing for a greater technology space. In the generalized model, the investment may be accompanied by the substitution of the fuel used, for example, in the case of heating investments, switching from a gas heating system to an electric heat pump. The integration of fuel substitution into the investment decision allows us to depict the existence of a zero emissions backstop technology.

We first examine the effect of the model generalization on Heutel's main propositions, assuming still that there is a welfare-optimal inner solution, i.e., that the backstop technology is not optimal. We then discuss the implications of the situation when the investment in the backstop technology is optimal. This may be the case if the assumed damage of the externality is high enough so that the backstop technology is welfare-optimal, or due to politically set climate neutrality targets. In a stylized case study for a representative building of the German building sector, we assume a politically set climate neutrality target. We numerically estimate real-world magnitudes of the present bias effect on heating-related investment and utilization decisions, emissions, policies, and associated deadweight loss.

In our analysis, we show that as long as social damage of carbon and the corresponding CO_2 price is not high enough to make the backstop technology optimal, households in the optimum will still emit CO_2. In this case, Heutels

propositions hold that to reach the social optimum, we need two policy instruments, one to address the internality and a second one to address the externality, that will still be present. Contrary to Heutel's propositions, if the social costs of carbon and the corresponding CO_2 price are high enough, a mark-up on the CO_2 price can also induce the social optimum. Therefore, present bias can be addressed by a tax or another single instrument when aiming at climate neutrality in the presence of a zero-emission backstop technology. In numerical simulations for a representative household in Germany and under the assumption of continuous investment choices, we quantify the target-consistent CO_2 price without present bias at $\tau_t^{neu} = 192€/tCO_2$. Applying τ_t^{neu} in the case of present bias leads to a welfare loss. In the case of a present-biased household, a higher CO_2 tax exists that reaches the target (in our exemplary building and an assumed present bias of β=0.7: $235€/tCO_2$ including an internality-mark-up of $43€/tCO_2$). While the optimal tax rate and subsidy depend on the level of present bias, we find that there exists an optimal tax-subsidy combination that is optimal regardless of the level of present bias.

2.1.2 Related literature and contribution

Ever since (Strotz, 1955) introduced the idea of time-inconsistent discounting with his theory of commitment, it has been recognized that consumers may deviate from the assumption of exponential, thus time-consistent, discounting.[1] In line with time-inconsistent discounting, Laibson (1997) coined the concept of present bias, i.e., agents' preference for immediate benefits over advantages in future periods beyond exponential discounting.[2] To represent this behavior, the literature has introduced and applied models of quasi-hyperbolic discounting (Laibson, 1997; O'Donoghue & Rabin, 1999; Phelps & Pollak, 1968).

One metric for policy evaluation is welfare. Assuming time-inconsistent preferences implies that preferences change over time, complicating welfare analysis. Economists provide several welfare criteria to overcome this complication. The two most prominent criteria are the Pareto criterion, i.e., considering each period's perspective in overall utility, and the long-run criterion, i.e., evaluating the "true" utility from a long-run perspective (O'Donoghue & Rabin, 2015). O'Donoghue and Rabin (1999) argue that the Pareto criterion is a too strong assumption when applied to intertemporal choice. O'Donoghue and Rabin (2015) claim that both approaches, as well as other thinkable welfare criteria, frequently yield the same

[1] Frederick et al. (2002) includes a critical review of the history and models of time discounting including time-consistent utility discounting models as well as time preferences and (quasi-) hyperbolic discounting models.

[2] See the reviews Frederick et al. (2002) and DellaVigna (2009) for empirical estimates for present bias in various circumstances and Imai et al. (2021) and Cheung et al. (2021) for recent meta studies of papers reporting present bias estimates.

conclusions but argue for the usage of the long-run criterion.[3] As Heutel (2015) utilizes the long-run criterion in his model, we will also apply it.

Applying the long-run criterion deviates from standard social welfare analysis, relying on revealed preferences as information about the consumer's true utility. The paternalistic assumption that the consumer's choices do not optimize her welfare is as critical as it is controversial. Saint-Paul (2011) argues that taxes levied for inducing a particular behavior might only lead to consumers paying higher prices instead of changing behavior, reducing overall welfare. According to Whitman (2006), the justifications of policy interventions for addressing internalities are based on the idea of Pigouvian taxation, ignoring Coase's theorem (Coase, 1960). The theorem states that externalities can be resolved by negotiation between individual parties when transaction costs are low. Since internalities consist of choices within the individual, Whitman (2006) argues that Coase's theorem is better suited for dealing with internalities. The information required to find the least costly option addressing the damage from time-inconsistent discounting is only available to the individual. Moreover, Krusell et al. (2002) argues that to tackle consumers' time-inconsistent preferences, only an intervention by a time-consistent social planner is welfare enhancing.

We apply our analysis to the case of households' heating system investment decisions. The empirical literature regarding behavioral biases in energy efficiency decision-making is limited (Gillingham et al., 2009). Schleich et al. (2019) investigated the role of present bias and other behavioral aspects in adopting energy-efficient technologies within different countries in the European Union. They provide evidence for the significance of present bias in reducing investments in energy-efficient appliances and building retrofitting. Werthschulte and Löschel (2021) find that present bias increases power consumption. Therefore, as households undervalue energy costs, price-based policies might fail to reduce household energy consumption. Furthermore, in the specific case of investment in household appliances in India, Fuerst and Singh (2018) find that present bias becomes more significant the larger the purchase object investigated. This finding is relevant to our work, as heating system replacement represents a particularly large investment decision for households. Overall, there is not yet a comprehensive empirical view on the effect of present bias on heating system investments. We account for this lack of estimates by considering a range of present bias factors in our numerical simulation.

This paper focuses on the consequence of present bias in agents' decision-making on policies for decarbonization. The model from Heutel (2015) constitutes the basis of our analysis. A detailed description of the model for analyzing optimal policy instruments for externality-producing durable goods under present bias can be found in Section 2.2.1. Heutel (2015) considers a technology space with efficiency and investment costs as dimensions. We expand this space by

[3] Kang (2015) shows that improvements in the Pareto criterion are also welfare-improving from the long-run perspective.

allowing technologies to differ in emission intensity and fuel price. As we will see, this generalization enables us to discuss the subject of climate neutral backstop technologies. Since Heutel (2015), recent work has deepened the understanding of present bias in economic policy design and welfare analysis (Bar-Gill & Hayashi, 2021; Drugeon & Wigniolle, 2021; Kang, 2022; Kotsogiannis & Schwager, 2022; Lades et al., 2021). Bar-Gill and Hayashi (2021) discuss the investment decisions for durable goods by present-biased agents. In contrast to our work, they focus on the effect of purchase financing. They find countervailing effects of present bias on the valuing of the benefits of an investment and the costs of financing said investment and derive recommendations for credit regulation. Since they discuss general durable goods, they do not consider the emission externalities from using energy technologies. Lades et al. (2021) examine investments from present-biased households in energy efficiency technologies. They illustrate particularly how administrative burden can reduce these investments. Similar to our work, they apply a theoretical model and a simulation with exemplary building data. As we will see, our key point of departure from Heutel (2015) and Lades et al. (2021) is that we consider policies reaching climate neutrality combined with the availability of a backstop technology.

While there is literature on policies in the context of present bias, to the best of our knowledge, there is no literature addressing the subject of policies for externality-producing durable goods aiming at climate neutrality. In the present work, we aim to close this gap by (i) generalizing the model from Heutel to more complex technologies also differing in emission intensity and fuel price to be able to account for zero emission backstop technologies, (ii) analyzing the consequences of the existence of an optimal backstop technology, and (iii) illustrating the consequence of such policies in the residential building sector numerically.

2.2 Analytical model

In this section, we first describe the representative agent model for investments in externality-producing durable goods under present-bias from Heutel (2015). Then we generalize the model and apply it to the building sector. By defining a larger technology set, we are able to represent technologies running on different fuels and thus zero emission backstop technologies. Based on the generalized model, we discuss two different cases: First, the case that the backstop technology is not optimal. Second, the case that the backstop technology is the optimal technology choice.

2.2.1 A representative agent model for investments in externality-producing durable goods under present-bias

Heutel (2015) describes the investment and operation problem for externality-producing durable goods under present bias in a representative agent model. We

present the model based on nomenclature for residential heating. The investment decision is made in the initial period ($t = 0$) and the good lasts T periods. In each period after the investment ($t = 1$ through $t = T$), the household decides on the operating intensity of the good: the generated heat or indoor temperature.

The model is defined by the household's problem and the social planner's problem. In the household's problem, future utility and costs are discounted using quasi-hyperbolic discounting. Quasi-hyperbolic discounting is a method for modeling the behavior of households who experience present bias, i.e., prefer immediate payoffs and undervalue future costs and payoffs.[4] To this end, two discount factors are introduced. δ is called the "long-run" discount factor, and β represents the "present bias". If a household experiences present bias, then $\beta < 1$.

The present-biased household perspective is contrasted with the social planner's problem. Present bias is a behavioral anomaly that a social planner does not experience due to fully rational behavior. One way to solve the social planner's optimization problem is to directly apply the long-run criterion while disregarding the household's present bias, i.e., setting $\beta = 1$. The approach assumes that the household's utility maximization deviates from optimal welfare even from the household's perspective. Thus, the household "makes a mistake" and does not optimize its "true utility".[5]

In the initial period, the household chooses the heating system's ratio of fuel input and generated heat, the so-called effort coefficient fph (fuel per heat), representing the investment decision for the durable good. In the subsequent periods, the heat generated in each period $h_t(t)$ is chosen, which translates into indoor temperature. $U(h_t)$, where $U' > 0$ and $U'' < 0$, describes the utility from generated heat in monetary terms. The costs per kWh of fuel are calculated as the sum of the time-dependent fuel cost (p_t) and a tax per kWh of fuel (τ_t). This fuel tax, hereinafter referred to as carbon tax, is intended to put a price on the GHG emissions. When choosing a level of fph, the household faces investment costs of $c(fph)$. It is assumed that $c' < 0$, meaning that less efficient goods (heating systems) are less expensive, and $c'' > 0$. The household's problem is thus described in Equation (2.1):

$$\max_{fph,\{h_t\}_{t=1}^{T}} \; -c(fph) + \beta \cdot \left[\sum_{t=1}^{T} \delta^t \cdot \Big[U(h_t) - [p_t + \tau_t] \cdot fph \cdot h_t \Big] \right] \tag{2.1}$$

[4] Technically speaking, present-biased households discount utility and costs in the near future at a higher implicit discount rate than in the distant future (Laibson, 1997).

[5] Alternative welfare criteria in the case of time-inconsistent discounting include the Paretian approach (e.g. Bhattacharya and Lakdawalla (2004)), or the "dictatorship of the present" approach discussed in Gruber and Köszegi (2004) or Laibson (1997), which prioritizes the preferences of the current self over the preferences of all future selves. Analogous to the approach in Heutel's basic model and following the arguments of O'Donoghue and Rabin (1999), we apply the long-run criterion.

The social planner's problem is characterized by including the externality of fuel consumption. The external damage from fuel consumption, i.e., damage from GHG emissions, depends on h_t, the kWh of fuel used in each period t, times fph, the fuel used for producing the heat. The damage is denoted as $d(h_t \cdot fph)$, where $d(0) = 0$, $d' > 0$ and $d'' = 0$. The corresponding social planner's problem, using the long-run criterion for discounting and including external damages, is described in Equation (2.2):

$$\max_{fph,\{h_t\}_{t=1}^{T}} -c(fph) + \sum_{t=1}^{T} \delta^t \cdot [U(h_t) - p_t \cdot fph \cdot h_t - d(h_t \cdot fph)] \tag{2.2}$$

2.2.2 Model generalization

In the model described in the previous section, consumers invest in one technology and can decide on its efficiency. By assumption, no backstop technology exists because efficiency improvements cannot reduce externalities to zero, and fuel cost differences between technologies used are neglected. We extend the technology set by allowing technologies running on different fuels. Therefore the investment decision affects fuel costs and GHG emissions per unit of generated heat. This enables us to analyze how optimal investment decisions depend on fuel cost ratios and to include a zero emission backstop technology. An example for a zero emission backstop technology in the building sector would be the switch to renewably generated heat from solar thermal energy or to electric heating powered by renewably generated electricity.

By allowing technologies to vary in fuel price and emission intensity (down to zero), we extend the technology set and generalize the model. In this generalized model, the fuel price $p_t(fph)$ and the CO_2 factor of the heating system $epf(fph)$ are represented as functions of the effort coefficient fph.[6] The functional form of $p_t(fph)$ is ambiguous: it is conceivable that the change to a more efficient heating system, e.g., from a gas boiler to an electric heat pump, is accompanied by decreasing fuel prices, in € per kWh_{fuel}, but also that the fuel price increases, if, for example, electricity is more expensive than gas. We incorporate a backstop technology with finite costs fph^{BS} by assuming that the emission function $epf(fph)$ equals zero for all $fph <= fph^{BS}$, and $epf' > 0$ for $fph >= fph^{BS}$. This means that when investing in the reduction of fph, $epf(fph)$ decreases linearly until the backstop technology fph^{BS} is reached, where emission intensity is zero. Further investments in reducing fph cannot further reduce the emission intensity.

[6] We model the choice of fph, the investment costs, the change in fuel price, and CO_2 factor as continuous. This serves the theoretical tractability of the model.

The household's problem, including quasi-hyperbolic discounting as defined in Section 2.2.1, is thus described as follows:

$$\max_{fph,\{h_t\}_{t=1}^{T}} \; -c(fph) + \beta \cdot \left[\sum_{t=1}^{T} \delta^t \cdot \Big[U(h_t) - [p_t(fph) + epf(fph) \cdot \tau_t] \cdot fph \cdot h_t \Big] \right] \tag{2.3}$$

The household's problem differs from Heutel (2015), since the investment decision fph depends on p_t and the newly introduced CO_2 factor epf. This yields first-order conditions for fph and each h_t. Assume that there exists a unique interior solution.[7] The solutions to the household's problem are called fph^* and h_t^*.

$$\begin{aligned} &- c'(fph^*) \\ &- \beta \cdot \sum_{t=1}^{T} \delta^t \cdot h_t^* \cdot [p_t(fph^*) + epf(fph^*) \cdot \tau_t] \\ &- \beta \cdot \sum_{t=1}^{T} \delta^t \cdot h_t^* \cdot \Big[[p_t'(fph^*) + epf'(fph^*) \cdot \tau_t] \cdot fph^* \Big] = 0 \end{aligned} \tag{2.4}$$

$$U'(h_t^*) - [p_t(fph^*) + epf(fph^*)\tau_t] \cdot fph^* = 0, \forall t \tag{2.5}$$

In Equation 2.4, considering the negative sign, the first term $-c'(fph^*)$ is positive. The term represents the benefit of a marginal increase in fph. Since $c' > 0$, it is cheaper to choose a system with higher fph and hence, lower efficiency. Similar to Heutel (2015), the first sum represents the discounted cost of a marginal increase in fph due to the decrease in efficiency: the utility in each future period decreases as heating costs increase. The second sum adds the changes in fuel prices $p_t'(fph)$ and changes in emission costs $epf'(fph) \cdot \tau_t$. While epf_t' is positive, p_t' can be positive or negative, depending on the constellation of fuel prices.[8] If both $p_t'(fph) = 0$ and $epf'(fph) = 0$, the third summand equals zero. In this case, neither the fuel price nor the emission intensity of the heating system depend on the investment decision, obtaining Heutels application with limited technology set. Equation 2.5 sets equal the marginal increase in utility of an additional kWh of heat with the marginal increase in costs for each period t.

The social planner's problem uses the long-run criterion and omits the term β. The external damage d depends on the GHG emissions emitted, which are calculated as the product of the emission intensity, the system efficiency, and the provided heat: $d(epf(fph) \cdot fph \cdot h_t)$, where $d(0) = 0$, $d' > 0$ and $d'' = 0$.

[7] It is assumed that $\lim_{h_t \to 0} U'(h_t) = \infty$ to ensure a unique interior solution.

[8] We will discuss the implications of this relationship under Proposition 2.

The social planner's problem is:

$$\max_{fph,\{h_t\}_{t=1}^{T}} -c(fph) + \left[\sum_{t=1}^{T} \delta^t \cdot \Big[U(h_t) - [p_t(fph) \cdot fph \cdot h_t] - d(epf(fph) \cdot fph \cdot h_t)\Big]\right] \tag{2.6}$$

The solutions to the social planner's problem are fph^{opt} and h_t^{opt}. The first-order conditions of the social planner's problem are:

$$\begin{aligned} & - c'(fph^{opt}) \\ & - \sum_{t=1}^{T} \delta^t \cdot h_t^{opt} \cdot \Big[p_t(fph^{opt}) + epf(fph^{opt}) \cdot d'(epf(fph^{opt}) \cdot fph^{opt} \cdot h_t^{opt})\Big] \\ & - \sum_{t=1}^{T} \delta^t \cdot h_t^{opt} \cdot \Big[[p_t'(fph^{opt}) + epf'(fph^{opt}) \cdot d'(epf(fph^{opt}) \cdot fph^{opt} \cdot h_t^{opt})] \cdot fph^{opt}\Big] \\ & = 0 \end{aligned} \tag{2.7}$$

$$U'(h_t^{opt}) - [p_t(fph^{opt}) + epf(fph^{opt}) \cdot d'(epf(fph^{opt}) \cdot fph^{opt} \cdot h_t^{opt})] \cdot fph^{opt} = 0, \forall t \tag{2.8}$$

2.2.3 Analysis

Optimal inner solution

First, we analyze the case that there is a welfare-optimal inner solution, i.e., that the backstop technology is not optimal and $fph^{opt} > fph^{BS}$. This is the case when the assumed external damage from GHG emissions is smaller than necessary for the backstop technology to be welfare-optimal. Thus, there exists a welfare-optimal quantity of GHG emissions that is greater than zero. The optimal solution is therefore found in the non-zero linear part of the emission intensity function $epf(fph)$.

From the first-order conditions of the household and the social planner, it follows that if $\beta = 1$, the household chooses the first-best outcome if $\tau_t = d'(epf(fph^{opt}) \cdot fph^{opt} \cdot h_t^{opt})\ \forall t$. This is the Pigouvian tax rate, called τ_t^{pig}, which internalizes fossil fuel usage's external damage.

As in Heutel (2015), the following holds for the adapted model:

Proposition 1.
Let $\beta < 1$: No set of emissions tax τ_t for all $t \epsilon [1, ..., T]$ exists that leads to the first-best outcome fph^{opt} and h_t^{opt}.[9]

[9]The proof is presented in Appendix 2.6.1.

If the Pigouvian tax rate is applied, Heutel (2015) obtains that too little is invested and the good is underutilized compared to the optimum of the social planner. In our case, when looking at heating investments, the question of whether too much or too little is invested due to present bias depends on how fuel and emission costs are affected by the investment decision, leading to Proposition 2:

Proposition 2.
Let $\beta < 1$: If $\tau_t = \tau_t^{pig}$ for all $t \in [1, ..., T]$ and
$\sum_{t=1}^{T} \delta^t \cdot h_t^* \cdot \left[[p_t(fph^*) + epf(fph^*) \cdot \tau_t] + [p_t'(fph^*) + epf'(fph^*) \cdot \tau_t] \cdot fph^* \right] \geq 0$
then $fph^* > fph^{opt}$ and $h_t^* < h_t^{opt}$ for all $t \in [1, ..., T]$.[10]

Proposition 2 states that present-biased households under-invest in the investment period and heat less than optimal in the subsequent periods, as long as the change in discounted future costs for a marginal increase in fph (marginally less efficient heating system) is greater or equal to zero. The scenario occurs if $p' >= 0$, meaning that the price for heating increases for less efficient heating systems. Then, the optimal solution is found as the trade-off between fph decreasing investment costs on the one side and the marginal increase in future heating costs consisting of the effects of the decreased efficiency, increasing emission costs, and increasing fuel costs on the other side. In the other scenario, in which $p' < 0$, the described relationship only continues to hold as long as the emission tax and lower efficiency offset the decrease in fuel costs for a marginal increase in fph. If this does not hold, i.e., $p_t' << 0$, a marginal increase in fph leads to lower investment costs and a decrease in future costs. In such a case, it would be optimal to invest as little as possible, thus $fph \to \infty$.

In the case of present bias, no set of CO_2 tax rates produces the first-best outcome regarding investments, fuel usage, and GHG emissions. A second-best policy solely based on CO_2 tax rates must consist of higher tax rates than the Pigouvian tax rate. The tax must address the usage of the heating system while also unfolding high incentives in the investment period, compensating for the present bias. A tax that incentivizes efficient investment despite present bias cannot be optimal because the tax is too high in subsequent periods to incentivize optimal heating use, given the optimal efficiency level, the utility of heating, and GHG emission damage. A second policy instrument has to be introduced to achieve the first-best result. In Heutel (2015), the author discusses a tax on the goods effort coefficient in the starting period and a fuel effort coefficient standard. In the case of the building sector, there is another policy measure often applied by the regulator: A subsidy on capital expenditures. We define this subsidy as a monetary benefit σ that is scaled with $\frac{1}{fph_{min} - fph_{max}} \cdot fph + \frac{1}{1 - \frac{fph_{min}}{fph_{max}}}$. The subsidy thus decreases linearly in fph. The household gets the full value of the subsidy if the household chooses fph_{min} and no subsidy if the household chooses fph_{max}:

[10] The proof is presented in Appendix 2.6.1.

Proposition 3.
Let $\beta < 1$: The first best is achieved by setting $\tau_t = \tau_{pig}$ in each period $t > 0$ and setting a technology subsidy in the form of $(\frac{1}{fph_{min} - fph_{max}} \cdot fph + \frac{1}{1 - \frac{fph_{min}}{fph_{max}}}) \cdot \sigma$ with $\sigma = (fph_{min} - fph_{max}) \cdot (\beta - 1) \cdot \sum_{t=1}^{T} \delta^t \cdot h_t^{opt} \cdot \big[[p_t(fph^{opt}) + epf(fph^{opt}) \cdot \tau_t^{pig}] + [p_t'(fph^{opt}) + epf'(fph^{opt}) \cdot \tau_t^{pig}] \cdot fph^{opt}\big]$.[11]

Since the household is present-biased, in the investment period, the household only considers a share of β of the future discounted benefits from decreasing fph. The subsidy is therefore composed of the benefit from investing in lower fph, expressed in the sum, times $(\beta - 1)$, offsetting the present bias in the investment period. In contrast to the fuel economy tax in Heutel (2015), our model's subsidy depends not only on h_t^{opt} but also on fph^{opt}. The intuition behind this is that due to the fuel switch when investing, fph^{opt} is relevant for determining the marginal benefit from an increase in fph as it defines fuel and emission costs in the optimal case. This means that for the optimal design of the subsidy, it is crucial to know how the optimal investment changes the fuel and emission costs. Besides the level of fuel and emission costs at fph^{opt}, also their slopes at this point determine the optimal subsidy. In contrast to Heutel (2015), marginal changes in investment affect the fuel price and the emission intensity. Therefore, the subsidy accounts for the marginal variable cost changes, composed of fuel price and emission intensity, induced by investment decisions under present bias. The term can both increase or decrease the optimal subsidy, as the fuel price can have a positive or negative slope in fph^{opt}.

Optimal backstop technology

In the model so far, we assumed that there exists a welfare optimal amount of GHG emissions that relates to the Pigouvian tax rate, internalizing the external emission damage. It was not optimal to invest in the backstop technology. In contrast, in the current political debate around the decarbonization of the building sector, the declared target is climate neutrality. The implicit assumption is thus, that the damage from GHG emissions is higher then corresponding abatement costs, and correspondingly, the optimal amount of GHG emissions is zero: fph is optimal if epf is zero. The same applies to a situation where the zero emission backstop technology is optimal due to sufficiently high assumed external emission damage. In the following, we discuss the case that $fph^{opt} = fph^{BS}$.

For the case without present bias, i.e., $\beta = 1$, there exists a set of tax rates τ_t^{neu} that is defined as the set of lowest tax rates, which achieves climate neutrality, which is thus the target-consistent set of CO_2 prices. As discussed before, this set

[11] The proof is presented in Appendix 2.6.1.

of tax rates is insufficient to reach climate neutrality in the case of present bias, as it only addresses the externality.

In contrast to Proposition 1, if the backstop technology is the optimal investment choice, a set of emission taxes $\tau_t > \tau_t^{neu}$ can be used to address both the externality and the internality. This is the case because of the added property of the emission function: We can choose taxes high enough for optimal investment, which induces climate neutrality. But since $epf(fph^{opt}) = epf(fph^{BS}) = 0$, the taxes do not influence the heating decision of households anymore. That means that any set of taxes high enough to induce investments in climate neutral heating technologies would be optimal since it does not affect heating decisions in the subsequent periods, as the heating decision becomes independent of the tax. This finding is, in principle, unaffected by the presence of present bias. Present bias only increases the minimum level of the taxes, inducing investments in climate neutral heating technologies.

Following that logic, the optimal investment decision can be derived from a set of taxes or a subsidy alone, a combination of both, or a command-and-control policy, i.e., a ban on new investments in conventional technologies. In our stylized model framework, except for the distributional effects of subsidies, there is no difference between those policies regarding the household's welfare, investment, or heating.[12]

2.3 Numerical simulation

In the numerical case study, we estimate real-world magnitudes of the present bias effect on under-investment, under-consumption of thermal energy, over-emissions, and associated deadweight loss. We obtain optimal single instrument magnitudes of CO_2 prices and subsidies representing the internality-mark-ups. Lastly, we show how present bias differentially affects CO_2 prices and subsidies and therefore numerically obtain optimal policy mixes.

2.3.1 Case study set-up

Metric for evaluation of sub-optimal policies

We numerically investigate the effects of present bias under policy measures aimed at reaching the politically set emission target with the help of a two-step procedure. First, excluding present bias internalities, we determine the minimal target-consistent carbon tax rate inducing investments suitable for climate neutrality

[12] See Section 2.4 for a discussion of the distributional effects of different policies.

goals, i.e., in the climate neutral backstop technology.[13] In the reference case, this carbon tax rate τ_t^{neu} is 192€ /tCO_2.[14] Second, we use this carbon tax rate as the implied damage to evaluate social welfare and deadweight loss.

Building and system characteristics

The functional form and parametrization of the utility of heating determine the household's choices. Mertesacker (2021) develops a utility function for domestic heating accounting for the properties of the technical heating system and building envelope. He estimates the utility's parameters within a German case study. We utilize this function and its estimated parameters. Equation (2.9) shows the utility function of our household $U(T_t)$ depending on the ideal indoor temperature $\overline{T}_t$ of 21 °C and chosen indoor temperature T_t. The utility function thus reflects the willingness to pay for the heating temperature. γ expresses the marginal utility of indoor temperature. We also refer to γ as *valuation factor* since it expresses the valuation of a specific household for indoor temperature.

$$U(T_t) = -\gamma \cdot (\overline{T}_t - T_t)^2 \tag{2.9}$$

We specify the utility function for the case study by defining an example household by its estimated marginal utility of indoor temperature γ, and an ideal indoor temperature. The characteristics and estimates of the corresponding marginal utility from indoor temperature stem from the median household in Mertesacker (2021). For this household, we obtain a γ of 25€ /ΔT^2.[15] Figure 2.1 shows the resulting utility function and variations for the exemplary household.

The heat demand in the case study, associated with the indoor temperature choice, is based on a representative building from Diefenbach et al. (2015) and IWU (2016).[16]

To evaluate a continuous investment choice of households, we estimate functions for investment costs, CO_2 emissions, and fuel prices based on real data (BAFA, 2021; Danish Energy Agency, 2021; Pickert et al., 2022). The heating technologies include oil and gas condensing boilers with and without solar thermal support and an air-source heat pump. As in the theoretical model, the functions are formulated concerning the heating technology's energy intensity level fph. We assume a system lifetime and an assessment period of 20 years. Table 2.1 shows the

[13] In our numerical simulation, we define the backstop technology with finite cost as an air-to-water heat pump. This applies under the assumption of continuously climate neutral electricity generation or based on political determinations that anticipate long-term decarbonization of power generation.

[14] In the numerical simulation, for simplicity, we assume constant fuel prices over time and utilize the same CO_2 tax rate in each year of the heating system lifetime.

[15] The underlying assumption of the household characteristics, the marginal utility estimates, and the computation of the valuation factor is described in Appendix 2.6.2.

[16] In Appendix 2.6.2, the computation of the heat demand and the underlying assumptions is described in detail.

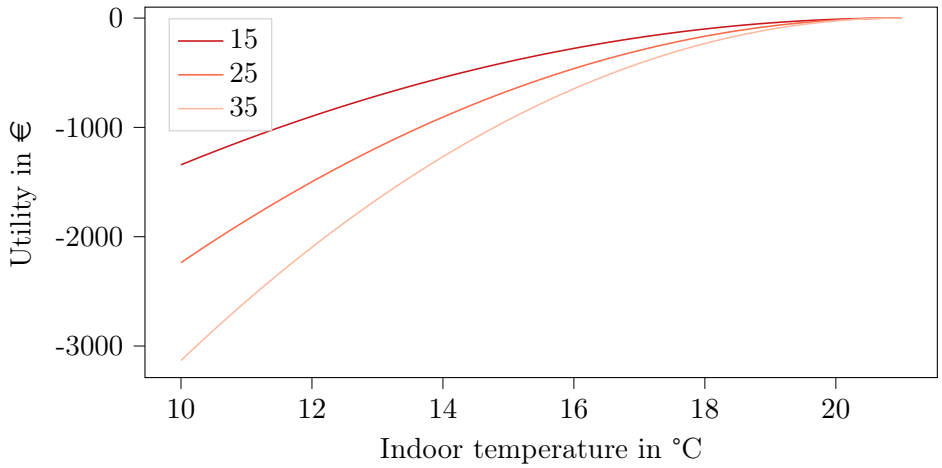

Figure 2.1: Utility Functions of indoor temperature for varying valuation factors

resulting technology functions.[17] It should be noted that fuel prices incorporate consumer taxes, including value-added tax, as well as electricity and gas taxes. Additionally, electricity prices include the costs of emission certificates derived from the European Emission Trading System. When interpreting the numerical results, one should keep in mind that these intricacies introduce distortions in optimal policy instruments and deadweight loss.

	Unit	Function
Investment costs	€	$c(fph) = 14,100e^{-1.019 \cdot fph}$
CO_2 emissions	kg/kWh	$epf(fph) = -0.110 + 0.358 \cdot fph$
Fuel price	€/kWh	$p(fph) = 0.394 - 0.331 \cdot fph$

Table 2.1: Estimated continuous functions of investment costs, CO_2 emissions, and variable costs.

2.3.2 Results

Continuous model

From the negative gradient of the fuel price in Table 2.1 follows that $p'(fph) < 0$. Considering Proposition 2 from Section 2.2, $p'(fph) < 0$ means that a CO_2 price (or a subsidy) has to at least offset the decrease of the heating system's variable fuel price induced by increasing fph. For such a CO_2 price, present bias leads to under-investment and, consequently, under-consumption of thermal energy. The numerical results replicate this finding on the relationship between present bias,

[17] Appendix 2.6.2 presents the underlying data and the computation of the technology functions.

investment, and consumption choices as illustrated in Figure 2.2. In case of no present bias, $\beta = 1.0$, there is no investment up to a CO_2 price of 137€ /tCO_2. The chosen indoor temperature at this price is 17.8°C. With an increasing CO_2 price, the investments in lower fph increase. As heating costs decrease, the indoor temperature increases, which is commonly referred to as the rebound effect. At a CO_2 price of 192€ /tCO_2, the household invests in climate neutral heating technology and reaches the corresponding indoor temperature of 18.2°C. As described in Section 2.3.1, we interpret this carbon tax rate τ_t^{neu} as the implied emission damage to evaluate social welfare and consequently deadweight loss. In the presence of present bias, the household invests less and chooses a lower indoor temperature.

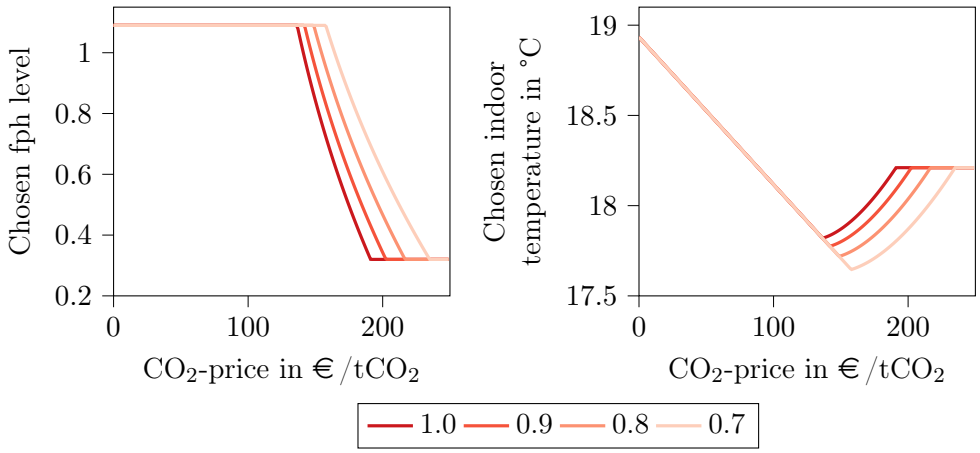

Figure 2.2: The chosen fph and indoor temperature levels depending on the CO_2 price for present biases of 1.0, 0.9, 0.8, and 0.7.

Figure 2.3 shows that the total CO_2 emissions over the 20 years of heating system lifetime follow the household's investment and consumption choices. As discussed in Section 2.2.3, the investment in lower fph impacts emissions more than decreasing indoor temperature. In case of $\beta = 0.7$, emissions decrease from 81 tCO_2 to 75 tCO_2 for a CO_2 price increase from 0€ /tCO_2 to 157€ /tCO_2, due to the decrease in temperature. The emission decline turns more significant once the investments in lower fph start at 158€ /tCO_2. At an emission price of 235€ /tCO_2, the household invests in the climate neutral technology so that total CO_2 emissions are 0.

The deadweight loss over the heating system's lifetime of 20 years is illustrated in Figure 2.3. It is based on the two-step procedure described in Section 2.3.1 and follows the chosen fph level. Without a CO_2 price, the household invests in the option with the highest fph, leading to a deadweight loss above 3,000€ due to the emissions. With an increasing CO_2 price, the indoor temperature first decreases slighty and with it consequently the emissions. Once the household invests in lower fph, the deadweight loss decreases convexly. Without present bias, the carbon tax rate τ_t^{neu} of 192€ /tCO_2 is sufficient to incentivize investment in the

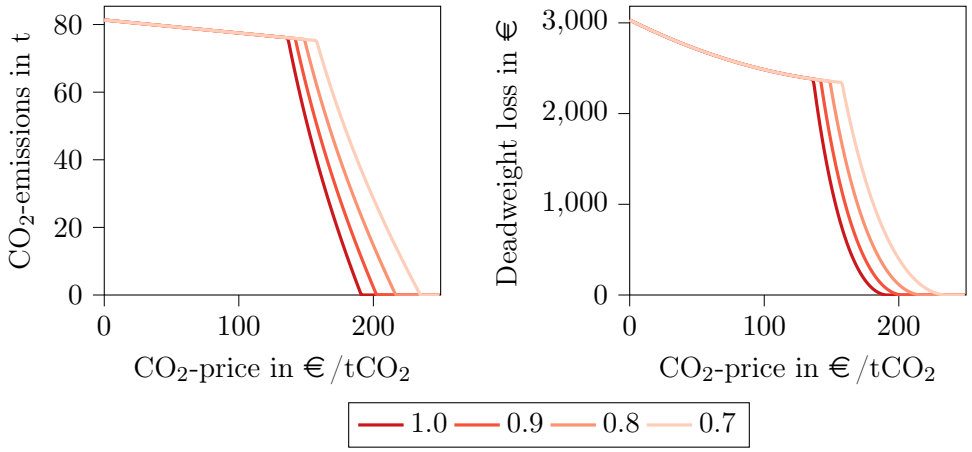

Figure 2.3: Total emissions and deadweight loss over the heating system's lifetime of 20 years depending on the CO_2 price for present biases of 1.0, 0.9, 0.8, and 0.7.

climate neutral technology. As Proposition 2 in Section 2.2.3 suggests, present bias leads to a deadweight loss caused by under-investment and, consequently, under-consumption. For $\beta = 0.9$, $\beta = 0.8$ and $\beta = 0.7$ the deadweight loss at τ_t^{neu} is 58€, 252€, and 613€, respectively. The loss results from the present bias internality as the τ_t^{neu} addresses the emission externality. In Section 2.2.3, we argue that under a climate neutrality regime, a mark-up on top of the CO_2 price which addresses the externality can address the internality and reach the climate neutral technology. The required mark-ups in the case study for $\beta = 0.9$, $\beta = 0.8$ and $\beta = 0.7$ are 11€ /tCO_2, 25€ /tCO_2, and 43€ /tCO_2, respectively.

According to Proposition 3 in Section 2.2.3, a subsidy is an alternative to a mark-up on the carbon tax. If the subsidy is high enough to induce investments in heat pumps, no CO_2 price is needed since subsequent heating does not emit CO_2. If the mark-up is high enough to induce investments in climate neutral heat pumps, no subsidy is needed. Consequently, a negative relationship exists between the two policies. All policy combinations that lead to the social optimum are illustrated in Figure 2.4. The function's slope describing the relationship between policies depends on the level of present bias and is lower for a high present bias. The slope differences originate from the differing times at which subsidies and CO_2 prices affect the household. Present bias hinders households from fully considering the CO_2 price in their optimal choice problem. Subsidies take effect directly at the time of the investment. The higher the level of present bias, the more the CO_2 price must increase to reduce the required subsidy.

At a CO_2 price of 89€ /t and a subsidy of 8,000€, there is an intersection of the functions for the different levels of present biases. Thus, at this combination of CO_2 price and subsidy, the required policy for the social optimum is independent of the level of present bias. The policy combination's CO_2 price creates parity between the variable costs of all technology options. In other words, the variable

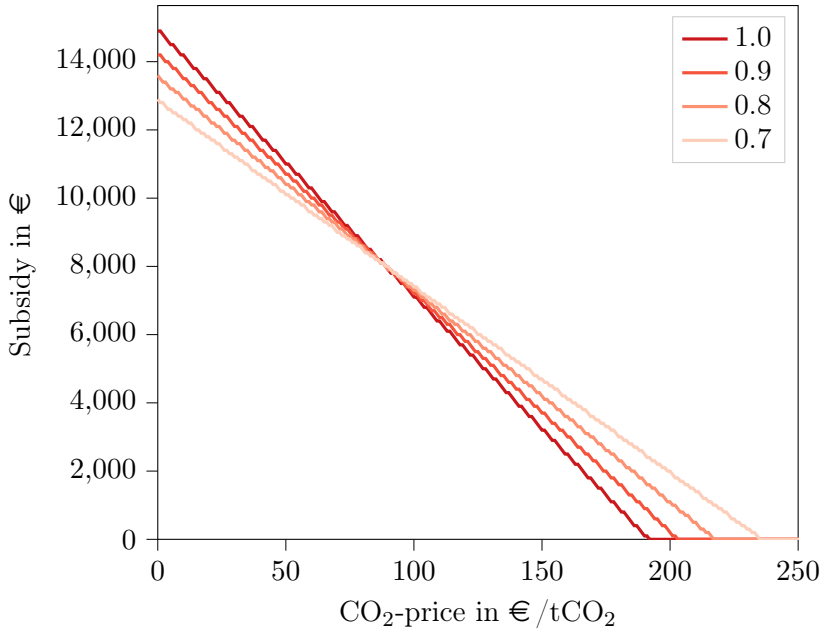

Figure 2.4: Combinations of CO_2 price and subsidy that lead to the social optimum for present biases of 1.0, 0.9, 0.8, and 0.7.

costs become independent of the chosen fph. We identify this intersection in Proposition 2 in Section 2.2.3 by stating that present bias leads to under-investment and, consequently, under-consumption as long as total future discounted heating costs, including fuel and emission costs, for a marginal increase in fph are greater or equal to zero. If this is not the case, i.e., less efficient heating systems have lower future heating costs, present bias will lead to over-investment. At the intersection between both cases, when future discounted heating costs are equal for all fph, the investment costs determine the investment choice. As present bias affects the household's weighting between marginal changes in investment costs and marginal changes in total future discounted costs, it does not affect the household's decision for equal future discounted costs. 89€ /t is the CO_2 price, which offsets the differences in the fuel costs. In this case, the subsidy must compensate households for the difference in investment costs between CO_2-emitting and climate neutral technologies. This subsidy is 8,000€. As a result, the policy mix at the intersection of the functions is optimal, independent of the level of present bias.[18]

The utility function of households is a critical assumption. As shown in Appendix 2.6.2, we identify different valuation levels for indoor temperature. Figure 2.5 shows the fph level and chosen indoor temperature over CO_2 price for three different valuation factors given a present-bias of $\beta = 0.8$. A higher valuation factor implies a lower necessary CO_2 price to incentivize investments

[18]The values of the optimal policy mix depend on the assumptions fed into the model, like fuel prices, heating efficiencies, and the utility function.

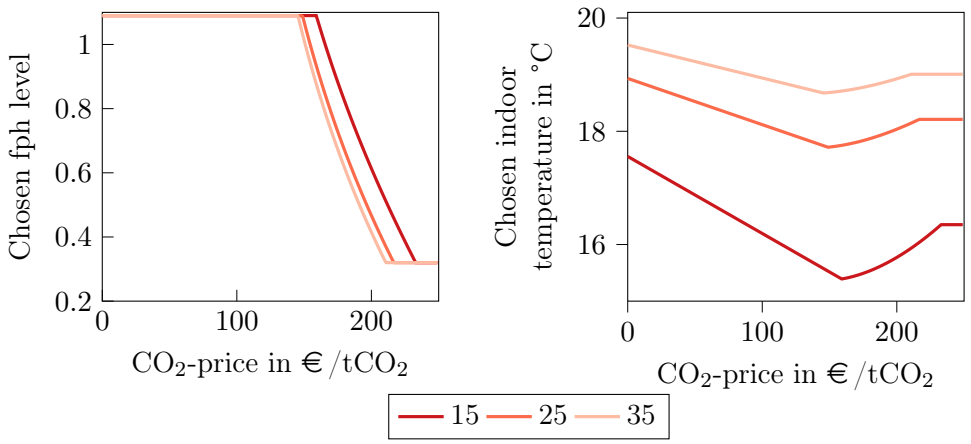

Figure 2.5: The chosen fph and indoor temperature levels depending on the CO_2 price for valuation factors of 15€ $/\Delta T^2$, 25€ $/\Delta T^2$, and 35€ $/\Delta T^2$.

in fph. In the case of a low valuation factor, the household reacts first with decreasing indoor temperature, as this yields lower utility loss compared to the additional costs of investing, as is shown in the right part of Figure 2.5. As soon as investments in more efficient technologies are profitable, efficiency increases, and the household increases the indoor temperature until the installation of the climate neutral backstop technology.

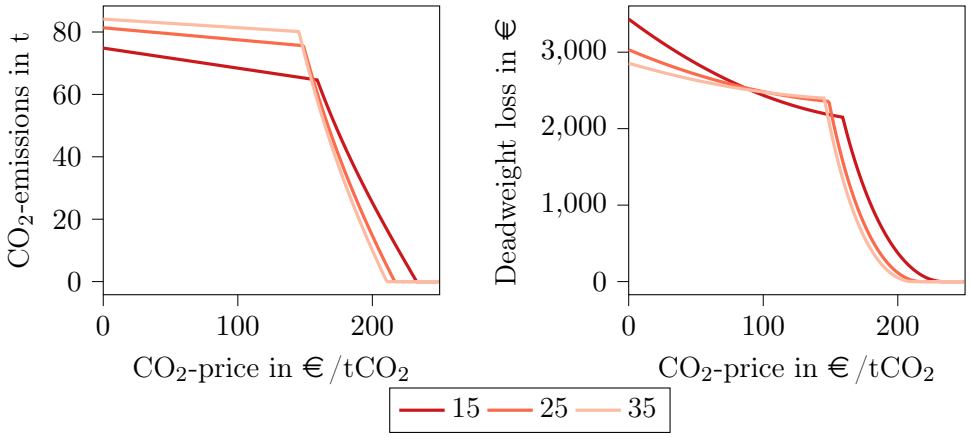

Figure 2.6: Total emissions and the deadweight loss over the heating system's lifetime of 20 years depending on the CO_2 price for valuation factors of 15€ $/\Delta T^2$, 25€ $/\Delta T^2$, and 35€ $/\Delta T^2$ and a present bias of 0.8.

The CO_2 emissions and deadweight losses over the heating system's lifetime of 20 years illustrated in Figure 2.6 show a slight decline until the start of investments in lower fph followed by a convex decline until the investment into the climate neutral technology. Before investments in more efficient technologies start, the deadweight loss is the highest for the high valuation factor since the under-consumption of indoor temperature weighs the most. The same logic also

applies to why households with a high valuation factor start investing in more efficient heating systems at lower CO_2 prices than households with lower valuation factors. As a higher level of investments decreases the deadweight loss not only through increased efficiency but also through reduced fuel costs, they exhibit a quadratic effect on the deadweight loss. Thus, the decline in welfare is less significant for lower valuation households, which still react by decreasing indoor temperature.

Discrete model

So far, the presented theoretical and numerical results assume continuous technology options so that all fph levels are feasible between the climate neutral and the least efficient option. In reality, there is only a limited set of heating technologies. Figure 2.7 illustrates the household's investment and consumption choices, given a discrete technology set, including an oil condensing boiler, a gas condensing boiler, both boiler combined with solar thermal, and an air-to-water heat pump. We define the set of technologies as the available fph levels from Section 2.3.1 and choose the cost and emission levels according to the functions from the continuous model (see Appendix 2.6.2).

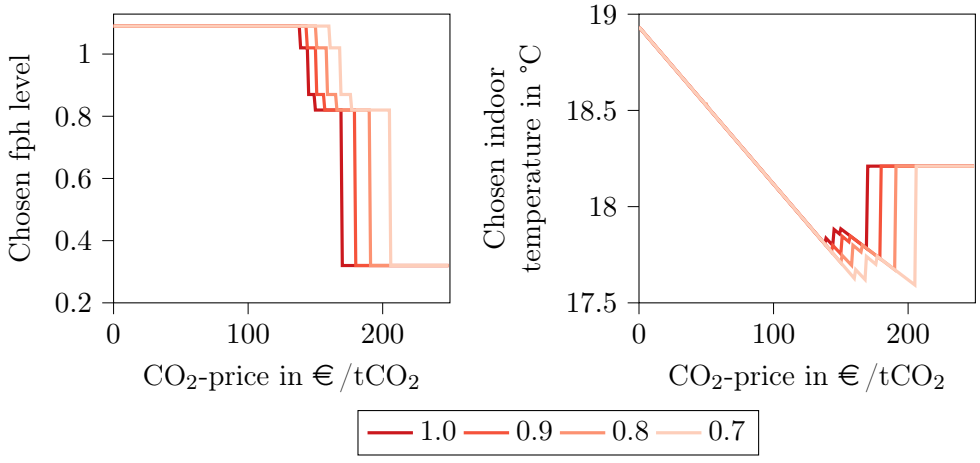

Figure 2.7: The chosen fph and indoor temperature levels in case of discrete technology options depending on the CO_2 price for present biases of 1.0, 0.9, 0.8, and 0.7.

For each present bias level, there are four break-even CO_2 prices that lead to a technology switch. In case of no present bias, i.e., $\beta = 1.0$, the household invests in the highest fph of 1.09, i.e., the oil condensing boiler, until a CO_2 price of 139€ /tCO_2. For higher prices, the household chooses a fph of 1.02, i.e., the gas condensing boiler. The break-even points for investing in the oil condensing boiler combined with solar thermal and the gas condensing boiler combined with solar thermal are at 145€ /tCO_2 and 150€ /tCO_2 respectively. At

a CO_2 price of 170€ /tCO_2, the household invests in the heat pump. Thus, in the discrete case 170€ /tCO_2 is the carbon tax rate τ_t^{neu} that induces investment in the climate neutral technology. The τ_t^{neu} is lower in the discrete case than in the continuous case because the CO_2 price only has to create a break-even between the gas condensing boiler with solar thermal and the heat pump, and not between an infinitesimal less efficient heating technology and the climate neutral backstop technology. Analogously to the continuous case, present bias leads to under-investment and under-consumption.

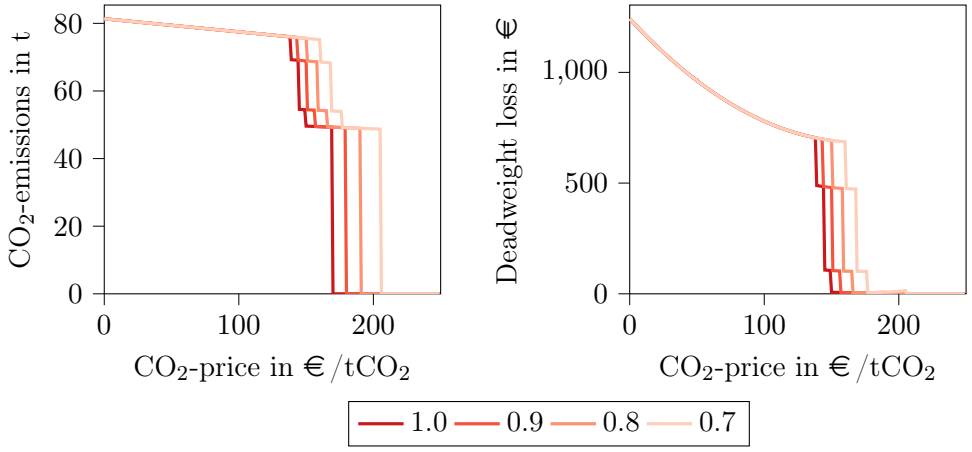

Figure 2.8: The total emissions and deadweight loss over the heating system's lifetime of 20 years in case of discrete technology options depending on the CO_2 price for present biases of 1.0, 0.9, 0.8, and 0.7.

The total CO_2 emissions over the heating system's lifetime of 20 years in Figure 2.8 mirror the step function of fph. There is a nearly linear decrease in CO_2 emissions following the household's temperature decreases and a more significant step whenever the CO_2 price causes a switch between two heating technologies. At the carbon tax rate τ_t^{neu}, there are zero CO_2 emissions in case of no present bias. The under-investment, due to present bias, leads to CO_2 emissions increases. These increases are for present biases of $\beta = 0.9$, $\beta = 0.8$, and $\beta = 0.7$, 49tCO_2, 49tCO_2, and 54tCO_2. This step is significantly higher than in the continuous case as the next available technology is a gas condensing boiler with solar thermal compared to a technology with infinitesimal higher emission intensity. A mark-up on the CO_2 price can address the internality and incentivize investment in the heat pump as stated in Section 2.2.3. For $\beta = 0.9$, $\beta = 0.8$, and $\beta = 0.7$, the mark-up is 10€ /tCO_2, 21€ /tCO_2, and 36€ /tCO_2, respectively. Following the two-step procedure described in Section 2.3.1, the implied damage from CO_2 emissions τ_t^{neu} is lower than in the continuous case, naturally resulting in a lower total level of deadweight loss. The deadweight loss due to present bias from under-investment and under-consumption is 101€ for a present bias of $\beta = 0.7$. The household chooses the oil condensing boiler with solar thermal instead of a heat pump. For present biases of $\beta = 0.9$ and $\beta = 0.8$ the household chooses a

gas condensing boiler with solar thermal, which leads to neglectable deadweight loss since τ_t^{neu} is defined as the necessarily implied damage to break-even between the two heating technologies.

2.4 Discussion

In our stylized model, we find that single-instrument policies can be welfare optimal and target-consistent even if the household is present biased. We implicitly assume that all households, their valuation factors, and their level of present bias are homogeneous. Accounting for household heterogeneity, however, implications of policy instruments can differ, especially in distributional effects.

According to our analysis, the lower the valuation for heat, the higher the CO_2 price must be to induce investment in the zero-emission backstop technology. Assuming the policymaker introduces a CO_2 price sufficient for incentivizing investment into the zero-emission backstop technology for a household with an average valuation factor, low-valuation households would not invest in the climate neutral technology. Instead, they would pay the CO_2 price and heat less, while high-valuation households invest in the zero-emission backstop technology. Similarly, if instead of a CO_2 price, the policymaker sets a target-consistent subsidy for average households, low-valuation households will not invest sufficiently. For households with higher valuations, however, the subsidy is not only sufficient but too high: they receive more money from the state than would have been necessary to stimulate the investment. The empirical literature suggests that high-income households have a higher valuation for thermal energy than low-income households (Cayla et al., 2011; Mertesacker, 2021). This would imply that a single, uniform subsidy, which aims to reach households with low valuation factors as well, favors high-income households.

Households also show heterogeneity with respect to their level of present bias. Assume the policymaker sets a CO_2 price that is target-consistent for households with average present bias. As shown in Section 2.3.2, households with stronger present bias ($\beta < \bar{\beta}$) would underinvest and pay the CO_2 price in future periods, heating less than optimal. Literature estimations of the correlation between income and the present bias level range between no correlation and a negative correlation, suggesting that low-income households experience higher levels of present bias (Can & Erdem, 2013; Filippini et al., 2021; Meier & Sprenger, 2010). We show in Section 2.3.2 that an optimal policy combination of a CO_2 price and subsidy exists that can account for different (unknown) levels of present bias.

Further real-world issues that our stylized model does not consider are investment distortions, hindering households from investing. Possible distortions and, thus, obstacles to investment include budget constraints, lack of access to capital, technological or regional circumstances, or split incentives between landlords and tenants. In cases where households cannot invest, otherwise target-consistent CO_2

prices may lead to high costs. Subsidies can help to overcome budget constraints and lack of access to capital. Suppose a subsidy is introduced as a single instrument. In that case, there is no price signal to at least partially internalize the externalities of households that cannot invest and whose heating is still associated with GHG externalities.

The policy instruments also differ regardless of households' heterogeneity. In the case of a singular implementation of a CO_2 price or bans on GHG emitting technologies, the households bear the full costs. With (supplementary) subsidies, by contrast, the state pays (part of) the costs. The latter may make sense from a social justice point of view or to increase acceptance among the population.

Given the heterogeneity of households and their potential investment constraints, as well as the possible desirability of distributing costs between households and the state, there are arguments in favor of combining taxes (or bans) with subsidies. By distinguishing the effects of policies on investment and utilization decisions, our analysis can support a nuanced discussion of appropriate policy mixes.

2.5 Conclusion

The present paper examines the impact of present bias on optimal environmental policies aimed at achieving climate neutrality. The study generalizes Heutel's model for policy design for externality-producing durable goods when internalities are present. Besides increasing efficiency, investments in a new heating system may substitute the fuel used. Accounting for this substitution adds the dimensions of fuel price and emission intensity to our technology space. The generalization allows us to include a backstop technology with finite cost and analyze policy choices that reach climate neutrality.

This work contributes to the scientific literature in three ways. First, we generalize Heutel's model by allowing technologies to differ in fuel price and emission intensity. Second, we introduce a model framework for developing target-consistent environmental policies given a backstop technology. It can serve as one element within a toolbox for welfare analysis given political targets beyond externality pricing. Third, we apply the model framework to the case of decarbonization in the German heating sector of private households under present bias and derive numerical magnitudes of the present bias effects.

We find that contrary to Heutel's propositions, one instrument can be sufficient to address both externality and internality. Still, a combination of subsidies and taxes can be advantageous as we show that there exists a tax-subsidy combination that is optimal regardless of the present bias level. This finding can be applied to comparable investment decisions in externality (GHG emission) producing durable goods, such as private mobility investments. The existence of the optimal policy mix is particularly relevant because the level of present bias is private information unknown to the policymaker and heterogenous among households. Policymakers

could avoid distributional effects by utilizing the present bias agnostic optimal policy mix. There are further arguments supporting policy mixes that fall short in our stylized model, including heterogeneity in the valuation of heating, investment distortions, and the costs' distribution between households and the state.

Based on our analysis, there remains room for further research. In contrast to our greenfield analysis with constant prices, in reality, households already own heating systems, and the heating system stock's age structure is heterogeneous. Therefore, households are faced not only with the question of which technology to invest in but also whether it is worth investing in a new heating system early on before the existing one breaks down. This raises questions about the timing of policy instruments, e.g., concerning the interdependencies of price paths of CO_2 taxes or fuel prices over time. Here, as well, the question arises as to what constitutes target-consistent policy instruments. The issue could prove complicated, as it is difficult to determine under which circumstances early heating systems replacement is required to achieve climate targets. Further, we discussed the role of household heterogeneity in our findings qualitatively. Households differ in their level of present bias, their current heating systems, and their financial capabilities. A more detailed examination of these properties could, in addition to theoretical analyses, e.g., concerning optimal policy mixes across households, also quantify effects at the level of the entire German building stock.

2.6 Appendix

2.6.1 Proofs

Proof 1:

Proposition:
There does not exist any set of emission tax rates τ_t for all $t \in [1, ..., T]$ that leads to the first-best outcome fph^{opt} and h_t^{opt}.

Proof analogous to Heutel (2015):
Suppose the contradiction: there exists a set of tax rates $\tau_t^{opt\beta}$ that lead to $m_t^* = m_t^{opt}$ for all $t > 0$ and $gpm^* = gpm^{opt}$. The first-order condition for choice of m_t in period t is $U'(m_t^*) = [p_t(fph^*) + epf(fph^*) \cdot \tau_t^{opt\beta}] \cdot fph^*$ or $U'(m_t^{opt}) = [p_t(fph^{opt}) + epf(fph^{opt}) \cdot \tau_t^{opt\beta}] \cdot fph^{opt}$. Since U'' is strictly negative the only optimal solution, when $\beta = 1$, is $\tau_t^{opt\beta} = \tau_t^{pig}$. When $\beta < 1$, the optimal solution does not change, since the planner does not consider the quasi-hyperbolic discount factor, but first order conditions of the consumer change. Thus, it does not equal the planner's solution.

Proof 2:

Proposition:
If $\tau_t = \tau_t^{pig}$ for all $t \in [1, ..., T]$ and
$\sum_{t=1}^{T} \delta^t \cdot h_t^* \cdot \Big[[p_t(fph^*) + epf(fph^*) \cdot \tau_t] + [p_t'(fph^*) + epf'(fph^*) \cdot \tau_t] \cdot fph^*\Big]$ then $fph^* > fph^{opt}$ and $h_t^* < h_t^{opt}$ for all $t \in [1, ..., T]$.

Proof analogous to Heutel (2015):
Note that the consumer's choice of fph^* is given by her first-order condition; call this equation F:

$$\begin{aligned} F = & -c'(fph^*) \\ & - \beta \cdot \sum_{t=1}^{T} \delta^t \cdot h_t^* \cdot \Big[[p_t(fph^*) + epf(fph^*) \cdot \tau_t] + [p_t'(fph^*) + epf'(fph^*) \cdot \tau_t] \cdot fph^*\Big] \end{aligned} \tag{2.10}$$

The implicit function theorem can be used to show how fph^* varies with β:

$$\frac{dfph^*}{d\beta} = \frac{-dF/d\beta}{dF/dfph} = \frac{\sum_{t=1}^{T} \delta^t \cdot h_t^* \cdot \Big[[p_t(fph^*) + epf(fph^*) \cdot \tau_t] + [p_t'(fph^*) + epf'(fph^*) \cdot \tau_t] \cdot fph^*\Big]}{dF/dfph} \tag{2.11}$$

The denominator is negative from the second-order condition of the consumer's optimization problem. The numerator is positive (or zero) if

$$\sum_{t=1}^{T} \delta^t \cdot h_t^* \cdot \Big[[p_t(fph^*) + epf(fph^*) \cdot \tau_t] + [p_t'(fph^*) + epf'(fph^*) \cdot \tau_t] \cdot fph^* \Big] \geq 0 \tag{2.12}$$

If the numerator is positive, then $dfph^*/d\beta < 0$. Since when $\beta = 1$ $fph^* = fph^{opt}$, it follows that in the case of $\beta < 1$ $fph^* > fph^{opt}$.

The consumer's choice of h_t^* in each period is a function of the total price of one kWh of heating, $[p_t(fph) + epf(fph) \cdot \tau_t] \cdot fph$, from the first-order condition $U'(h_t^*) = [p_t(fph) + epf(fph) \cdot \tau_t] \cdot fph$. Since $U'' < 0$, $dh_t^*/dfph < 0$. When $fph = fph^{opt}$, $h_t^* = h_t^{opt}$. But when $\beta < 1$, $fph^* > fph^{opt}$, so $h_t^* < h_t^{opt}$ for each period t>0 (and vice versa).

Proof 3:

Proposition:
Let $\beta < 1$: The first best is achieved by setting $\tau_t = \tau_{pig}$ in each period $t > 0$ and setting a technology subsidy in the form of $(\frac{1}{fph_{min} - fph_{max}} \cdot fph + \frac{1}{1 - \frac{fph_{min}}{fph_{max}}}) \cdot \sigma$ with $\sigma = (fph_{min} - fph_{max}) \cdot (\beta - 1) \cdot \sum_{t=1}^{T} \delta^t \cdot h_t^{opt} \cdot \Big[[p_t(fph^{opt}) + epf(fph^{opt}) \cdot \tau_t^{pig}] + [p_t'(fph^{opt}) + epf'(fph^{opt}) \cdot \tau_t^{pig}] \cdot fph^{opt} \Big]$.

Proof:
The subsidy is defined as a monetary benefit σ that is scaled with $\frac{1}{fph_{min} - fph_{max}} \cdot fph + \frac{1}{1 - \frac{fph_{min}}{fph_{max}}}$. The consumer's problem is:

$$\begin{aligned} \max_{fph, \{h_t\}_{t=1}^T} \; & -c(fph) + (\frac{1}{fph_{min} - fph_{max}} \cdot fph + \frac{1}{1 - \frac{fph_{min}}{fph_{max}}}) \cdot \sigma \\ & + \beta \cdot \left[\sum_{t=1}^{T} \delta^t \cdot \Big[U(h_t) - [p_t(fph) + epf(fph) \cdot \tau_t^{pig}] \cdot fph \cdot h_t \Big] \right] \end{aligned} \tag{2.13}$$

Subject to

$$U'(h_t) - [p_t(fph) + epf(fph) \cdot \tau_t^{pig}] \cdot fph = 0, \forall t \tag{2.14}$$

Consider this problem's Lagrangian, where the constraint from the period t choice of h_t^* has a multiplier λ_t. The first-order condition with respect to h_t is:

$$\beta \cdot \delta^t \Big[U'(h_t^*) - [p_t(fph^*) + epf(fph^*) \cdot \tau_t^{pig}] \cdot fph^* \Big] + \lambda_t \cdot U''(h_t^*) = 0 \tag{2.15}$$

The term in brackets is zero from the first-order condition from the static choice of h_t, Since U'' is strictly negative, $\lambda_t = 0$ for all $t > 0$. Then, the first-order

condition for fph is:

$$\begin{aligned}
&- c'(fph^*) + \frac{1}{fph_{min} - fph_{max}} \cdot \sigma \\
&- \beta \cdot \left[\sum_{t=1}^{T} \delta^t \cdot h_t^* \cdot \Big[[p_t(fph^*) + epf(fph^*) \cdot \tau_t^{pig}] \right. \\
&\qquad \left. + [p_t'(fph^*) + epf'(fph^*) \cdot \tau_t^{pig}] \cdot fph^* \Big] \right] \\
&= 0
\end{aligned} \tag{2.16}$$

With the value of σ as given, this first-order condition can be written as:

$$\begin{aligned}
&- c'(fph^*) \\
&- \sum_{t=1}^{T} \delta^t \cdot \left[\beta \cdot h_t^* \cdot \Big[[p_t(fph^*) + epf(fph^*) \cdot \tau_t^{pig}] + [p_t'(fph^*) + epf'(fph^*) \cdot \tau_t^{pig}] \cdot fph^* \Big] \right. \\
&\qquad + (1-\beta) \cdot h_t^{opt} \cdot \Big[[p_t(fph^{opt}) + epf(fph^{opt}) \cdot \tau_t^{pig}] \\
&\qquad\qquad \left. + [p_t'(fph^{opt}) + epf'(fph^{opt}) \cdot \tau_t^{pig}] \cdot fph^{opt} \Big] \right] \\
&= 0
\end{aligned} \tag{2.17}$$

When $fph^* = fph^{opt}$, then $h_t^* = h_t^{opt}$ for all $t > 0$ since $\tau_t = \tau_t^{pig}$. Plugging $fph^* = fph^{opt}$ and $h_t^* = h_t^{opt}$ in Equation 2.17 makes it equal to the social planner's first-order condition. So fph^{opt} and h_t^{opt} solve the consumer's problem, and by the second-order condition this is a unique solution.

2.6.2 Numerical simulation

Household's heating valuation

Mertesacker (2021) provides a utility function and estimates of its parameters for a case study on energy consumers in Germany. The utility function from Equation (2.9) includes a household's indoor temperature valuation factor γ. γ is obtained by multiplying household characteristics x as binary vector and the estimated coefficient for each characteristic δ. We specify the utility function for the case study by defining an example household by its characteristics x and corresponding estimated marginal utility of indoor temperature δ. The characteristics and estimates of the corresponding marginal utility from indoor temperature stem from Mertesacker (2021) as listed in Table 2.2. For the case study in this paper, we construct three sample households covering the potential spread of valuations as shown in Table 2.2. The base household has a valuation of 25€ $/\Delta T^2$, while the minimum obtained value is 13€ $/\Delta T^2$ and the maximum 38€ $/\Delta T^2$. For

simplicity, we utilize valuations of 15€ $/\Delta T^2$, 25€ $/\Delta T^2$, and 35€ $/\Delta T^2$ in the valuation sensitivity.

Parameter		δ Coefficent	x Base	x Min	x Max
Constant		12,256	1	1	1
Age	30-39	1.262	0	0	0
	40-49	0.094	1	1	0
	50-59	3.918	0	0	0
	≥ 60	4.811	0	0	1
# adults	2	3.014	1	1	0
	3	6.654	0	0	1
	≥ 4	3.850	0	0	0
# children	1	-0.368	0	1	0
	≥ 2	2.964	1	0	1
Is employed		-2.234	1	1	0
Has Abitur		3.271	1	0	1
Is owner		-0.033	1	1	0
Income	$<$ 1,500€	2.329	0	0	1
	$\geq$ 3,500 €	0.320	0	1	0
Dwelling size	Small: $<$ 1st tercile	-1.103	0	1	0
	Large: $>$ 2nd tercile	5.322	1	0	1
Valuation βx in € $/\Delta T^2$			25	13	38

Table 2.2: Estimates of a household's characteristic's effect on marginal utility from indoor temperature from Mertesacker (2021).

Building's heat demand

The heat demand for the representative building used in the numerical case study is based on the building "SFH 1" from the building stock model of Diefenbach et al. (2015) and IWU (2016)[19]. The building definition in Diefenbach et al. (2015) is part of a model for the German building stock of the year 2009 via six representative average buildings. In this model "SFH 1" represents the most common average building in Germany. It is a single-family home with 147.1 m^2 of floor area. Based on the calculations implemented in IWU (2016), the specific heat demand of the household (including domestic water supply, storage and distribution losses) for the ideal room temperature of 21°C is set to 224 kWh/m^2. This value includes an assumed reduction factor of 0.86 which corrects for the heated area and the reduction of temperatures during the night. Using the calculation methods and definitions from IWU (2016), the heat demand is determined for different temperature levels. Theoretical calculation methods for

[19]Specified with the code DE.National.2009.002.01

determining heat demand tend to overpredict the real heat demand (Loga et al., 2012; Mertesacker, 2021). To account for this we assume an adaptation factor of 0.8 for our representative building, based on Loga et al. (2012) and IWU (2016). The choice of this factor is consistent with the results of Mertesacker (2021), who estimates lower adaptation factors, but does not take into account domestic hot water generation. The heat demand in our model h [kWh] is then approximated as a linear function, depending on the chosen temperature T [°C]:

$$h = 0.8 \cdot 147.1\, m^2 \cdot (11.61 \frac{kWh}{m^2 \cdot^{\circ} C} \cdot T - 19.85 \frac{kWh}{m^2}) \tag{2.18}$$

Heating technologies

Within the case study, we utilize stylized continuous functions of investment costs, CO_2 emissions, and fuel prices depending on the chosen fph-level. These functions are based on technical and economic heating system parameters from Danish Energy Agency (2021), emission intensities from BAFA (2021), and fuel price trajectories from Pickert et al. (2022). Danish Energy Agency (2021) provides data on real heating systems including reference capacities, efficiencies, and cost components as shown in Table 2.3. We combine the solar thermal system with both an oil boiler and a gas boiler to obtain in total five investment options for the household in the case study. fph is the reciprocal of the efficiency. The efficiency of the combined heating system of a boiler and solar thermal results from the assumption that the solar thermal accounts for 20% of heat demand (BDEW, 2020). The investment costs of for each technology are obtained by scaling the equipment costs from Table 2.3 to the uniform heating system size of 12.5 kW for the conventional technologies and 6.25 kW for the heat pump and adding the corresponding installation costs. Figure 2.9 illustrates the resulting investment costs depending on fph, both for the discrete heating systems and a fitted exponential function.

The fuel data in Table 2.4 contains the CO_2-intensites from BAFA (2021) and the average fuel prices over the next 20 years from Pickert et al. (2022). Note that the fuel prices are final consumption prices accounting for grid fees and other levies. Accounting for the efficiencies of the heating systems, Figure 2.9 shows the resulting discrete emission intensities and fuel prices in dependence of fph as well as fitted linear functions.

Heating technology	Capacity kW_{th}	Efficiency	Equipment costs €	Installation costs €
Oil boiler	20	0.92	4260	1300
Gas boiler	14	0.98	2702	1158
Air-to-Water heatpump	7	3.15	6780	3830
Solar thermal	4,2		2872	1228

Table 2.3: Technical and economic properties of oil boiler, gas boiler, air-to-water heatpump, and solar thermal systems (Danish Energy Agency, 2021).

Fuel	Fuel price € /kWh	CO_2-intensity $kgCO_2$/kWh
Oil	0.0738	0.266
Gas	0.0743	0.201
Electricity	0.3142	0

Table 2.4: Energy prices based on Pickert et al. (2022) and CO_2-intensities based on BAFA (2021).

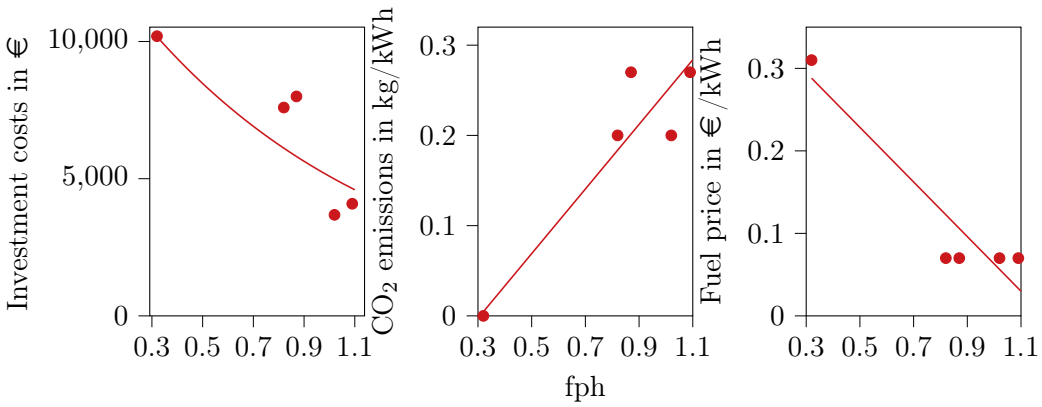

Figure 2.9: Investment costs, CO_2 emissions, and fuel prices for different heating technologies, including gas and oil condensing boiler, gas and oil boiler combined with a solar thermal system respectively, and an air-source heat pump. Both the discrete technologies as well as fitted functions are displayed.

3 How prices guide investment decisions under net purchasing - An empirical analysis on the impact of network tariffs on residential PV

3.1 Introduction

Solar photovoltaic (PV) is generally expected to have a substantial share in the future electricity generation mix around the globe (IEA, 2020). In Germany, residential PV systems already count for around 1.2 million installations in 2020 (Bundesnetzagentur, 2021b). These PV systems are typically installed by individual households and, thus, distributed decentrally. To limit network expansion and reduce congestion costs, an efficient coordination of these investments is essential. Recent findings suggest that economic factors are among the main drivers for PV adoption in the residential sector (e.g. Jacksohn et al., 2019). In principle, households can use the self-generated PV electricity to either feed it into the grid or replace electricity consumption from the grid. The profitability of these options depends on the regulatory framework. In Germany, a net purchasing system is in place for residential PV installations, which is also the predominant metering scheme in Europe (Gautier et al., 2018). That is, grid feed-in and grid consumption are metered separately and billed at two different prices. The remuneration of grid feed-in is based on the feed-in tariff, which is the main subsidy for residential PV in Germany, granted under the Renewable Energy Sources Act (EEG.). The value of self-consumption depends on the consumption costs, which households can reduce for each kilowatt-hour (kWh) of grid consumption substituted with self-generated PV electricity.

Higher tariffs for grid consumption increase the consumption costs of the household and raise the incentive for self-consumption and residential PV installations. This relationship is unambiguous under net metering, where grid feed-in and grid consumption are billed at the same price (c.f. Gautier & Jacqmin, 2020). Under net purchasing, the same rationale should apply, although the incentive structure also depends on the remuneration for grid feed-in. In particular, the effect should increase the more profitable self-consumption is compared to the revenue from grid feed-in (c.f. Jägemann et al., 2013).

Additionally, tariffs follow a nonlinear pricing schedule. The investment decision should be incentivized only by the volumetric price rather than the fixed price component or an average price calculated from both. Empirical findings suggest that consumers confuse nonlinear price schedules, which contrasts with the the-

oretical expectation (Ito, 2014). Such an effect would raise concerns regarding the effect of regulatory changes in electricity price components on residential PV installations. In Germany, for example, reform proposals for the network tariff system plan to shift network costs from predominantly volumetric network tariffs to a more substantial share of fixed network tariffs. Other proposals aim for a change in the EEG-levy that is currently paid exclusively on a volumetric basis. Knowing whether and how consumers respond to the different price components is crucial to assess the consequences of such policy reforms on PV adoption.

We empirically investigate whether and how price signals impact the adoption of residential PV installations in Germany. More specifically, we analyze the impact of network tariffs on PV adoption and exploit the fact that network tariffs are a considerable part of retail tariffs and the decisive driver for their regional variation. The heterogeneity of network tariffs allows us to identify the impact of price signals on a high regional resolution. In contrast, the other components of the retail tariff depend on markets and regulations that are equal across Germany. We use a panel data set of PV installations, network tariffs, and socioeconomic covariates on postcode level covering the years of 2009-2017 and apply a Poisson quasi-maximum likelihood estimator (PQMLE) with fixed effects to capture unobserved heterogeneity across regions and time.

We find evidence that network tariffs significantly impact PV investments across Germany. An increase in network tariffs by one within standard deviation (0.34 eurocent per kWh) is estimated to increase PV installations by 2 %, all else equal. This effect has grown, supporting the hypothesis that the incentive for self-consumption has increased over time. Furthermore, it is indeed the volumetric network tariff that impacts PV adoption rather than the average price. Our results provide valuable insights into the driving forces of residential PV adoption in Germany, which allows evaluating upcoming policy reforms regarding the regional allocation of PV installations and the structure of electricity prices.

The paper is organized as follows. Section 3.2 provides an overview of the empirical literature on residential PV adoption. Section 3.3 outlines the policy framework and the economic rationale for investment in residential PV installations in Germany. Section 3.4 introduces the empirical strategy while Section 3.5 presents our panel data set. Our results are shown and discussed in Section 3.6 and we discuss our findings and conclude in Section 3.7.

3.2 Literature review

Our analysis contributes to two streams of the literature: first, the drivers of residential PV expansion, and second, the impact of nonlinear tariff structures on investment decisions in the residential energy sector.

The main drivers for residential PV investments can be classified by socio- and techno-economic factors, behavioral factors, and economic factors.[20] The first and most extensively researched category are socioeconomic factors such as education, per capita income, environmental awareness, and techno-economic factors, such as solar irradiance and specific house characteristics. Schaffer and Brun (2015) conduct a comprehensive analysis on the drivers for adopting residential PV in Germany between 1991 and 2012. They find strong effects for solar irradiance, house density, home-ownership, and per capita income, while the environmental awareness hardly affects PV investments.[21] Subsequent studies, for example, Dharshing (2017), Baginski and Weber (2019), Jacksohn et al. (2019) and Gutsche et al. (2020), generally confirm these findings: environmental awareness has only little explanatory power, while the other socio- and techno-economic factors are important drivers of residential PV adoption in Germany.

Second, behavioral factors, such as myopia, inertia, or peer effects, are also likely to drive PV adoption in the residential sector. For example, regarding peer effects, i.e., the impact of previously installed PV in a surrounding area on the current investment decision of an individual household, findings in the empirical literature are mixed. In their seminal work, Bollinger and Gillingham (2012) examine peer effects on residential PV expansion in the US and find a significant impact. Rode and Weber (2016) conduct a similar analysis for Germany and confirm the impact of imitative adoption behavior. Though Baginski and Weber (2019) also find regional dependencies in their analysis, social imitation does not seem to be the main driver of the regional spillover effects. Similarly, Rode and Müller (2020) find that the impact of previously installed PV on current adoption decreases over time and might be mistaken with the regional concentration of craft skills or solar initiatives.

The third category contains literature on the influence of economic factors, i.e., expected costs and revenues of the PV installation.[22] We observe a growing research interest regarding the economic factors due to two simultaneous developments. First, Palm (2020) suggests that in the first stage of the diffusion process, early adopters have fewer concerns for costs or concrete financial benefits. In contrast, in the later stages, the economic factors become more decisive. Hence, the impact of socioeconomic and behavioral factors on PV investments should decrease over time as these factors become less pivotal during the diffusion process of new technologies. Second, in the early years of PV expansion in Germany, a PV installation has been financially attractive mainly due to the feed-in tariffs granted as a subsidy for PV deployment. Ossenbrink (2017), and Germeshausen

[20] Comprehensive reviews on the adoption of building-scale renewable energy systems in European countries can be found in, for example, Heiskanen and Matschoss (2017) and Selvakkumaran and Ahlgren (2019). In this literature review, we mainly focus on analyses for Germany to derive a better understanding of the empirical case for the reader. However, most findings of the literature also apply to other regions.

[21] Balta-Ozkan et al. (2015) find similar factors for the UK.

[22] Intuitively, cost and revenues also depend on techno-economic factors, like irradiance. However, we think of economic factors as monetary metrics.

(2018) analyze the impact of feed-in tariffs in Germany and, in particular, the impact of (changes in) the policy framework on PV adoption. Jacksohn et al. (2019) analyze the impact of the costs of PV panels and revenues from feed-in tariffs in Germany from 2008 to 2015 on the individual household level. They find that these economic factors mainly drive the investment decisions in PV installations and solar thermal facilities. Also in other countries, economic factors impact households' PV investment decisions. As for the case of feed-in tariffs in Germany, governmental pricing policies play a substantial role for the PV adoption in many countries. Best et al. (2019) quantify the impact of Australia's spatially-differentiated small-scale renewable energy scheme on residential PV investments using postcode-level data. Their results indicate that postcodes receiving a higher subsidy factor have significantly more residential PV investments, after controlling for solar exposure and spatial patterns in the data. Similarly, De Groote et al. (2016) find that local policies have a significant impact on PV adoption in Flanders. Focusing on the residential PV adaption in California, e.g., Hughes and Podolefsky (2015), show a significant regional effect of upfront rebates on PV investments, exploiting variation in rebate rates across electric utilities over time. Similarly, Crago and Chernyakhovskiy (2017) show that rebates have the biggest impact among financial incentives on residential PV adoptions in the Northeast. They further indicate positive impacts of electricity prices.[23] With the increasing attraction of self-consumption, the economic rationale of residential PV installations is further influenced by the costs for electricity consumption and, therefore, not only by the feed-in tariff but also by the retail tariff. Klein and Deissenroth (2017) show that the overall German residential PV expansion is impacted by the anticipation of profitability, including both feed-in and retail tariffs in their analysis. Sahari (2019) analyzes the choice of heating systems in Finland. She finds a significant impact of electricity prices on long-term technology choices. Further and closest to our analysis, Gautier and Jacqmin (2020) analyze the impact of volumetric network tariffs on PV investments under a net metering system in Wallonia. They find a positive and significant effect of network tariffs on PV installations. In a similar vein, de Freitas (2020) analyzes PV investments in Brazil. Both regions currently apply net metering systems, where grid feed-in and self-consumption are both valued at the retail tariff. Therefore, higher retail tariffs should encourage higher PV investments. In a net purchasing system, the incentive is two-fold and depends on the remuneration for grid feed-in, which is determined separately (see Section 3.3).

Moreover, we extend the analysis of price signals by examining how the nonlinear tariff structure influences investment decisions. In his seminal work, Ito (2014) analyzes the price perception of consumers in US electricity markets. His results suggest that consumers are short-sighted in their response to electricity prices by deciding on their electricity bill of the past rather than current tariffs or future expectations. Further, Ito (2014) examines the impact of nonlinear multi-tier

[23] See Ossenbrink (2017), for a comparison of the impact of feed-in tariff designs and their interplay with retail electricity prices between Germany and California.

tariffs on electricity consumption, and Shaffer (2020) conducts a similar analysis for British Colombia. The authors analyze whether consumers respond to nonlinear tariffs in the way microeconomic theory suggests, i.e., whether they respond to the marginal price rather than the fixed or an average price. Both find that consumers respond to average rather than marginal prices, which contrasts with the theoretical expectation. However, a further analysis by Ito and Zhang (2020) for heating usage in China finds that consumers do indeed respond to the marginal price in the context of a simpler tariff form, i.e., a two-part tariff.

To the best of our knowledge, we are the first to empirically analyze the impact of price signals on PV adoption in a net purchasing system. We use the regional variation in network tariffs in Germany to investigate whether and how prices impact PV investments. We examine whether the incentives for self-consumption have become more relevant in recent years and conduct the first empirical study that analyzes how the price components of a nonlinear tariff impact residential PV adoption.

3.3 Residential PV in Germany: policy framework and investment incentives

PV installations enable individual households to generate their own electricity so that they no longer participate in the market only as consumers.[24] To illustrate the economic rationale behind residential PV adoption in Germany, we derive the microeconomic foundation of the investment incentives for an individual household. The regulatory framework in Germany is a net purchasing system. In contrast to a net metering system, where one single price for electricity consumption from the grid (imports) and grid feed-in (exports) exists, these two options are measured separately (c.f. Gautier et al., 2018).

The PV installation offers two options for the household how the self-generated electricity (q_{PV}) can be used:

$$q_{PV} = q_{togrid} + q_{self} \tag{3.1}$$

The household can feed the electricity into the grid (q_{togrid}) or use it for self-consumption (q_{self}), i.e., substitute electricity consumption that is otherwise imported from the grid (d_{total}).[25] We structure the economic incentives by

[24] As households with PV installations both produce and consume electricity, the term prosumer has also been established. Prosumers are of general interest in recent literature, seeking to understand their decision-making and how regulatory policies impact them in more detail, (e.g. Gautier et al., 2018).

[25] To fully reflect the potential temporal discrepancy of PV generation and the household's electricity consumption, an (hourly) time index could be introduced (see e.g. Ossenbrink (2017) for a more detailed representation). However, for simplicity and without loss of generality, we refrain from this issue in the following representation.

analyzing the net present value (NPV)[26] of the PV installation in Equation (3.2):

$$NPV = -C_I + \sum_{t=0}^{T} \frac{R(q_{togrid}) - C(d_{total} - q_{self}) - c_{OM}}{(1+r)^t} \tag{3.2}$$

One-time costs occur due to the initial investment C_I. Once the PV system is installed, continuous costs for operation and maintenance c_{OM} incur and the PV installation offers the opportunity to generate revenue by selling electricity to the grid ($R(q_{togrid})$) and to reduce electricity costs by self-consuming electricity from the PV installation ($C(d_{total} - q_{self})$). By assumption, costs and revenues are constant over time, but discounted on a yearly basis t at an interest rate r. We briefly describe the institutional and regulatory framework in Germany and discuss the incentives for PV investments over the years.

3.3.1 Regulatory framework for residential PV in Germany

The grid feed-in of a residential PV installation is regulated under the EEG, and residential PV owners receive a feed-in tariff, paid for each kilowatt-hour (kWh) of electricity fed into the grid. The feed-in tariff varies depending on the date, size, and type (roof-top or ground-mount) of the installation.

Feed-in tariffs are determined administratively by the government, and the level and the categorization are regularly adjusted for new installations. Residential PV installations with 10 kW or smaller have always been eligible to receive the highest possible feed-in tariff. In contrast, larger installations have been subject to some changes in the definition of their support categories over the years. Adjustments of the level of feed-in tariffs are mainly based on the development of PV investment costs which has led to a declining trend over the past years (see Figure 3.1). While the feed-in tariff was about 43 ct/kWh in 2009, this has been reduced to about 12 ct/kWh by 2017. In addition to the feed-in tariff, from 2009 until 2012, the EEG granted an additional remuneration for self-consumption. Although this remuneration was lower than the feed-in tariff, e.g., 25 ct/kWh compared to a feed-in tariff of 43 ct/kWh in 2009, households benefited from self-consumption on top of the savings from reduced electricity consumption costs (Bundesnetzagentur, 2021a).

[26] We focus on the economic rationale in terms of cash flows and do not consider the utility function of the household. One can think of factors that increase the utility beyond the financial aspects, e.g. environmental preferences, and those that have a negative impact, e.g. behavioral biases like inertia or myopia.

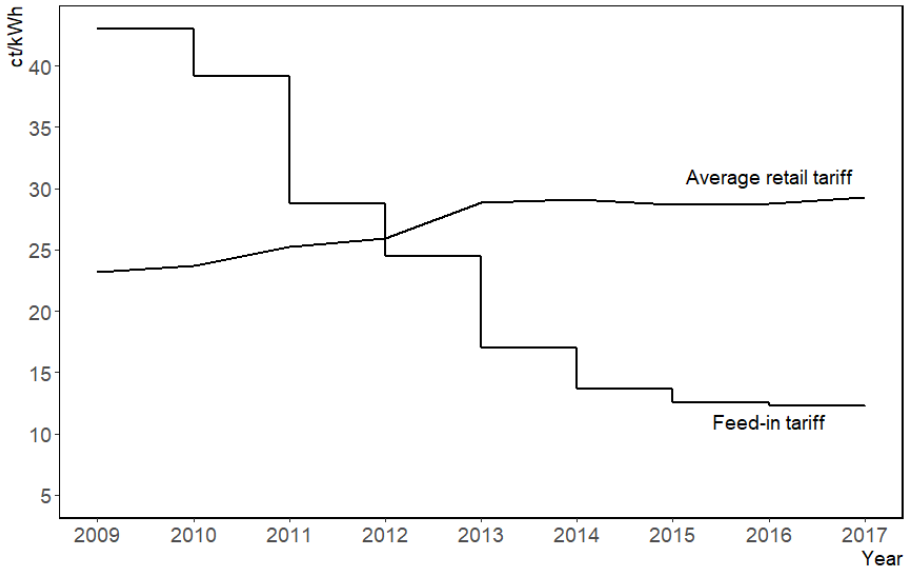

Figure 3.1: The development of feed-in tariffs for PV installations < 10 kW and average retail tariffs for households in Germany between 2009 and 2017. Own illustration based on data from Bundesnetzagentur (2021a) and BDEW (2021).

3.3.2 Retail electricity tariffs and the incentive for self-consumption

The value of self-consumption depends on the consumption costs that can be reduced for each kWh of grid consumption substituted with self-generated PV electricity. PV owners can profit from self-consumption because the household's electricity bill in Germany mainly depends on the actual consumption. The retail tariff for grid consumption is nonlinear and consists of a volumetric and a fixed price component, i.e., it constitutes a two-part tariff.

The volumetric price per kWh typically predominates, whereas the fixed component, i.e., the basic price for being served and connected to the network, accounts for a smaller proportion of total retail costs. Furthermore, the retail tariff in Germany comprises of three elements: procurement and sales costs of the retailing firm, network tariffs, and administratively determined taxes, charges, and levies. The latter include, for example, the tax on electricity, the EEG-levy, and the concession fee. In 2017, for instance, these three elements split up into 19 % procurement and sales costs, 26 % network tariffs, and 55 % taxes, charges, and levies (BDEW, 2021). Households do not have to pay the volumetric parts of the network tariff and all taxes, charges, and levies for self-consumption.[27] Following the theory on nonlinear pricing, the fixed price component of the retail tariff should not affect the economic rationale to invest in PV installations. These

[27] Though there were changes regarding the EEG-levy for self-consumption in 2012, residential PV installations with 10 kW or less have always been exempted.

costs always have to be paid unless the household becomes fully independent and, thus, disconnected from the grid. The volumetric tariff describes the opportunity to purchase electricity from the grid and thus, represents the value of self-consumption.

Furthermore, and in contrast to the feed-in tariff that applies equally for all households across Germany, retail prices vary regionally. While wholesale market prices and taxes, charges, and levies are the same across Germany, the network tariff is the only cost component that systematically differs on a regional level.[28] In particular for residential consumers connected to the low-voltage network, network tariffs are increasingly diverging.[29] The regional variation of distribution network tariffs in Germany is due to the allocation mechanism, a so-called vertical mechanism, by which network operators allocate the network costs to network users (c.f. Jeddi & Sitzmann, 2019). In Germany, the network costs are refinanced by electricity consumers. The allocation is based on the principle that costs incurred in a particular network area are borne by consumers connected to the respective network. Network operators calculate the network tariffs on an annual basis, based on their individual, regulated revenue cap. In practice, this regulatory procedure means that network costs of the current year are decoupled from this year's network tariffs and rather passed on to the network tariffs in later years.

3.3.3 The economic rationale for investments in PV installations

The profitability of a PV investment hinges on the the value of self-consumption, the feed-in tariff and the interaction of both options. On the one hand, substituting electricity from the grid reduces electricity costs. On the other hand, each kWh used for self-consumption cannot be fed into the grid, i.e., the PV owner does not receive the feed-in tariff. Therefore, it is not only the absolute level of prices and tariffs compared to the PV installation costs that is decisive, but also the relation of the feed-in tariff to the retail electricity price. We apply the regulatory setting in Germany to Equation (3.2). The expected revenue consists of the subsidization of grid feed-in via feed-in tariffs (p^{fit}), self-consumption via a reduction of electricity consumption costs valued at the volumetric tariff (p^{retail}), plus, if applicable, the additional subsidy for self-consumption (p^{self}):

$$NPV = -C_I + \sum_{t=0}^{T} \frac{q_{togrid} \cdot p^{fit} - [(d_{total} - q_{self}) \cdot p^{retail} + q_{self} \cdot p^{self} - c_{OM}]}{(1+r)^t} \quad (3.3)$$

Equation (3.3) shows that as soon as the volumetric retail tariff (p^{retail}) rises above the feed-in tariff (p^{fit}), self-consumption becomes financially more profitable compared to grid feed-in.

[28] The concession fee can also vary depending on the network area. However, the magnitude is legally fixed, so that the differences are minor compared to the variation in network tariffs.
[29] See e.g. Hinz et al. (2018) and Schlesewsky and Winter (2018) for further investigations.

The feed-in tariff has been continuously decreasing to accommodate the declining costs of PV installations and technological developments. Contrarily, the average retail tariff across Germany has been increasing in most years. Both developments are depicted in Figure 3.1 for the period between 2009 and 2017. Since 2012, the average retail tariff is higher than the feed-in tariff by a constantly increasing margin. Therefore, we expect the investment incentives for residential PV adoption to be increasingly affected by the incentive for self-consumption rather than the feed-in tariff. If this holds, the impact of price signals should have become more relevant since 2012. The abolition of the explicit subsidy for self-consumption in 2012 should have further strengthened the influence of the implicit incentive of the retail tariff.

However, one should keep in mind that self-consumption is attractive only if the household can use the electricity when the sun shines or if a storage opportunity exists. Installation numbers of batteries in households only recently begin to increase as storage is still relatively costly (Figgener et al., 2021). If storage opportunities become economically attractive, the incentive for self-consumption might increase in the upcoming years. Thus, it could become interesting to distinguish between PV systems with and without battery storage.[30]

In principle, the economic incentives of PV adoption apply equally to all households. The feed-in tariff does not vary regionally across Germany, and thus, all else equal, it should have a similar impact on the investment decision. In contrast, network tariffs of the distribution grid vary throughout Germany and over time. Therefore, the implicit investment incentive from self-consumption can differ between regions. As summarized in Section 3.3.2, network tariffs are the only price component, which varies substantially between regions, and, therefore, are the main driver for regional retail price variation in Germany. Our empirical strategy takes advantage of this heterogeneity to investigate the impact of price signals on PV investments in Germany.

3.4 Empirical strategy

Our objective is to identify whether network tariffs influence investments in PV installations. Therefore, we set up our analysis on postcode-specific panel data for Germany and exploit the regional variance of network tariffs across Germany. Our dependent variable, the number of new PV installations ($Y_{i,t}$) per postcode (i) and year (t), is a count variable, i.e., it follows a non-negative distribution and can only take on integer values. Given the characteristic of the dependent variable and the panel data structure, we employ a Poisson quasi-maximum likelihood estimator with multiple fixed effects (PQMLE) (c.f. Wooldridge, 2010). The

[30] Due to the low number of installed batteries and data availability, we refrain from including batteries in this analysis. Predictive simulations for the development of combined PV and storage systems in Germany can be found, for example, in Kaschub et al. (2016), Fett et al. (2021) and Günther et al. (2021).

consistency of the estimator neither requires that our dependent variable follows a Poisson distribution nor any additional assumptions concerning the distribution of our dependent variable. As part of the estimation procedure, we calculate robust standard errors. By clustering the standard errors at a regional level, we accommodate for arbitrary correlation across clusters. The choice of the PQMLE approach as our preferred estimation method is in line with recent research by Gautier and Jacqmin (2020) and de Freitas (2020), who apply it in a similar setting.

The formulation of our preferred estimation model is as follows:

$$Y_{i,t} = exp(\beta \cdot \mathit{tariff}_{i,t-1} + \gamma \cdot X_{i,t} + \phi_t + \mu_i + \theta_i \cdot t) \cdot \epsilon_{i,t} \tag{3.4}$$

where $\mathit{tariff}_{i,t-1}$ is our primary explanatory variable, $X_{i,t}$ is a vector of postcode-specific covariates, ϕ_t are year-specific fixed effects, μ_i are postcode-specific fixed effects and θ_i are postcode-specific time trends. $\epsilon_{i,t}$ is an error term.

In our preferred model specification, we lag our primary explanatory variable by one year. Although fully rational households should form an expectation about future electricity costs, in practice, it may be reasonable to assume that households are rather short-sighted and base their expectation on the currently observed electricity costs (c.f. de Groote & Verboven, 2019; Ito, 2014). In Germany, households pay their electricity bill annually and ex-post, which results in a time lag of one year between the temporal validity of the network tariff and the cost realization. In addition, some time passes between the investment decision and the actual PV installation, e.g., due to administrative reasons. Therefore, we assume that households are more likely to respond to the previous year's tariff than the current one and use the network tariff lagged by one year as our explanatory variable.[31] We check the robustness of our assumption against the current network tariff $\mathit{tariff}_{i,t}$ in Section 3.6 and for tariffs further in the past, i.e., $\mathit{tariff}_{i,t-2}$ and $\mathit{tariff}_{i,t-3}$, in Appendix 3.8.2.

An advantageous effect of using the time lag is that it helps us to alleviate the strict exogeneity assumption of our primary explanatory variable. The endogeneity concerns arise because, in recent years, network tariffs increase mainly due to network expansion costs which in turn are due to the integration of renewable energy sources, including residential PV installations (c.f. Just & Wetzel, 2020). However, PV adoption in the current year does not affect the network tariffs of the previous year. Therefore, based on our choice of lagged network tariffs as our explanatory variable and because network tariffs reflect historical network costs, we suggest that reverse causality is not a concern in our setting.

[31] Our assumption is supported, for example, by an empirical analysis regarding electricity consumption behavior by Bushnell and Mansur (2005), who find that households respond more strongly to recent past electricity bills than to new retail tariff price information, even when the new tariff has already been announced. Also, Gautier and Jacqmin (2020) find the assumption of using a lagged network tariff to be justified in their analysis on the effect of network tariffs on PV installations under a net metering scheme in Wallonia.

We further include a vector of covariates to control for observable heterogeneity of postcode areas. This vector contains the average income and age of the population, the share of detached and semi-detached houses in the building stock, and the number of residential buildings.

The fixed effects approach takes advantage of the panel data structure of our data and allows us to control for unobserved heterogeneity. By applying multiple fixed effects, we can isolate and identify the impact of our primary explanatory variable on the dependent variable based on the within-postcode variance in our data. A random effects model would not be consistent as we expect a correlation between the individual effects and the independent variables.[32] By including year-specific fixed effects, we control for overall developments over time. Examples are declining prices for solar modules, overall trends in electricity demand[33] or national policy changes, in particular changes in feed-in tariffs. Another aspect covered by these effects is the development of retail price components that do not vary across Germany, such as the EEG-levy or wholesale electricity prices. Postcode-specific fixed effects account for factors that regionally differ between postcode areas but are constant over time, e.g., socioeconomic aspects and solar irradiance.[34] Postcode-specific time trends control for any linear postcode-specific development over time that is not addressed by the nationwide year-specific fixed effects. Examples of such trends include local demographic change or local economic growth.

In addition to the PQMLE, other commonly used models in count data applications are, for example, negative binomial regression models or OLS models with a logarithmized dependent variable. We include these models as robustness checks for our main findings.

To analyze the effect of the nonlinear pricing schedule, we apply the encompassing approach by Davidson and MacKinnon (1993), which can be used to identify a preferable model specification for non-nested models. We specify the encompassing model as an augmented model of (3.4) and include both alternative explanatory variables, i.e., the volumetric tariff ($tariff_{i,t-1}$) and the average tariff ($\varnothing\text{-}tariff_{i,t-1}$):

$$Y_{i,t} = exp(\beta \cdot tariff_{i,t-1} + \delta \cdot \varnothing\text{-}tariff_{i,t-1} + \gamma \cdot X_{i,t} + \phi_t + \mu_i + \theta_i \cdot t) \cdot \epsilon_{i,t} \tag{3.5}$$

[32] A Hausman test rejects the null hypothesis that there is no significant correlation at the significance level of 1 %, which supports the choice of a fixed effects approach.

[33] In Germany, the overall electricity demand has decreased over the past years, which is covered by the year-specific fixed effects. If spatial heterogeneity in demand exists, this is covered by the postcode-specific fixed effects. We do not expect substantial variation in both dimensions, as we see no indication that energy efficiency gains should vary significantly across regions over time.

[34] Generally, solar irradiance is a decisive variable influencing residential PV investments. However, we assume that households do not account for the (relatively small) solar irradiance variation over time. Instead, we expect that households consider it as a spatial component, such as whether one lives in a generally sunnier region. Therefore, we do not include solar irradiance as a covariate in our model, as it is reflected in the postcode-specific fixed effects.

We want to test our hypothesis that the volumetric tariff impacts PV investments rather than the average tariff. Hence, we expect that as long as the model accounts for the volumetric tariff, the coefficient of the average tariff δ is statistically insignificant, i.e., not influencing the number of PV installations, and we can check this hypothesis with a standard F-test (c.f. Greene, 2003).

3.5 Data

For our analysis, we use a unique panel data set at the German postcode level. The panel data set covers 8,148 postcodes (PLZ) for 2009-2017, a total of 73,329 observations. For our dependent variable we rely on data from the Marktstammdatenregister (MaStR) (Bundesnetzagentur, 2021b). For each unit, the MaStR documents the energy carrier, the installed capacity, the postcode, the installation date, and various additional information. In this paper, we focus on PV installations with a size up to 10 kW as this is the typical size installed on residential buildings. Our data consists of 708,555 PV installations commissioned between 2009 and 2017. By aggregating the number of new PV installations per year and postcode, we receive our dependent variable (*# of PV*).

Furthermore, we use detailed data on annual network tariffs on postcode level from ene't, a German data provider for the electricity industry (ene't, 2021). The data contains information on the annual fixed component of network tariffs (*fixed_tariff*, in Euro/year) and the volumetric component (*tariff*, in ct/kWh). For our investigation of price perception, we use both components to calculate an average tariff (*∅-tariff* in ct/kWh) by assuming a reference load profile of 3,500 kWh annual consumption. Figure 3.2 illustrates the regional distribution of the volumetric network tariff and the number of PV installations per 1000 residential buildings for the year 2017. The maps show regional heterogeneity for both variables. The volumetric tariffs are highest in north-east and south-west Germany, driven by the high wind penetration, especially in the north. PV installations per 1000 buildings concentrate in the southern regions, which is in line with the general expectations, as these regions show the highest solar irradiance. Note that the fixed effects of our estimation approach capture this persistent difference between regions. The spatial heterogeneity of the variables differs over time, shown in further illustrations of the temporal variation of our data in Appendix 3.8.1.

To analyze whether network tariffs had a greater impact on the number of PV installations after 2012, we define two binary dummy variables: One that takes on the value 1 for all years before 2012 ($d_{<2012}$), and one that takes on the value 1 otherwise ($d_{\geq 2012}$).

We further control for the heterogeneity of postcode areas by including socioeconomic drivers of PV expansion that have been identified in the literature described in Section 3.2. We use yearly and postcode-specific data for these socioeconomic

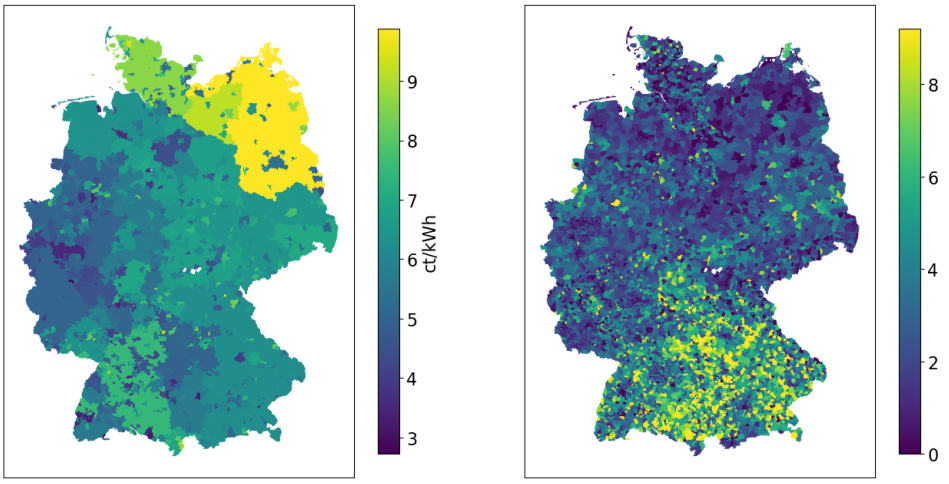

(i) (ii)

Figure 3.2: Regional resolution of (i) the volumetric network tariff and (ii) # of PV per 1000 residential buildings, both for the year 2017.

Table 3.1: Descriptive statistics, 2009-2017 (N = 73,329)

Variable	Mean	Median	SD	Min	Max	Source
Dependent variable						
# of PV	9.66	6	11.57	0	184	MaStR
Independent variables						
tariff (ct/kWh)	5.29	5.08	1.04	2.38	9.90	ene't
fixed_tariff (Euro/year)	21.56	18.00	17.72	0	95.00	ene't
∅-tariff (ct/kWh)	5.90	5.65	1.24	2.67	11.55	ene't
income (log of)	9.95	9.95	0.19	9.30	11.01	RWI
housetype (% of 1- and 2-family homes)	58.32	63.64	20.69	0.30	100	RWI
age	43.74	43.58	2.35	35.11	58.48	RWI
buildings (log of)	7.40	7.46	0.92	0.69	9.80	RWI

covariates from RWI-GEO-GRID, a data set from the Leibniz Institute for Economic Research (RWI) (RWI & Microm, 2020). First, we consider the average purchasing power of households per capita (*income*, in Euro/year). We expect a positive impact of the purchasing power of households on PV expansion as the investment costs of the installation are more likely to be afforded by more affluent people. The variable *age* denotes the average age of inhabitants in a specific postcode area. One would assume that a younger population is more aware of

the possibility to invest in PV, thus leading to a negative influence of average age on our dependent variable. For the number of residential buildings (*buildings*), which is closely correlated with the number of inhabitants, we would expect a positive effect on our dependent variable as more buildings in a postcode mean more opportunities for PV investments. Further, we include the share of detached and semi-detached houses in the building stock (*housetype*, in %). Detached and semi-detached houses are well suited for residential PV installations, for example, due to the unity of electricity consumer and investor. Therefore, we would expect a positive impact of the housetype on our dependent variable. Another factor that could have an influence on PV investments but is not included in our analysis is environmental awareness. Election results, i.e. the proportion of green voters, are usually taken into account as a measure of environmental awareness. There is no continuous annual data for this, so the approach conflicts with the panel-based fixed-effects approach of our model. Moreover, the existing literature shows that environmental awareness has little to no effect on PV investment (see Section 3.2).

3.6 Results

We estimate the impact of network tariffs on residential PV installations in Germany within our preferred model specification, described in Section 3.4. Further, we analyze whether the incentives for self-consumption have become more relevant in recent years compared to the early years of PV adoption and how the nonlinear pricing schedule affects PV adoption. Using additional model specifications, we also check the robustness of our results.

We present our main results regarding the impact of network tariffs on PV adoption in Table 3.2. Regression (1) shows our preferred model specification (c.f. Equation 3.4), which estimates the impact of lagged network tariffs on the number of new PV installations, controlling for socioeconomic covariates. Our estimation suggests that network tariffs have a positive and significant impact on the number of PV installations. All else equal, an increase of one within standard deviation (0.34 eurocent per kWh) in network tariffs is estimated to increase the number of PV installations by 2 %.[35] The magnitude of this effect is in line with the findings of Gautier and Jacqmin (2020) for PV investments in Wallonia. The results further confirm the findings of Frondel et al. (2019), who show that households in Germany are aware of yearly price variations and change their electricity consumption respectively. Furthermore, the impact of the other covariates in our model is not statistically different from zero. The fixed effects

[35] Within standard deviation refers to the variation of the network tariffs that is not accounted for by the applied fixed effects. The model results show an increase by 5.8 % for one cent per kWh increase in network tariffs. However, we cannot make reliable statements about the effect of a shift of that magnitude, because the within standard deviation of network tariffs in the model is significantly lower than one cent per kWh. We include a more detailed discussion in Appendix 3.8.3.

absorb their impact due to their relatively low within-variance, which is depicted in Appendix 3.8.3.

Table 3.2: Main results

Model:	(1)	(2)	(3)	(4)
Dependent Variable:	# of PV	# of PV	# of PV	# of PV
tariff_{t-1}	0.0578***			0.0914***
	(0.0061)			(0.0208)
$\text{d}_{<2012} \times \text{tariff}_{t-1}$		0.0112		
		(0.0083)		
$\text{d}_{\geq 2012} \times \text{tariff}_{t-1}$		0.0707***		
		(0.0064)		
$\varnothing\text{-tariff}_{t-1}$			0.0577***	-0.0386*
			(0.0066)	(0.0224)
income (log of)	-0.0334	0.0230	-0.0374	-0.0332
	(0.1497)	(0.1488)	(0.1502)	(0.1495)
housetype	0.0041	0.0050	0.0037	0.0042
	(0.0042)	(0.0042)	(0.0042)	(0.0042)
age	0.0168	0.0184	0.0160	0.0171
	(0.0136)	(0.0136)	(0.0137)	(0.0136)
buildings (log of)	-0.1225	-0.1363	-0.0988	-0.1287
	(0.1688)	(0.1688)	(0.1687)	(0.1689)
Fit statistics				
observations	64,531	64,531	64,531	64,531
AIC	330,230	330,094	330,271	330,225
BIC	476,772	476,644	476,812	476,776
Log-Likelihood	-148,967	-148,898	-148,987	-148,963

Robust standard errors clustered at the postcode level.
*Signif. Codes: ***: 0.01, **: 0.05, *: 0.1*

We further examine whether the incentives for self-consumption have become more relevant in recent years compared to the early years of PV adoption. Therefore, we analyze how the change in the economics of PV investments from 2012 onward has affected the impact of network tariffs on PV installations in Germany (c.f. Section 3.3). We include an interaction term between our binary dummy variables ($d_{<2012}$ and $d_{\geq 2012}$) and the network tariff in regression (2). This estimation allows us to compare the effect of network tariffs before and after 2012. The results suggest that network tariffs did not significantly impact PV adoption before 2012, while they do afterward. We estimate that, since 2012, an increase in network tariffs of one standard deviation (0.34 eurocent per kWh) increases PV installations by 2.4 %. A Chow test confirms the difference between the estimates

of the two time-subsets, revealing significance at the 1 % level. Hence, we can confirm our hypothesis that self-consumption has gained importance since 2012 when rising retail tariffs started to exceed declining feed-in tariffs.

We further examine how the different price components of nonlinear tariffs impact PV installations. We make use of the volumetric and the fixed component of network tariffs and test the theoretical expectation that PV adoption should only be affected by the volumetric tariffs. In a first step, we estimate the impact of average instead of the volumetric tariffs in regression (3). This estimation yields similar results compared to our preferred model specification with the volumetric tariffs in regression (1). In a second step, we jointly test the two alternatives in the encompassing model (c.f. Equation 3.5). In regression (4), we include both the volumetric ($tariff_{t-1}$) and the average tariff ($\varnothing$-$tariff_{t-1}$). The coefficient of the volumetric tariff is still positive and statistically significant, while the average tariff does not have a statistically significant impact on the number of PV installations. Thus, the encompassing test confirms the theoretical expectation that volumetric tariffs drive PV investments. The results indicate that consumers differentiate between the price components of the two-part tariff, which contributes to the empirical evidence on consumers' perception of nonlinear pricing. Consumers may understand the taxonomy of the two-part tariff and base their investment decision on the volumetric rather than an average tariff. However, given the aggregate nature of our data, this finding should be complemented by further analysis of microeconomic data.

In Table 3.3, we provide several robustness checks regarding our model specification and our estimation strategy. In regression (5), we check our assumption that PV adoption is impacted by the lagged network tariff rather than the contemporary one by using the contemporary tariff ($tariff_t$) as our explanatory variable instead of the lagged network tariff ($tariff_{t-1}$). The results indicate a positive effect of the current network tariff on PV adoption. However, the coefficient is smaller compared to the impact of the lagged network tariff in regression (1). Moreover, in regression (5), the values of the two information criteria, AIC and BIC, increase while the value of the log-likelihood decreases compared to regression (1), implying that the explanatory power of our preferred model specification is higher. This finding supports our assumption that households respond to their electricity bill rather than current tariffs and, thus, may have a rather short-sighted perception of prices.[36]

We aggregate our data to the next higher regional level (NUTS-3) in regression (6) to check whether our results remain valid at a higher regional aggregation. The estimation suggests that, even under a higher regional aggregation, network tariffs positively and significantly impact PV investments, supporting the results derived from postcode-level data.[37] In regression (7), we estimate our preferred model specification without the postcode-specific time trends. We observe that

[36] An additional robustness check on tariffs further in the past can be found in Appendix 3.8.2.

[37] In Appendix 3.8.2 we further analyze whether the impact of network tariffs may differ between regions and include a regression on state-specific effects of network tariffs on PV investments.

Table 3.3: Robustness checks

Model:	(5)	(6)	(7)	(8)	(9)	(10)
Dependent:	# of PV	# of PV	# of PV	log(# of	# of PV	# of PV
Variable:				PV+1)		>300 kW
tariff_t	0.0351***					
	(0.0056)					
tariff_{t-1}		0.0725***	0.0540***	0.0478***	0.0550***	-0.0468
		(0.0153)	(0.0047)	(0.0056)	(0.0045)	(0.0520)
income (log of)	-0.1770	-1.320**	0.6786***	-0.0810	0.7198***	0.6676
	(0.1468)	(0.5806)	(0.1241)	(0.1462)	(0.1140)	(1.2350)
housetype	0.0152***	0.0286**	0.0017	0.0051	0.0027	-0.0690*
	(0.0038)	(0.0144)	(0.0030)	(0.0036)	(0.0028)	(0.0342)
age	-0.0043	0.0547	-0.0997***	0.0153	-0.1025***	0.2476*
	(0.0131)	(0.0571)	(0.0076)	(0.0116)	(0.0070)	(0.1202)
buildings	-0.1371	-0.5982	0.1874	0.0796	0.2362*	-0.8075
(log of)	(0.1543)	(0.5511)	(0.1379)	(0.1386)	(0.1285)	(1.3720)
Fixed effects						
PLZ	Yes+slope		Yes	Yes+slope	Yes	Yes+slope
year	Yes	Yes	Yes	Yes	Yes	Yes
NUTS-3		Yes+slope				
Distribution	PQMLE	PQMLE	PQMLE	OLS	Neg.Bin.	PQMLE
Fit statistics						
observations	72,672	3,192	64,531	65,179	64,531	27,595
AIC	375,142	32,949	338,674	91,389	330,167	42,126
BIC	523,758	37,864	411,999	239,563	403,492	98,980
Log-Likelihood	-171,406	-15,664	-161,257	-29,384	-157,003	-14,151

Robust standard errors clustered at the regional level.
*Signif. Codes: ***: 0.01, **: 0.05, *: 0.1*

the positive and significant impact of network tariffs persists. Further, as expected, income has a significantly positive and age a significantly negative impact on the number of new PV installations. Hence, in our preferred model specification, the postcode-specific time trends do indeed capture the assumed postcode-specific demographic change and local economic growth.

To further check the robustness of our results, we apply alternative estimation strategies to determine the impact of network tariffs on the number of PV installations. First, regression (8) assumes a linear relationship, using an OLS regression. To accommodate for the non-negative nature of our count data, we take the log of the dependent variable to which we add one unit due to the presence of

zero outcomes. Second, we estimate a negative binomial regression (9). Negative binomial regressions make stronger assumptions regarding the distribution of the dependent variable, which do not fully hold for our data. However, the results can provide a robustness check. Overall, both results confirm the finding of our preferred model specification, that higher network tariffs lead to more PV installations.

Finally, we perform another robustness check of our hypothesis by replacing the dependent variable with a sample of PV systems that should not be affected by network tariffs. Regression (10) shows the results of such a placebo test. The dependent variable is defined as the number of PV installations larger than 300 kW. PV systems with this size can be assumed to be commercial systems, i.e., installed on non-residential buildings or ground-mounted. Although non-residential network users are also required to pay network tariffs, self-consumption should generally not be the driving factor for PV investments in these cases. Rather, investment decisions should be motivated by potential revenues from the sale of electricity. Therefore, we expect network tariffs not to affect investment decisions for PV installations larger than 300 kW. The regression results confirm this hypothesis, as they do not show a significant impact of network tariffs on PV installations larger than 300 kW.

3.7 Conclusion

Within a net purchasing system, investment incentives for residential PV arise from feed-in tariffs and the value of self-consumption. With the latter becoming the dominant economic driver, network tariffs, which constitute a substantial part of the consumption costs, are expected to gain importance. By exploiting the regional heterogeneity of network tariffs, we investigate whether network tariffs encourage to invest in PV systems using a unique panel data set at the German postcode level over the period 2009-2017. We further evaluate how the nonlinear tariff structure impacts residential PV adoption.

We use a Poisson quasi-maximum likelihood estimator with conditional fixed effects and provide additional robustness checks for various distributional assumptions and the regional aggregation level. All else equal, an increase in network tariffs by one standard deviation (0.34 eurocent per kWh) is estimated to increase PV installations by 2 %. Thus, our results indicate that network tariffs impact PV adoption across Germany. We find evidence that the impact of network tariffs has increased over time, supporting our expectation that the economic incentives for self-consumption have become more important in recent years. Furthermore, our analysis of the different price components indicates that the volumetric network tariff drives PV adoption rather than the average price.

For policymakers, our results provide essential insights for upcoming reforms of electricity price components. Our results suggest that households do react to

price signals and that prices effectively guide investments. The current incentive for self-consumption is a side effect of the retail tariff design in Germany. Due to taxes, levies and the network tariff design, retail tariffs contain various price components that are not necessarily aligned and, thus, may distort the investment decision of the household in a way that is economically inefficient. If the retail tariff is higher than economically efficient, the incentives for PV investments are distorted. For instance, a feedback effect, as discussed in Jägemann et al. (2013), arises when rising retail tariffs lead to rising residential PV expansion and rising PV expansion, in turn, leads to increasing retail tariffs. Therefore, from an economic point of view, it is essential to create price signals in the least distorting way. In Germany, reform proposals are currently considered for the network tariff system and include a shift from predominantly volumetric network tariffs to a more substantial fixed network tariff. Other proposals aim for a change in the EEG-levy that is currently paid exclusively on a volumetric basis. Consequently, these reforms influence not only household consumption behavior but also investment incentives for PV installations.

The regional variation of price signals may explain at least part of the present heterogeneity of PV installations in Germany. However, as we use fixed effects to control for unobserved heterogeneity between regions, our analysis is limited in this regard. Further analyses could examine the impact of economic factors on the regional heterogeneity across Germany in more detail. Furthermore, declining costs for storage technologies, such as batteries, will further strengthen the case for self-consumption in the residential sector. Therefore, future empirical research could investigate the incentives that drive households to invest in combined PV and storage systems. In a similar vein and in the light of currently increasing adoption rates of electric vehicles and electric heating systems in the residential sector, future empirical analyses could shed light on the impact of price signals on these technologies. Finally, our analysis focuses on the influence of price signals on the initial decision to invest in a PV installation. Another promising field would be to supplement our results with empirical studies on consumption profiles to provide insights into the short-term price sensitivity of households with PV installations.

3.8 Appendix

3.8.1 Further data statistics

Figure 3.3 illustrates the variation of the volumetric network tariffs, the fixed network tariff and the number of PV installations between the years 2009 and 2017.

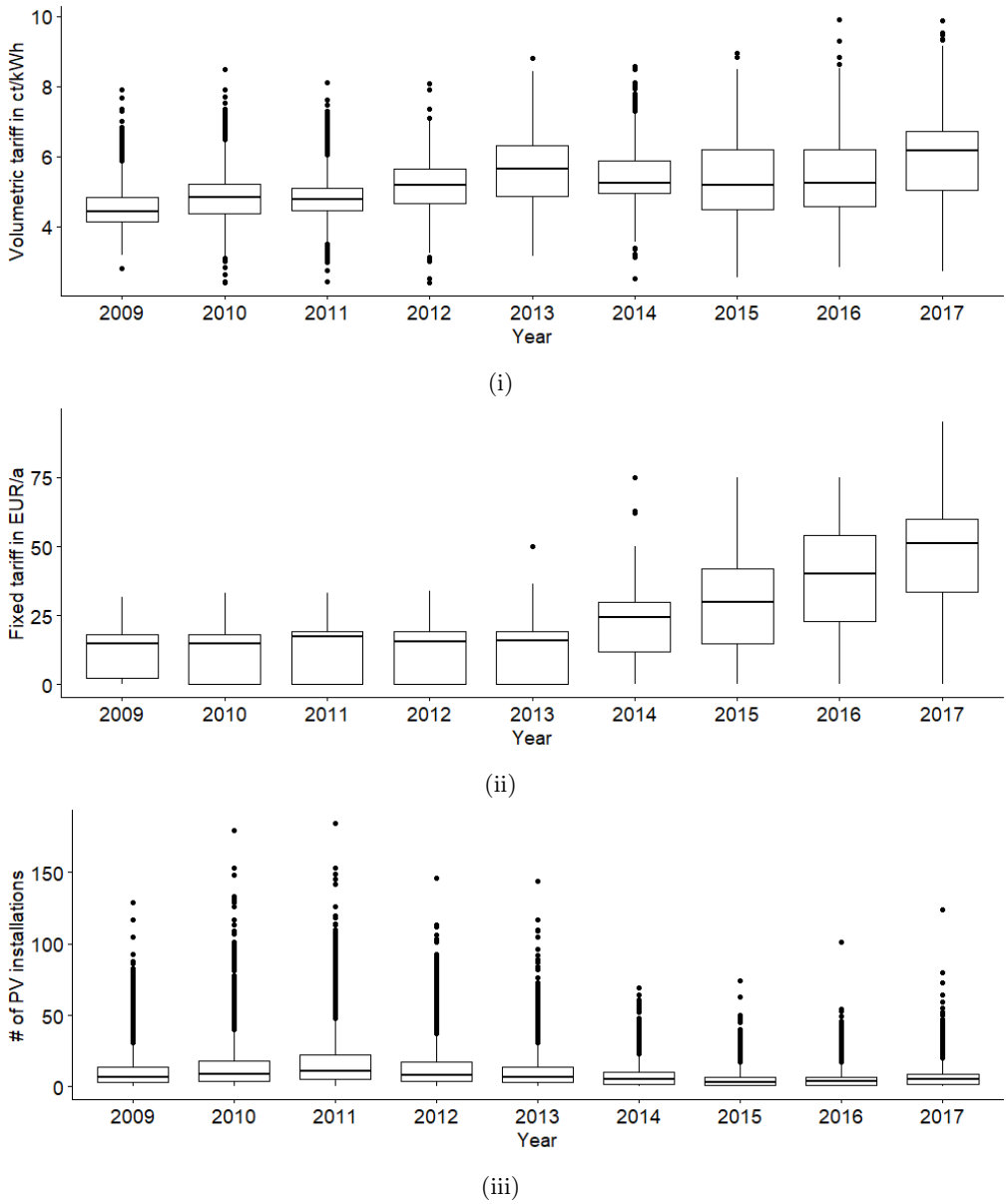

Figure 3.3: Temporal variation of (a) the volumetric network tariffs, (b) the fixed network tariff, and (c) the number of PV installations

As shown in Figure 3.3 (a) and (b) network tariffs have risen steadily over the period under consideration. In particular, the median fixed tariff more than doubled between 2009 and 2017. In addition, one can see that for both the volumetric and fixed tariff the regional dispersion in the 25th to 75th percentile across postcode areas has increased substantially, while the regional dispersion of the number of PV installations has tended to decrease (see Figure 3.3 (c)).

3.8.2 Further robustness checks

With the following robustness checks in Table 3.4, we additionally check our assumption that households respond to the previous years' tariffs, i.e., $tariff_{i,t-1}$, by including tariffs further in the past. We test a regression with $tariff_{i,t-2}$ and one alternative with $tariff_{i,t-3}$ instead of $tariff_{i,t-1}$.

Table 3.4: Further robustness checks: time lags

Model:	(11)	(12)	(13)
Dependent Variable:	# of PV	# of PV	# of PV
tariff_{t-1}			0.0231**
			(0.0086)
tariff_{t-2}	0.0245***		-0.0107
	(0.0071)		(0.0091)
tariff_{t-3}		-0.0050	-0.0031
	(0.0081)	(0.0082)	
income (log of)	-0.1004	-0.4194	-0.4253
	(0.2140)	(0.3182)	(0.3184)
housetype	-0.0014	0.0034	0.0038
	(0.0047)	(0.0054)	(0.0054)
age	0.0366*	0.0331	0.0336*
	(0.0155)	(0.0170)	(0.0171)
buildings (log of)	-0.0403	0.01267	0.1075
	(0.1839)	(0.2178)	(0.2186)
Fit statistics			
observations	56,269	48,084	48,083
AIC	282,959.3	235,622.8	235,605.7
BIC	426,858.3	376,482.9	376,483
Log-Likelihood	-125,380.6	-101,769.4	-101,758.9

Robust standard errors clustered at the postcode level.
*Signif. Codes: ***: 0.01, **: 0.05, *: 0.1*

The results show that the impact of the lagged network tariffs $tariff_{i,t-2}$ and $tariff_{i,t-3}$ decreases compared to the impact of $tariff_{i,t-1}$. An encompassing test

further supports this finding. The coefficient of $tariff_{i,t-1}$ is the only significant variable, at least at a 5 percent level, compared to $tariff_{i,t-2}$ and $tariff_{i,t-3}$. Hence, the results further support our assumption.

Table 3.5: Further robustness check: regional results

Model:	(14)
Dependent Variable:	# of PV
BW × tariff_{t-1}	0.1652*** (0.0197)
BY × tariff_{t-1}	0.0290*** (0.0085)
BE × tariff_{t-1}	-0.1352 (0.0929)
BB × tariff_{t-1}	0.0559* (0.0232)
HB × tariff_{t-1}	0.2740** (0.0872)
HH × tariff_{t-1}	0.0659 (0.1405)
HE × tariff_{t-1}	-0.0058 (0.0238)
MV × tariff_{t-1}	0.0869* (0.0368)
NI × tariff_{t-1}	0.0607** (0.0192)
NW × tariff_{t-1}	0.0570** (0.0198)
RP × tariff_{t-1}	-0.0678** (0.0255)
SL × tariff_{t-1}	-0.0508 (0.0624)
SN × tariff_{t-1}	0.1360*** (0.0257)
ST × tariff_{t-1}	0.0678* (0.0300)
SH × tariff_{t-1}	0.1550*** (0.0309)
TH × tariff_{t-1}	0.2682*** (0.0432)
income (log of)	-0.0273 (0.1487)
housetype	0.0044 (0.0043)
age	0.0158 (0.0136)
buildings (log of)	-0.1350 (0.1685)
Fit statistics	
observations	64,531
AIC	329,958
BIC	476,636
Log-Likelihood	-148,816

Robust standard errors clustered at the postcode level.
*Signif. Codes: ***: 0.01, **: 0.05, *: 0.1*

In another model variation (14, Table 3.5), we include an interaction term between binary dummy variables for the 16 German states and the network tariff. This estimation allows us to compare the regional effect of network tariffs on PV investments. The model specification is based on the assumption that while the effect of the network tariffs differs between states, the effects of the covariates and time-specific fixed effects do not. The results suggest that network tariffs significantly impact PV investments in a selection of states (BW, BY, SN, SH,

TH), with the highest effect being in HB and the lowest in BY. An explanation for the different sizes of the effect could be differences in awareness for PV investments in different states. A reason why we cannot identify a significant effect for most states could be the low within-variance of network tariffs in the respective state. Because of the low within-variance of the state-specific tariffs and because the results depend on the assumptions made about the effects of the covariates and the annual fixed effects, the results should be treated with caution. Therefore, we interpret the results as indicative of the existence of regional differences in the effect of network tariffs on PV investments. However, a detailed analysis of these differences is outside the scope of this paper and remains subject to future research.

3.8.3 Within-variance of the covariates in our sample

Using a fixed effects approach, we exploit the within-region variation of our explanatory variables to identify their impact on our dependent variable. By including time fixed effects, we control for overall developments over time. While this allows us to isolate the effects under investigation, i.e., the effect of network tariffs on PV investments, it prevents us from making statements about the influence of covariates that have little or no within-region variation after controlling for time fixed effects. By regressing the explanatory variables on our fixed effects, we calculate the variation in these variables used to estimate the coefficients in our fixed effects model. The standard deviations of these residuals, calculated for the preferred specification of our model (1) and the specification without the postcode-specific slope (7), are shown in Table 3.6. The given values may aid in interpreting and classifying the estimated treatment effects of the explanatory variables. For a detailed analysis on the interpretation of fixed effects, refer to Mummolo and Peterson (2018).

Table 3.6: Within standard deviation

Model:	(1)	(7)
tariff_{t-1} (ct/kWh)	0.34	0.49
income (log of)	0.02	0.03
housetype (%)	0.63	0.96
age	0.18	0.43
buildings (log of)	0.02	0.02

4 On the functional form of short-term electricity demand response - insights from high-price years in Germany

4.1 Introduction

In traditional, centralized power systems, demand is matched by supply from conventional and dispatchable electricity generation units. In this system, the potential of demand reacting flexibly to prices at short notice has played a subordinate role. With the increase in intermittent generation and the declining capacity of dispatchable power plants, understanding the short-term own-price elasticity of electricity demand becomes increasingly important in understanding market realities. Demand response becomes more relevant in the high-frequency matching of supply and demand as supply from intermittent generating units fluctuates.

Obtaining accurate estimates of short-term own-price elasticities of electricity demand is, therefore, important in planning the future electricity system. Assumptions on how electricity demand reacts to prices in peak load situations influence the extent of future capacity needs. Assumed short-term elasticities thus influence the design of capacity mechanisms such as capacity markets or payments.

In addition, reliable information about the demand response in the electricity market can improve operational decisions, e.g. in grid operation or the dispatch of generation units.

Both in the case of medium and long-term planning decisions and the case of short-term operational decisions, elasticity information is incorporated into quantitative models. Various models, e.g. electricity market models, price forecast models, infrastructure models or general-equilibrium models, exist in academia and the industry that inform policy and business decisions. All these models require precise information on price elasticities.

The level of short-run own-price elasticities of electricity demand[38] is of particular interest in high-price situations. In the last two years, prices in Germany have been drastically higher and more volatile than historically. The corresponding

[38] Since the present paper deals with own-price elasticities, for simplicity, "price elasticity" or "elasticity" is used synonymously with "own-price elasticity of electricity demand" in the remainder of the paper.

availability of new observations on demand response offers the opportunity to update estimates of demand elasticity, with a specific focus on situations characterized by high prices. Furthermore, this provides a chance to explore the functional relationship between demand response and price levels. By incorporating these new observations, a more refined understanding of how demand responds to varying price levels can be attained. So far, there are no estimates of short-term elasticities that include data from these high-price years or any other information concerning comparably high prices.

Demand responses are commonly characterized using either linear or exponential price-demand relationships. The latter is modeled by applying the natural logarithm to both variables and implies a constant elasticity (log-log specification). While the disparities between these two approaches are likely small at lower price levels, the question arises as to their compatibility with the observed wide-ranging price dispersion. Since the shape of the demand curve is unknown ex-ante, this research aims to address the superiority of one assumption over the other, drawing upon theoretical expectations derived from the electricity market under consideration and the available data. In the course of this, this study will explore the extent to which estimates of demand elasticities, considering the newly available data on high prices, differ from existing estimates.

Consequently, the present study firstly discusses the two distinct functional forms of demand-price response against the background of the German electricity market. Based on the insights gained from this examination, hypotheses are formulated for the empirical study. Subsequently, short-term own-price elasticities are estimated using data spanning the years 2015-2022 in the German wholesale electricity market, employing both functional forms. Recognizing the endogeneity issue between demand and prices, a two-stage least squares approach (2SLS) is employed, utilizing the day-ahead forecast of wind power generation as an instrumental variable for day-ahead electricity prices. Particular attention is paid to whether the short-term elasticity changed in 2021 and 2022 when consumers faced higher prices. To facilitate this examination, the analysis is divided into two distinct periods: the "low-price years" 2015-2020 and the "high-price years" 2021-2022.

Three hypotheses are put forward and then empirically confirmed: Firstly, in low-price years, the assumption of a linear relationship between demand and price yields similar average elasticities as the assumption of constant elasticities. This similarity, however, is not clear-cut and does not hold in high-price years. Secondly, when assuming a linear relationship between price and demand, the estimates for the demand response to a price increase of 1 EUR/MWh differ significantly between high- and low-price years (–34.3 MW/(EUR/MWh) vs –109.4 MW/(EUR/MWh)). The discrepancy arises, as the linear specification cannot account for decreasing absolute demand flexibility with increasing prices. Lastly, under the log-log specification, which assumes a constant elasticity, estimates are much closer together (–5.3 % vs –4.2 %). The exponential nature of the log-log function accounts for the decline in absolute demand response (per price change of 1

EUR/MWh) at high prices, resulting in more consistent estimations across the price range.

The paper is organized as follows. Section 4.2 provides an overview of the empirical literature on short-term (hourly) price elasticity estimation and the contribution of the paper at hand. Section 4.3 outlines basics of the German wholesale electricity market. Further, the Section introduces the two assumptions for the functional form of the demand function, discusses their properties and formulates hypotheses for the empirical study. Section 4.4 introduces the empirical strategy, drawing on the findings from Section 4.3, while Section 4.5 presents the data set utilized. The empirical results are shown and discussed in Section 4.6 before the paper concludes with Section 4.7.

4.2 Literature review and contribution

There is a wide range of literature on empirical estimation of price elasticities in the energy and electricity sectors. A general distinction is made between self-elasticity or own-price elasticity, i.e. the elasticity of demand to changes in the price of the good itself, and cross-price elasticities, i.e. the response of demand for one good to changes in the price of another good (in the case of electricity, for example, the price of electricity at other points in time (e.g. Filippini (2011)) or the price of natural gas (e.g. Woo et al. (2018) or Gautam and Paudel (2018)). Most papers, like the one at hand, deal with own-price elasticities. For readers who are interested in existing elasticity estimates, papers with comprehensive summaries of elasticity estimates and estimation methods have been published (Andruszkiewicz et al., 2019; Boogen et al., 2017; Ciarreta et al., 2023). In addition, explicit meta-studies have been conducted to review the state of research (Espey & Espey, 2004; Labandeira et al., 2017).

This paper seeks to estimate short-term price elasticities. Here, "short-term" refers to the hourly price reactions of consumers. The estimation and analysis of demand reactions in an hourly resolution (sometimes also called "real-time" elasticities (Lijesen, 2007)) constitutes a much smaller strand of literature. In this context, a distinction can be made between papers whose analyses are based on individual consumer consumption data and those that draw on aggregated data.

Taylor et al. (2005), Wolak (2011), Cosmo et al. (2014), and Fabra et al. (2021) use individual measurement data to examine the hourly demand response of individual consumers to various dynamic, time-of-use, or real-time pricing tariffs in different countries. These studies can be used, for example, to assess the impact and reactions of customers to the introduction of new price regulations. In contrast, there are studies that do not focus on individual consumers but on the overall demand response at the system level. As in the present paper, the goal is not to find out how pricing or taxation schemes affect individual consumers but rather to determine what demand reactions are caused by prices at

the national level in the status quo. The first paper addressing this question for the Netherlands, based on data for the year 2003, is Lijesen (2007). He utilizes the lagged electricity price as instrumental variable to account for the simultaneity issue between price and demand. He estimates the price elasticity based on a linear specification of the demand curve to be –0.0013 and based on a logarithmic form to be –0.0043 . These values are very low and imply an almost completely inelastic demand in the short run. Hirth et al. (2023), however, argue that the exogeneity assumption for the use of lagged prices as an instrumental variable, given the strong serial correlation and intertemporal interrelations, is unlikely to hold.

For Germany, three papers estimate hourly price elasticities of electricity demand. The first is Bönte et al. (2015). The paper uses ask prices from the EPEX SPOT power exchange for 2010-2014 to estimate a short-term elasticity of –0.43 . This approach fundamentally differs from the one used in the present paper, as I utilize day-ahead prices and data on the realized aggregated demand. In contrast to the realized aggregated demand, the demand curves of the power exchange do not include the entirety of demand. However, they do include power traded over several markets and financial stages (Hirth et al., 2023) as well as prior internal matching of supply and demand of the market participants (Knaut & Paulus, 2016) (see Section 4.3.1).

The two papers that are methodologically closest to the one at hand are Knaut and Paulus (2016) and Hirth et al. (2023). Both papers use wind power generation as instrumental variable to estimate the hourly price elasticity of electricity demand in Germany. Knaut and Paulus (2016) estimate the elasticity, based on data for 2015, to be between –0.02 and –0.13 , depending on the time of day. They assume a linear demand curve. Hirth et al. (2023) use data from 2015-2019 to estimate the average elasticity at –0.051 , assuming a linear price-demand relationship. The results are thus consistent with those of Knaut and Paulus (2016). The paper further includes regression models assuming a log-linear relationship[39] as well as non-parametric models and various sensitivities and robustness checks.

The present work adds to the literature in two ways. First, no previous work includes data from 2021 and 2022, the years in which prices were significantly higher than historically. The observations from recent years provide an opportunity to gain a better understanding of the demand response at high prices. Therefore, the analysis focuses on the two most commonly assumed functional forms of the demand curve: linear and log-log. While Lijesen (2007) uses both variants but does not discuss the differences in estimates, Bönte et al. (2015) uses only the log-log variant, Knaut and Paulus (2016) only the linear approximation, and Hirth et al. (2023) the linear, a log-linear, and non-parametric forms, but not the usual log-log variant. Given the wide dispersion of prices in recent years the implicit

[39] Log-linear here means that the dependent variable (demand) was logarithmized, but not the explanatory variables. Alternatively, this procedure is also referred to as semi-log or log-level, while confusingly log-linear can also refer to models in which the explanatory variables are also logarithmized (here refered to as log-log).

differences between the approaches could become more pronounced. Therefore, a well-founded discussion of the differences, implications and validity of both assumptions under current circumstances is needed.

4.3 Background

To support the interpretation of the applied method and results, this Section defines the estimated elasticities and explains the basics of the German wholesale electricity market and the demand response to be measured. Subsequently, the two applied assumptions for the functional form of the demand function are introduced, their properties are discussed, and hypotheses are formulated for the empirical study.

4.3.1 Short-term elasticity and wholesale prices

Price elasticity can be defined for different time scales. Long-run elasticity usually refers to demand adjustments over several years and thus include adjustments of the capital stock. Short-run elasticity is often defined as adjustments within one year (Labandeira et al., 2017). In the present analysis, *short-term* refers to an even shorter time scale: the demand response on an hourly basis. Sometimes this is also referred to as *real-time* elasticity (Hirth et al., 2023; Lijesen, 2007). Own-price elasticity of demand, the kind of elasticity covered in this paper, denotes the relative change in demand for a relative change in price for the product. As elasticities are not necessarily constant for all price-demand combinations, the own-price elasticity of demand (ϵ) can be calculated based on the absolute changes at a specific combination of *price* and *demand* using Equation 4.1.

$$\epsilon = \frac{\%\Delta demand}{\%\Delta price} = \frac{\Delta demand}{\Delta price} \cdot \frac{price}{demand} \tag{4.1}$$

In order to estimate the elasticity according to Equation 4.1, one needs information on price and demand. For the price, I rely on the hourly day-ahead prices from the German wholesale electricity market (EPEX SPOT). Via an auction, supply and demand are traded daily at noon for each hour of the following day. Not all electricity volumes are procured on the power exchange. Alternatively, there is the option of bilateral trading or own-generation of required electricity quantities. Nevertheless, the day-ahead prices can be seen as relevant benchmarks for the other procurement options, as they form the opportunity costs for consumers and producers. Two aspects have to be considered further to interpret the estimated short-term price elasticities when using wholesale day-ahead prices. First, not all consumers are exposed to the hourly variation of electricity exchange prices. Residential electricity customers, for example, usually purchase their electricity at a fixed price per kWh from their electricity supplier. Other consumers acquire their electricity demand directly, such as energy-intensive industries. These are

exposed to electricity price variations. Accordingly, the estimated demand response measures the demand response of these electricity consumers only. Second, electricity consumers are confronted with other price components besides the wholesale electricity price, such as taxes and surcharges, as well as regulatory incentives. Accordingly, the elasticity estimates are dependent on the existing regulatory background.

For the demand I utilize data on the hourly realized aggregated electricity demand in Germany. As described, while not all of the realized demand is traded at the day-ahead market, the day-ahead price is still a valid benchmark for the procurement cost of the entire demand. However, it should be emphasized that after the day-ahead prices are set, there is still continuous intraday trading that can affect realized demand. The estimate cannot reflect corresponding dynamics, e.g. triggered by unexpected events such as power plant outages (Lijesen, 2007).

As an alternative to using the day-ahead price and realized demand, it is also conceivable to use the aggregated hourly demand curves based on ask bids at the power exchange, e.g. EPEX SPOT, to estimate the price elasticities. Knaut and Paulus (2016) argue, however, that this is not easily possible, as market participants already match parts of their demand and supply internally before submitting their bids, which distorts the observable demand curve in the market. Furthermore, the observable demand curve on the wholesale market does not correspond to the real demand curve because it only reflects the volumes traded on the wholesale market and includes electricity that is traded over several market and financial stages (Hirth et al., 2023).

4.3.2 Functional forms of demand-price response and hypotheses

The actual demand curve in the electricity market is not known ex ante. When estimating elasticities, different functional forms of the demand-price relationship can be assumed. Two central options are the linear price-demand relationship and the exponential relationship described via constant elasticities (log-log specification).

In the literature, the linear approximation of the demand function according to Equation 4.2 is applied for example in Fabra et al. (2021); Hirth et al. (2023); Knaut and Paulus (2016); Lijesen (2007).

$$demand = b \cdot price + a \tag{4.2}$$

When estimating the demand response based on the linear formulation, one estimates the slope b of the demand-price curve. This slope is constant across all price levels. The elasticity corresponding to Equation 4.1 then varies depending on the point on the curve, since the absolute demand response $\frac{\Delta demand}{\Delta price}$ is constant, but the price-demand combination $\frac{price}{demand}$ is different at each point of the curve. The elasticity is then lower for low and higher for high prices. The results of this estimation are often communicated as average elasticity $\bar{\epsilon}$, calculated with

Equation 4.3. This approach is convenient, but one must keep in mind that this average elasticity value is only valid for a single point on the linear demand-price curve (see Figure 4.1 (a)).

$$\bar{\epsilon} = b \cdot \frac{\overline{price}}{\overline{demand}} \tag{4.3}$$

Alternatively, the demand function is often assumed to have a log-log functional form according to Equation 4.4 (e.g. Bönte et al. (2015); Boogen et al. (2017); Lijesen (2007)). This specification is based on the formation of the natural logarithm for both the dependent and the explanatory variables. The assumed relationship between demand and price is exponential. Confusingly, the term log-linear is also used to describe this specification. However, since this can lead to confusion with specifications in which only the dependent variable is logarithmized (also called semi-log or log-level), I use the term log-log specification in this paper, following Wooldridge (2013).

$$ln(demand) = c \cdot ln(price) + d \tag{4.4}$$

The parameter c, when estimated based on the assumption of a log-log demand function, can then be directly interpreted as a constant price elasticity of demand (see Figure 4.1 (a)). Using the approximation that $log(1 + x) \approx x$ for small x, the parameter c expresses the percentage change in demand for a one percent change in price, independent of the price level (Wooldridge, 2013). Thus, the log-log functional form assumes that the absolute effect of a price change on demand decreases with the price. Accordingly, the absolute demand response (per price change of 1 EUR/MWh) differs between linear and log-log specification, particularly at the edges of the curve, i.e. at very high prices.

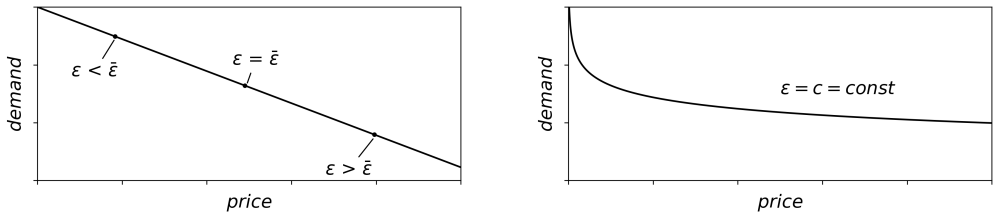

(i) (ii)

Figure 4.1: Stylized demand-price functions: linear (i) and log-log (ii)

As previously discussed, not all electricity market participants are confronted with the wholesale electricity price signal, resulting in a portion of demand that is completely unresponsive to short-term price changes. Figure 4.2 presents a highly stylized depiction of the composition of electricity demand during a specific hour. The total demand is divided into segments based on the maximum price that consumers are willing to pay before they curtail or shift their consumption. The shaded segment ($< d_1$) represents the perfectly inelastic portion of demand,

such as the demand from household customers not exposed to price signals. Additionally, there are demand segments comprising customers who can adjust their consumption in response to wholesale market price signals (yellow areas). The extent to which these customers reduce or shift their consumption depends on their flexibility and opportunity costs. The figure illustrates this flexible demand using six equally sized demand shares. Starting from the bottom, the first segment represents industrial companies that only modify or shift their production at very high electricity prices (p_1). This is followed by increasingly flexible industrial and service applications, ultimately leading to flexible consumers such as storage units that curtail consumption even at relatively low prices. The size and number of these segments, the extent of demand reduction at different price levels, and, thus, the actual shape of the demand function are, in reality, unknown.

Function $D_1(p)$ serves as an illustrative linear demand function that captures the demand behavior in the low price range ($< p_1$). However, at high prices, the linear demand function deviates significantly from the assumed demand structure. Increasing the slope of the function may improve its representation of the low demand response to high prices, but this improvement comes at the cost of accurately depicting the demand response at low prices.

In contrast, Function $D_2(p)$ represents an exemplary log-log demand function. It maintains similarity to the linear description in the low price range, effectively capturing the demand structure. However, the model exhibits a good fit for the price range characterized by predominantly inelastic demand, thanks to its exponential characteristics that effectively capture the diminishing demand response as prices increase.

Certainly, there are other possible functional forms for the demand curve, such as piecewise linear functions, that can accurately represent these relationships. However, for the purpose of this paper, I focus on the two central options presented. In doing so, I aim to capture the fundamental characteristics of the demand response to price changes without delving into the complexities introduced by alternative functional forms.

Three hypotheses are derived from these observations, which will be substantiated in the following through empirical estimation:

Hypothesis 1: At low prices, estimates based on both assumptions yield similar results. The average elasticity based on the linear assumption will be similar to the constant elasticity derived from the log-log description.

Hypothesis 2: The estimators based on linear functions will exhibit significant differences depending on whether low or high prices are considered. This discrepancy arises from the observation that demand at high prices tends to have limited flexibility, leading to distinct estimations.

Hypothesis 3: Estimators using the log-log approach will demonstrate smaller differences between estimates based on low and high prices. This is because the exponential nature of the log-log function takes into account the decrease

in absolute demand response (per price change of 1 EUR/MWh) at high prices, leading to more consistent estimations across the price range.

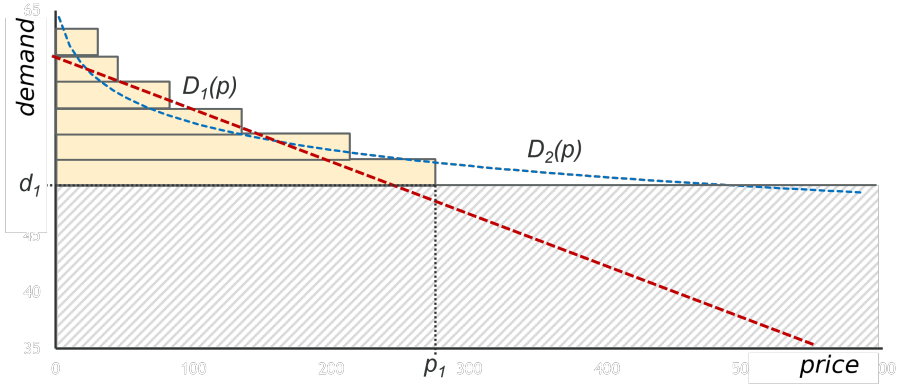

Figure 4.2: Stylized demand structure.

4.4 Empirical strategy

The objective of the analysis is to estimate the short-term (i.e. hourly) response of electricity demand in Germany to changes in electricity prices. Equation 4.5 shows the estimated relationship as a linear regression model.

$$Demand_t = \alpha_0 + \alpha_1 \cdot Price_t + \boldsymbol{\alpha_2} \cdot \boldsymbol{X_t} + \epsilon_t \tag{4.5}$$

The variable $Demand_t$ represents the hourly realized electricity demand in Germany, while the variable $Price_t$ represents the deflated (real) hourly day-ahead electricity price in the German electricity market. X_t denotes a vector of covariates.

The interaction of demand and supply endogenously determines price and realized demand. Due to this simultaneity, the explanatory variable $Price_t$ is endogenous: In a linear regression model (as shown in Equation 4.5), the $Price_t$ is correlated with the error term ϵ_t. An estimation of the response of demand to changes in price using a common linear regression model is therefore biased.[40]

To handle the simultaneity issue, I apply a two-stage least squares (2SLS) approach, using an instrumental variable (IV) for the endogenous explanatory variable of the electricity price. As IV, I utilize the grid operators' day-ahead wind power generation forecast. Figure 4.3 illustrates the relationship between the outcome $Demand_t$, the central explanatory variable, or treatment, $Price_t$, and the IV day-ahead forecast of wind power generation $Wind_t$.

[40] In Appendix 4.8.1, the main model results of this paper are compared to the results of an OLS estimation to show magnitudes of bias.

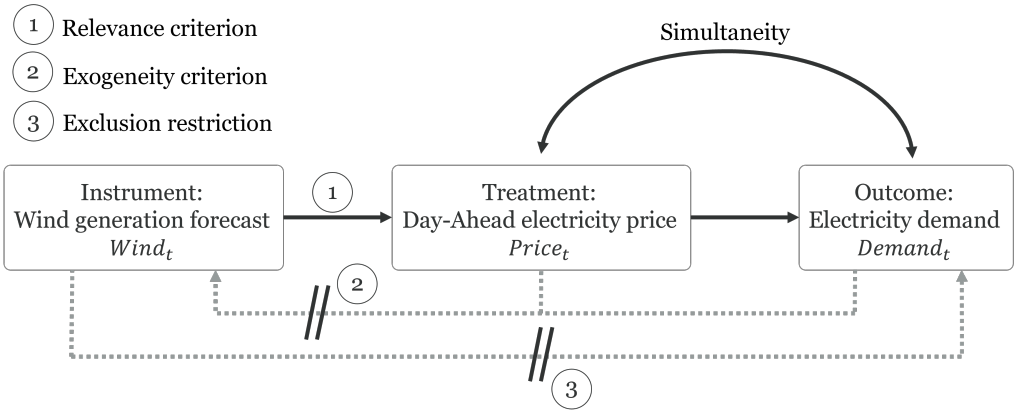

Figure 4.3: Instrumental variable estimation approach.

The chosen IV meets the three criteria central to an appropriate instrument choice: The relevance and exogeneity criteria as well as the exclusion restriction (indicated in Figure 4.3). First, $Wind_t$ is relevant as an instrument for the treatment variable $Price_t$ as it is correlated with $Price_t$: electricity generation from wind has, ceteris paribus, a negative effect on the price of electricity because electricity from wind turbines is offered in the market at marginal costs close to zero. As a result, more expensive forms of generation, such as coal or gas-fired power plants, are priced out of the market equilibrium. In Section 4.6, it is shown quantitatively that $Wind_t$ has significant and high explanatory power for $Price_t$. Since day-ahead prices are determined by auction at noon the day before delivery, they are not driven by the realized wind generation but rather by the market participants' expectation of the wind generation of the following day. The grid operators in Germany are obliged to publish a forecast for the wind power generation of the following day.[41] The forecast is transmitted daily at 6 pm. Thus, it represents the best publicly available approximation of the generation expectation at the time of price formation and is therefore used as IV.[42].

As the second criterion, the IV must be exogenous with respect to the instrumented and explained variables. The wind power generation forecast is unaffected by price and demand changes. It depends only on the installed capacity of the wind turbines and the weather forecast for the delivery time.

Third, the exclusion restriction must apply to the IV. That is, the wind power generation forecast does not affect electricity demand in any way other than through the price of electricity. This should be true in principle, but there might be correlations between wind power generation and electricity demand due to

[41] Art. 14 Par. 1 c) Commission Regulation (EU) No. 543/2013

[42] Alternatively, using the realized wind power generation as IV would also be possible (e.g., Hirth et al. (2023)) However, the actual wind power generation is unknown at the moment of pricing. Also, data on actual generation includes curtailment, e.g. due to grid congestion. However, using actual wind power generation as IV hardly changes the results of the present analysis, as is shown in Appendix 4.8.2

weather coincidences. For example, it is conceivable that periods of high wind generation (i.e. in winter) coincide with periods of increased electricity demand for heating applications. To isolate these weather correlations from the estimation, dummies for months and hours of a day as well as heating and cooling degrees are introduced in the estimation model.

As an alternative or addition to the selected IV, day-ahead wind generation forecast, one could utilize the photovoltaic (PV) generation or the day-ahead PV generation forecast as instruments. However, there are two reasons to assume that the exclusion restriction of a valid IV is not met for PV generation (and the forecast of it). First, small rooftop PV systems do not consistently provide hourly metering data, so the grid operators' data are partly based on estimates. Therefore, measurement errors that correlate with prices are conceivable and would distort the price-demand response estimation (Hirth et al., 2023). Second, Frondel et al. (2022) show that there exists a so-called solar rebound effect, i.e. more electricity is consumed when solar electricity is generated. A potential correlation between PV generation and demand would violate the exclusion restriction. However, to account for the potential correlation between solar generation and demand, the day-ahead PV generation forecast is included in the model as a control variable.[43]

Equation 4.6 and 4.7 show the simultaneous equation model. Here a linear relationship between $Demand_t$ and $Price_t$ is assumed. As alternative model specification logarithmized variables are utilized, following the discussion in Section 4.3.2.

$$Price_t = \gamma_0 + \gamma_1 \cdot Wind_t + \boldsymbol{\gamma_2} \cdot \boldsymbol{C_t} + \boldsymbol{\gamma_3} \cdot \boldsymbol{D_t} + \epsilon_t \tag{4.6}$$

$$Demand_t = \beta_0 + \beta_1 \cdot Price_t + \boldsymbol{\beta_2} \cdot \boldsymbol{C_t} + \boldsymbol{\beta_3} \cdot \boldsymbol{D_t} + \mu_t \tag{4.7}$$

Due to the simultaneity of the two equations, the model is solved via the two-stage least squares (2SLS) approach. In the first stage, $Price_t$ is the response variable, and the IV $Wind_t$ is the primary explanatory variable. In the second stage, $Price_t$ is then replaced with the predicted values from the first stage to estimate the causal effect of $Price_t$ on $Demand_t$. In both stages, there are further controls included in the model. C_t is a vector of covariates, including the hourly day-ahead forecast for PV generation, daily deflated gas, coal and European emission allowances (EUA) prices, as well as hourly heating and cooling degrees. D_t is a vector of dummy controls. Yearly dummies account for changes in generation capacity over time, while monthly dummies correct for seasonal effects in demand and prices. Dummies for the different days of the week and for the different hours of a day control for varying demand structures over time.[44] ϵ_t and μ_t are error terms.

[43] As a sensitivity analysis, in Appendix 4.8.2, the estimations are run with the day-ahead PV generation forecast as an additional instrument. The results differ only slightly from the main result, with the estimators for the demand response being slightly lower.

[44] Appendix 4.8.3 shows the effect of adding each dummy control to the model

For a precise understanding and interpretation of the model results, it is crucial to acknowledge the presence of autocorrelation in variables within the model. The selected estimation model does not only estimates the demand response to the price in a specific hour but also implicitly includes intertemporal cross-price elasticities with the preceding and subsequent hours (Hirth et al., 2023). This implies that the effects of price fluctuations extend beyond a single hour, capturing interdependencies across time. For instance, due to the possibility of load shifts, the expectation of high prices in a particular hour may influence demand in preceding and subsequent hours.

Following the discussion in Section 4.3.2, the model is further estimated with logarithmized variables, namely as a log-log specification. For heating and cooling degrees as well as PV generation, a constant of 1 is added beforehand, owing to the presence of zero values. Since the natural logarithm of negative and zero values is not defined, respective data points of negative prices are removed. This eliminates 1.4% (909) of the data points under consideration. Thus, information about demand response to negative prices is lost. However, this is not a problem since the present analysis focuses on demand response when prices are high.

To account for the serial correlation in the data, heteroscedasticity and autocorrelation (HAC) robust standard errors are calculated, for all model specifications. Specifically, the standard errors are calculated using Newey-West kernel with automatic bandwidth selection.[45]

4.5 Data

The basis of the analysis is an hourly data set for 2015-2022, with a total of 70,024 observations.[46] To ensure that special effects of public holidays and bridge days do not distort the estimation, corresponding data points and the period between Christmas and New Year were removed from the data set, leaving 65,920 observations.

The hourly values of the dependent variable $Demand_t$ are taken from the *Total Load* timeseries published by the European Network of Transmission System Operators (ENTSO-E)(ENTSO-E, 2023).[47] Figure 4.4 depicts the temporal variation in German electricity demand in the dataset. Over the course of a day demand is highest around 11:00 am and lowest at night at around 2:00 am. Demand is lower at weekends than on weekdays and lowest on Sundays. The

[45] Estimates are carried out using *ivregress* from StataCorp (2021).

[46] The data set does not include the first 96 hours of 2015, as data on day-ahead electricity prices is not available.

[47] All data from the ENTSO-E Transparency Platform used in this analysis is on country level "Germany" and was downloaded on 28.02.2023. The latter is important as values are regularly updated, especially on electricity demand. Information on the ENTSO-E data can be found at `https://transparency.entsoe.eu/content/static_content/Static%20content/knowledge%20base/knowledge%20base.html`

electricity demand also shows a seasonal trend, with demand being higher in winter than in summer. When comparing the years, two years, 2020 and 2022, stand out, in which the median electricity demand deviates downward from the other years. For 2020, the effect of the Covid-19 pandemic can be assumed as the cause; for 2022, the reason could be the energy crisis and the associated high electricity prices.

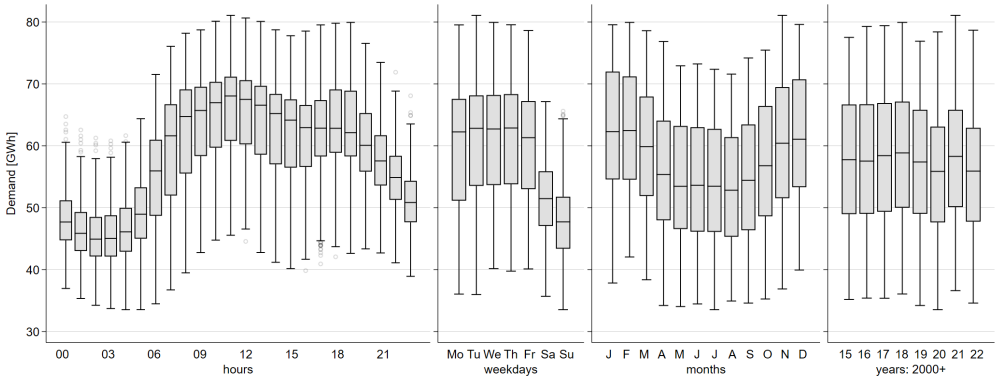

Figure 4.4: Temporal variation in the variable $Demand_t$, 2015-2022, from (ENTSO-E, 2023).

Hourly day-ahead wholesale electricity prices $Price_t$ are taken from *Day-ahead prices* timeseries of ENTSO-E (2023). These prices are the result of the German day-ahead auction at the EPEX power exchange. The nominal prices from ENTSO-E (2023) are deflated using the Consumer Price Index (CPI) from Statistisches Bundesamt (Destatis) (2023) to the level of January 2015 in order to account for the impact of inflation and accurately assess the demand response without the confounding effects of rising prices over time.[48] In Figure 4.5, the variance of real prices over time is shown. With the exception of the annual figure, the price distributions are characterized by a large number of positive outliers. These occur due to the extremely high electricity prices in 2021 and 2022 compared to previous years. Prices above 100 EUR/MWh occurred very rarely in the years 2015 to 2020, which is evident in the annual figure. Due to this significant difference in price levels and variance, the analysis performed is based on the split of the data set into the low-price years (2015-2020) and high-price years (2021-2022). According to the literature (e.g. Wolff and Feuerriegel (2017)), one would expect prices to be higher in winter than summer, as demand increases and solar generation declines. Based on the figure, this relationship can not be clearly demonstrated, due to the extremely high prices in July to October 2022. Prices tend to be lower on

[48] For the same purpose, other price data (gas, coal and EUA prices) are also adjusted for inflation using the CPI. Thus, with the exception of the literature results, all EUR values presented reflect real values based on the reference point of January 2015. The central results of the analysis remain unchanged even if nominal prices are used. However, the linear estimates for the price variables are slightly lower in that case.

weekends than during the week, and there are two price peaks during the day, once at 8:00 am and once at 7:00 pm.

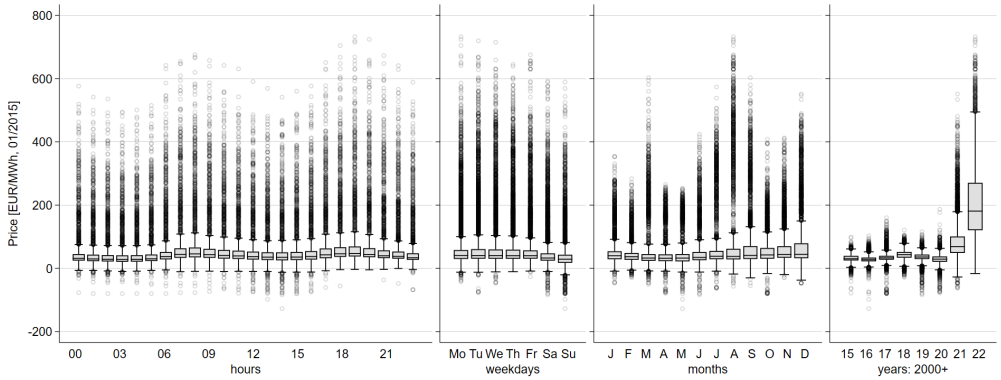

Figure 4.5: Temporal variation in the variable $Price_t$, 2015-2022, from (ENTSO-E, 2023).

As described in the methodological discussion in Section 4.4, the day-ahead wind generation forecast of the grid operators $Wind_t$ is used as IV for the endogenous variable $Price_t$. Together with the forecast for solar generation, the forecast values are available from ENTSO-E (2023) as the hourly time series *Day-Ahead generation Forecast Wind and Solar*. The forecast of solar generation PV_t is used as a covariate in the model, as PV generation is potentially correlated with the demand (see Section 4.4). For both variables, a negative effect on the electricity price is to be expected. Figure 4.6 shows the time variation of the two variables. Both variables show an increasing trend over the past years, corresponding to the increase in generation capacities. However, due to the weather dependency, this is subject to a wide dispersion. Both variables also show a strong seasonal structure: While electricity generation from wind is particularly high in winter, solar electricity generation is high in summer. The intra-day structure is much more pronounced for solar electricity than wind generation: while no PV electricity is generated at night, most electricity is generated at noon.

Besides the day-ahead PV generation forecast, several additional covariates are used in the model. Further covariates that affect the supply side of electricity pricing are fuel prices and prices for emission allowances, which determine the marginal costs of conventional power plants. As they are not available on hourly basis, they further do not qualify as IV in this setting. Since the marginal cost of generating electricity in conventional power plants increases with the fuel and certificate prices, a positive effect on the electricity price can be expected for all three variables. For the coal price $Coal_t$ the daily prices for coal imports at the Amsterdam-Rotterdam-Antwerp (ARA) trading point are utilized.[49] As gas price, the daily prices for natural gas at the reference trading point TTF are

[49] Coal (API2) CIF ARA (ARGUS-McCloskey).

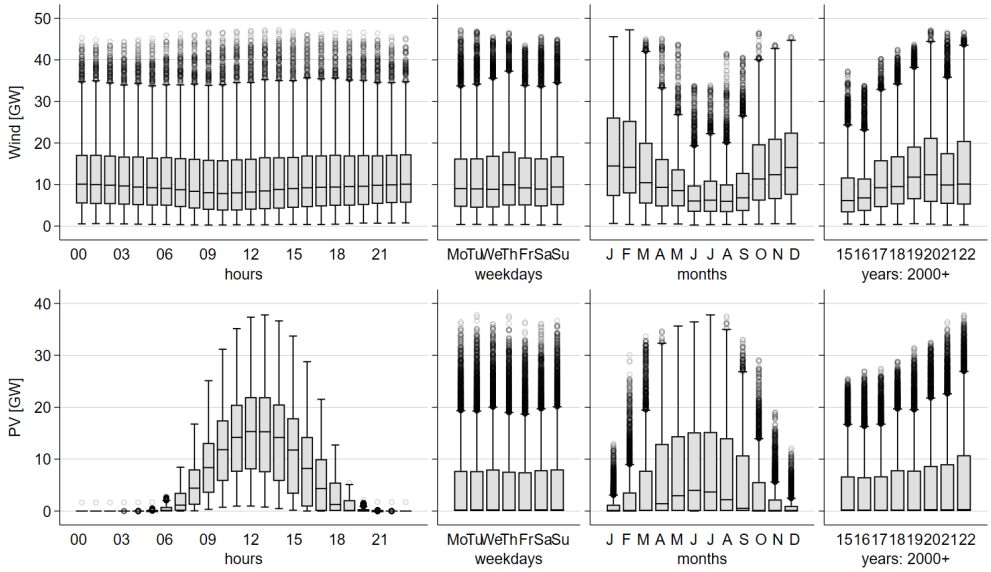

Figure 4.6: Temporal variation in the variables $Wind_t$ (top) and PV_t (bottom), 2015-2022, from (ENTSO-E, 2023).

included.[50] Daily prices for European Emission allowances (EUA) are taken from ICAP (2023). Figure 4.7 shows the deflated fuel and certificate prices compared to daily averages of the deflated day-ahead electricity price. The increase in prices in 2021 and especially in 2022 is particularly noteworthy. As a result of the war in Ukraine, gas prices in particular reached record levels. The electricity price follows the development of the underlying fuel prices. The correlation is particularly evident for the gas price.

Heating and cooling degrees are used as covariates on the demand side. The need for heating or cooling implies correspondingly higher electricity demand. Therefore, a positive correlation between electricity demand and heating or cooling degrees can be expected. For the calculation of hourly heating degrees and cooling degrees temperature data by region is taken from Copernicus Climate Change Service (2020)[51]. By weighting the temperatures with the region specific population from Eurostat (2023), I derive population weighted average temperatures for Germany. Hourly heating and cooling degrees are then calculated based on a temperature threshold of 15 °C.

[50] Dutch TTF Natural Gas Futures.
[51] Air temperature at an altitude of 2m for NUTS3 regions.

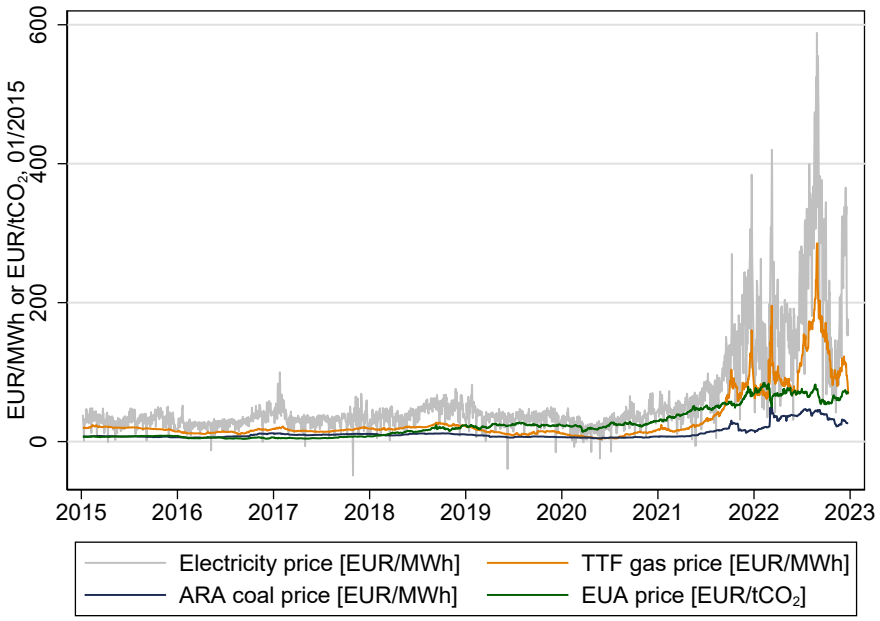

Figure 4.7: Daily average electricity price, gas, coal and EUA price in 2015-2022.

Table 4.1 gives an overview over descriptive statistics of the used data.

Table 4.1: Descriptive statistics, 2015-2022 (N = 65,920)

Variable	Mean	Median	SD	Min	Max	Source
Demand (MW)	57348	57393	9963	33542	81077	ENTSO-E
Price (EUR/MWh, 01/2015)	61.84	37.44	75.64	-127.35	732.52	ENTSO-E
Wind (GW)	11.95	9.17	9.39	0.24	47.23	ENTSO-E
PV (GW)	4.88	0.21	7.48	0	37.78	ENTSO-E
Gas (EUR/MWh, 01/2015)	31.02	17.55	37.33	3.25	285.27	ICE Dutch TTF
Coal (EUR/MWh, 01/2015)	11.98	8.88	9.37	4.71	49.13	API2 CIF ARA
EUA (EUR/tCO_2, 01/2015)	24.46	19.19	21.73	3.81	84.68	ICAP
HD (°C)	5.84	4.86	5.63	0	27.04	CDS
CD (°C)	1.43	0	2.98	0	20.75	CDS

4.6 Empirical results

I estimate the short-run elasticity of electricity demand for Germany using the 2SLS approach described in Section 4.4, both for the linear and the log-log model specification. First, the results for the first stage are examined concerning the

validity of the approach before the second-stage model results are discussed. I distinguish between low-price and high-price years to investigate whether the elasticities differ for the time periods and, thus, for the different price ranges. In addition, further sensitivities are discussed.

4.6.1 First stage

Table 4.2 shows the results of the model in linear (1a) and log-log (1b) specification. In both variants, the estimator for the instrumental variable $Wind_t$, i.e., the day-ahead wind generation forecast, is significant. In the linear model, 1 GW of additional wind generation, ceteris paribus, leads to a price decrease of around 1.8 EUR/MWh. Similarly, the second model results state that a one percent increase in wind generation leads to a 0.31 % decrease in price.[52] The partial R squared shows for both models that $Wind_t$ explains a relevant part of the variance of the price. In addition, the Montiel-Pflueger robust weak instrument test was performed for both model specifications. The F-statistics of the tests at 5% confidence level are 11,151 and 8,110, respectively, which is well above the critical value of the test of 37.42. Based on the test result and the significance at the first stage, I conclude that $Wind_t$ is indeed a strong instrument for $Price_t$. The estimators of the other covariates have the expected signs and magnitudes. PV power generation has a negative impact on the electricity price, similar in magnitude to wind power generation. Fuel and certificate prices enter positively, with the gas price having the largest effect on the price at 1.7 EUR/MWh. This order of magnitude is also intuitively plausible if one assumes that an average gas-fired power plant has an efficiency of about 50%. When gas-fired power plants determine the price of electricity, an increase in the price of gas of 1 EUR leads to an increase in the price of electricity of 2 EUR. Since gas-fired power plants do not determine the price at every hour, the estimated value is lower.

4.6.2 Second stage

Linear model results

Table 4.3 shows the second stage results for the linear specification. For Model (2a), where data from all eight years under consideration was utilized, the estimator for the linear demand response to price is –61.81 , i.e. when the price increases by 1 EUR/MWh, demand decreases by 61.81 MW. In contrast, the data set used in Model (3a) includes only the low-price years (2015-2020), and Model (4a) includes only the high-price years (2021-2022). The estimation results differ significantly from the results of the joint estimation. While the estimator for the low-price years is significantly higher (–109.4), the estimator for the high-price years is lower (–34.35). The intuition behind this result follows the explanations in Section 4.3.2.

[52] The within-variance of the price, after accounting for the dummy control variables, is shown in Appendix 4.8.4.

Table 4.2: First stage results

	(1a) linear		(1b) log-log	
Wind [GW]	-1.765***	[-1.80,-1.73]	-0.314***	[-0.32,-0.31]
PV [GW]	-2.495***	[-2.58,-2.41]	-0.298***	[-0.31,-0.29]
Gas [EUR/MWh]	1.707***	[1.66,1.75]	0.537***	[0.51,0.56]
Coal [EUR/MWh]	0.259**	[0.10,0.41]	0.163***	[0.13,0.20]
EUA [EUR/tCO2]	0.925***	[0.84,1.01]	0.268***	[0.24,0.30]
Heating degrees [°C]	0.555***	[0.48,0.63]	0.079***	[0.07,0.09]
Cooling degrees [°C]	1.341***	[1.21,1.47]	0.061***	[0.05,0.07]
Dummy variables				
Hours	Yes		Yes	
Weekdays	Yes		Yes	
Months	Yes		Yes	
Years	Yes		Yes	
Fit statistics				
Partial R^2 Wind	0.215		0.187	
Adjusted R^2	0.869		0.684	
Observations	65920		65011	

95% confidence intervals in brackets. * $p < 0.05$, ** $p < 0.01$, *** $p < 0.001$.
Coefficients of dummy variables can be found in Appendix 4.8.5.

In contrast to the linear relationship between price and demand assumed in the model, the absolute demand response (per price change of 1 EUR/MWh)decreases with the price level. At low prices, a price increase of 1 EUR is relatively large, and consumers in the market are willing or able to not consume or postpone their consumption at this price increase. In contrast, the same price increase in years with high prices is relatively small. Consumers who buy electricity at the price level of high price years have already exhausted their potential to reduce consumption: demand can hardly be reduced any more, e.g. because the delivery is contractually fixed. Demand at this price level is less flexible in absolute terms. Calculating demand response as a linear model across all price levels ignores this decrease in absolute flexibility as prices rise. Therefore, the joint Model (2a) estimate forms a weighted average over the demand flexibility of different price levels. The results, thus, confirm Hypothesis 2.

Figure 4.8 illustrates the difference between the estimators via linear demand functions. The estimator of the linear model corresponds to the slope of the function. In addition to the three estimated values from Table 4.3, the figure includes linear estimators of the demand response from Hirth et al. (2023) (–79.6) and based on Knaut and Paulus (2016) (–99.1).[53] The estimations from Models (2a)-(4a) and their confidence intervals differ substantially. The estimate based

[53] In Knaut and Paulus (2016), the demand response is derived individually for the different hours of the day. The values range from –42.1 at 10:00 am to –201.8 at 5:00 pm. For comparability, I assume the non-weighted daily average of these values (–99.1).

Table 4.3: Second stage results of the linear specification

	(2a) 2015-2022	(3a) 2015-2020	(4a) 2021-2022
Price [EUR/MWh]	-61.81***	-109.4***	-34.35***
	[-69.95,-53.66]	[-123.75,-95.07]	[-39.50,-29.21]
PV [GW]	-204.0***	-164.1***	-211.8***
	[-231.02,-176.93]	[-191.23,-137.00]	[-248.38,-175.29]
Gas [EUR/MWh]	86.41***	226.5***	53.43***
	[65.83,106.98]	[151.79,301.26]	[39.21,67.65]
Coal [EUR/MWh]	61.79	76.99	83.41***
	[-3.53,127.12]	[-77.66,231.64]	[34.63,132.20]
EUA [EUR/tCO2]	150.8***	110.8**	140.0***
	[115.42,186.16]	[37.22,184.30]	[116.10,163.93]
Heating degrees [°C]	379.1***	351.3***	416.0***
	[337.44,420.73]	[310.82,391.72]	[357.24,474.71]
Cooling degrees [°C]	176.4***	144.0***	153.8***
	[140.67,212.10]	[109.39,178.58]	[81.72,225.81]
Dummy variables			
Hours	Yes	Yes	Yes
Weekdays	Yes	Yes	Yes
Months	Yes	Yes	Yes
Years	Yes	Yes	Yes
Fit statistics			
Adjusted R^2	0.868	0.885	0.883
Observations	65920	49434	16486

95% confidence intervals in brackets. * $p < 0.05$, ** $p < 0.01$, *** $p < 0.001$.
Standard errors are calculated as Newey-West HAC robust standard errors.
Coefficients of dummy variables can be found in Appendix 4.8.5.

on Knaut and Paulus (2016) aligns closely in magnitude with the estimate for the low-price years. This similarity is not surprising, considering that the estimate is derived from 2015 data, which corresponds to the low-price period. On the other hand, the estimate from Hirth et al. (2023) is, in absolute terms, lower than the estimate for the low-price year, despite being based on data from 2015-2019. There are two main reasons for this disparity. Firstly, the estimate does not include data from 2020, a year characterized by exceptionally low prices. Secondly, the study does not account for inflation in the price data, which, in comparison to my estimation, also leads to, in absolute terms, lower demand response estimates.

In all three model variants, the PV generation forecast enters negatively. A potential explanation may be that small-scale PV generation volumes are partially estimated by the transmission system operators (see Section 4.4). As a result, part of the small-scale PV generation appears as a reduction in $Demand_t$. Moreover,

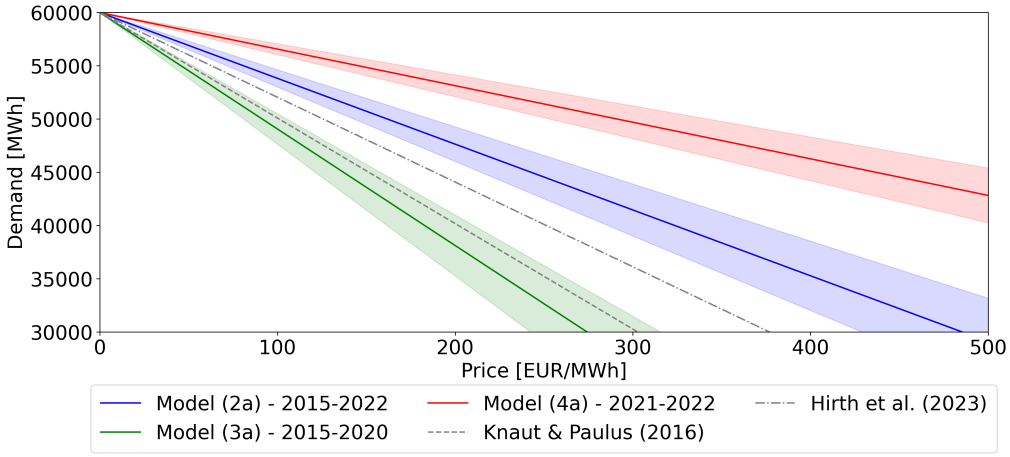

Note: For the illustration of the price-demand functions, an example intercept of 60,000 MW of demand was assumed for a price of 0 EUR/MWh.

Figure 4.8: Linear demand functions based on estimation results from different models. The shaded areas represent the 95%-confidence intervals of the estimators.

the negative sign indicates that this effect of measurement errors dominates a potential solar rebound effect in demand.[54]

Log-log model results and average elasticities

As discussed in Section 4.3.2, the log-log specification is a formulation of the demand function that considers that the absolute demand response (per price change of 1 EUR/MWh) decreases with the price level. Models (2b)-(4b) are based on logarithmized data for the variables. The estimator for the demand response in Model (2b), i.e., using the entire data set, is –0.045 . This estimator can be directly interpreted as a constant elasticity, i.e., for a price increase of 1 %, demand decreases by –4.5 %. The elasticities for the two subsets are –4.2 % and –5.3 %, respectively. The differences between elasticities for the low and high price years and the entire data set are much smaller than for the linear formulation. A look at the confidence intervals shows that these even overlap significantly. A Chow test shows that the estimators of the Models (3b) and (4b) differ at the 5% level but not at higher significance levels.

In the linear formulation, estimation results exhibit a strong dependence on the subset of data considered, highlighting the sensitivity of the estimates to the price range. In contrast, the estimators in the log-log specification demonstrate less pronounced variations. Consequently, when comparing the two models that cover the entire data set, (2a) and (2b), the log-log formulation (2b) provides a better representation of the underlying relationships across the entire price range. The empirical findings, thus, align with Hypothesis 2, as they indicate that the

[54] This is in line with findings in Hirth et al. (2023).

log-log formulation captures the true relationships more effectively than the linear specification when considering the entire data set.

Table 4.4: Second stage results of the log-log specification

	(2b) 2015-2022	(3b) 2015-2020	(4b) 2021-2022
Price [EUR/MWh] (log)	-0.0455***	-0.0418***	-0.0533***
	[-0.05,-0.04]	[-0.05,-0.04]	[-0.06,-0.04]
PV [GW] (log+1)	-0.0240***	-0.0212***	-0.0288***
	[-0.03,-0.02]	[-0.02,-0.02]	[-0.03,-0.02]
Gas [EUR/MWh] (log)	0.0355***	0.0722***	0.0401**
	[0.02,0.05]	[0.06,0.09]	[0.02,0.06]
Coal [EUR/MWh] (log)	0.0006	-0.0061	0.0353*
	[-0.02,0.02]	[-0.03,0.01]	[0.01,0.06]
EUA [EUR/tCO2] (log)	0.0400***	-0.0034	0.0805***
	[0.02,0.06]	[-0.02,0.01]	[0.05,0.11]
Heating degrees [°C] (log+1)	0.0279***	0.0244***	0.0314***
	[0.02,0.03]	[0.02,0.03]	[0.03,0.04]
Cooling degrees [°C] (log+1)	0.0225***	0.0207***	0.0241***
	[0.02,0.02]	[0.02,0.02]	[0.02,0.03]
Dummy variables			
Hours	Yes	Yes	Yes
Weekdays	Yes	Yes	Yes
Months	Yes	Yes	Yes
Years	Yes	Yes	Yes
Adjusted R^2	0.885	0.895	0.880
Observations	65011	48670	16341

95% confidence intervals in brackets. * $p < 0.05$, ** $p < 0.01$, *** $p < 0.001$.
Standard errors are calculated as Newey-West HAC robust standard errors.
Coefficients of dummy variables can be found in Appendix 4.8.5.

Figure 4.9 shows the log-log demand functions based on the estimators from Table 4.4. The figure also includes the average elasticities derived from the linear models of Knaut and Paulus (2016) (–5.4 %) and Hirth et al. (2023) (–5.1 %) as well as average elasticities obtained from the results of the linear formulation (Table 4.3, Model (2a): –6.7 %, Model (3a): –6.4 %, Model (4a): –8.9 %).[55] It is evident that the curves are much closer to each other compared to the linear functions (Figure 4.8), particularly at higher price levels. The plotted confidence intervals for models (2b)-(4b) overlap, further highlighting the consistency of the log-log estimators. Moreover, the average elasticity estimates from Knaut and Paulus (2016) and Hirth et al. (2023) fall within the range of values obtained from the log-log specification.

The similarity between the average elasticities obtained through the linear formulation in these studies and those derived from the log-log formulation supports

[55]The average elasticity is derived from the linear model specifications with Equation 4.3.

Hypothesis 1. It suggests that, for low price ranges, the linear approximation of the demand curve does not deviate too much from the log-log formulation. The average elasticity based on the linear estimators of the models (2a) and (3a) are somewhat higher, in absolute terms, than the corresponding constant elasticities of the models (2b) and (3b). However, this contrasts with the average elasticity estimated using the linear model specification for high prices (Model (4a)), which is considerably higher, in absolute terms, than the constant elasticities determined with the log-log specification. This much larger disparity arises because the assumption of a linear demand response is invalid, particularly at higher price levels.

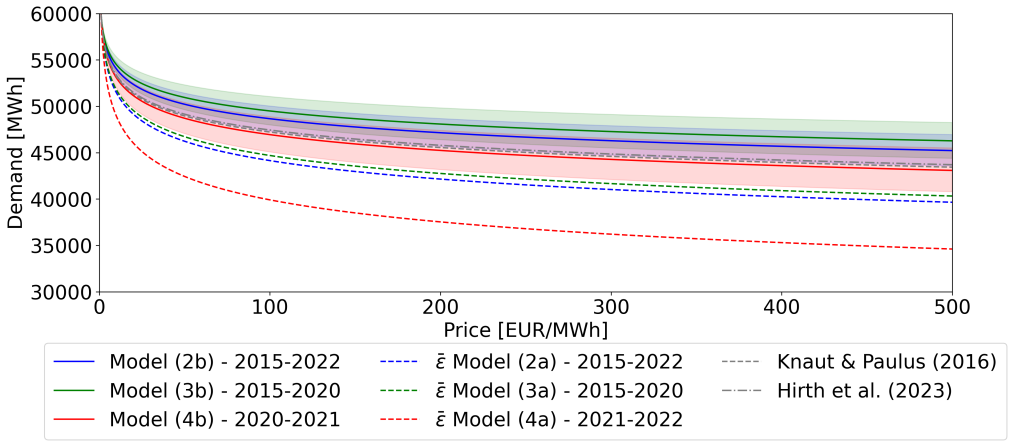

Note: For the illustration of the price-demand functions, an example intercept of 60,000 MW of demand was assumed for a price of 0 EUR/MWh.

Figure 4.9: Log-log demand functions based on estimation results from different models. The shaded areas represent the 95%-confidence intervals of the estimators.

4.6.3 Further model specifications

A key aspect of the present analysis is the separation of the data into low-price and high-price years. However, this separation is not perfectly unambiguous. As shown in Figure 4.5, the price of electricity has increased steadily since the beginning of 2021. Alternative separation dates for the start of the high-price period are, for example, after the first or second quarter of 2021. However, choosing a separation date that differs from the one in the main specification does not drastically affect the analysis results.[56]

In addition to the selected covariates, there may be other potentially beneficial covariates to be added, particularly on the supply side. For example, the availability of hydroelectric or nuclear power generation in Germany and neighbouring countries influences the electricity price, as does the available coal-fired power

[56] Appendix 4.8.6 contains the results for alternative separation dates. The results strengthen the validity of statements based on the main model specifications.

plant capacity. Including possible proxies for these influencing variables hardly changes the results.[57] That is because these effects are already absorbed by the corresponding time dummy variables in the main model specification.

In similar price elasticity analyses, realized wind generation is used as the instrumental variable for price instead of the day-ahead forecast (e.g., Hirth et al., 2023). However, this alternative model specification does not greatly impact the model results.[58]

In the primary model specifications, fuel and certificate prices are utilized as covariates in both estimation stages. This approach aims to enhance the precision of estimation in the first stage, in identifying the relationship between the forecast of wind power generation and the electricity price. However, the potential for endogeneity issues arises when incorporating these covariates in the second stage: It is conceivable that electricity demand influences gas, coal, and EUA prices, given the impact of electricity demand on the demand for these commodities. An alternative model specification is employed to address this concern, wherein these price data are omitted from both stages. Although this may reduce the precision of estimation in the first stage, the estimation remains fundamentally valid as long as the instrumental variable requirements are met, and a strong relationship exists between the instrument and the variable being explained (Angrist & Pischke, 2008). The corresponding model results (Appendix 4.8.6) confirm the presented results of the primary model specifications (Models 1 to 5). Even without the price covariates, the wind energy forecast remains a strong instrument, and the estimated demand responses exhibit only minimal changes. These results further validate the analysis presented, indicating that any potential endogeneity concerns arising from the price covariates have negligible impact on the main findings.

4.7 Conclusion

In a power system with a large share of intermittent generators, it is increasingly important to understand how demand responds to price signals, especially when prices are high. Electricity prices in 2021 and 2022 were higher than ever. This offers the opportunity to better understand how demand responds under these circumstances. Against this backdrop, this paper focuses on examining the short-term (hourly) elasticity of electricity demand in Germany. By analyzing the new observations of high prices, I aim to explore the functional relationship between demand response and price levels across a broader range of price dispersion. I analyze both linear and log-log demand-price relationships, exploring the dynamics and complexities of demand response to varying price levels.

[57] Appendix 4.8.6 contains the results for model specifications, including covariates for the availability of nuclear, hydro and coal-fired power generation.

[58] Appendix 4.8.2 contains the results for model specifications using wind electricity generation as an instrument.

To this end, I first examine the characteristics of the two functional forms of the demand curve and establish three hypotheses for empirical analysis. I employ a two-stage least squares (2SLS) approach to address the simultaneity between demand and prices. The hourly demand response to hourly day-ahead prices is determined using the day-ahead wind power generation forecast as an IV for the price. I calculate separate models for the entire 2015-2022 period, as well as subsets of the high- and low-price years.

In the linear model that includes all observation years, an increase in price by 1 EUR/MWh, all else equal, leads to a decrease in demand of about 62 MW. The estimate of the decrease in demand for the low-price years is higher (–109.4) and lower (–34.35) for the high-price years. The estimates for the different time subsets in the log-log model are closer together. All else equal, the 1 % increase in price leads to a 4.5 % decrease in demand when considering all observations, 4.2 % for the low-price years, and 5.3 % for the high-price years. Whereby the confidence intervals of the individual estimators overlap.

The quantitative findings provide confirmation for the formulated hypotheses. Consistent with Hypotheses 1 and 2, the results demonstrate that while a linear relationship between demand and price can yield similar average elasticities to the assumption of constant elasticities for low prices, this is no longer the case for high-price years. The linear demand response decreases with the price. Therefore, the linear estimators for the high-price and low-price years differ significantly, and this also carries over to the average elasticity values derived from them. In contrast, as anticipated by Hypothesis 3, the use of the log-log formulation effectively captures the decrease in absolute demand response (per price change of 1 EUR/MWh), making it a preferable approach when dealing with substantial price spreads.

For researchers and policymakers, the results imply that using elasticities based on the linear approximation of the demand curve should be critically questioned. Possible applications for such elasticity estimates could be electricity market, energy system or price forecasting models. In particular, if the application purpose includes the occurrence of high prices, the decreasing linear demand response to prices should be accounted for.

The estimated elasticity values can be used in further research, e.g. in electricity and energy market models, to address diverse inquiries. In addition to the already mentioned example of estimating necessary controllable capacities, this could also include other questions of infrastructure planning, market design and operational decisions in the electricity sector. It is worth noting that the potential influence of autocorrelation on the estimation results should be duly considered, as the estimators capture time-crossing effects of price movements on demand. This presents an avenue for further investigation into isolating the individual effects and quantifying their magnitude. This paper limits its consideration to two possible assumptions for specifying the demand function, linear and log-log. The idea behind this is that these two represent the most common specifications that are

widely used. However, both can, of course, only be approximations of reality. In further research, the use of piece-wise linear models or quantile regression models would be conceivable to investigate the dependence of the demand response on the price level in a more detailed way. Moreover, the present research is limited to the investigation of short-term elasticities. Long-term elasticities and the extent to which they have changed as a function of price levels would be a promising topic for further research.

4.8 Appendix

4.8.1 OLS estimation

Table 4.5 shows the results of the main models (2a) and (2b) compared to the results of simple OLS estimations. The results of the OLS estimation are biased due to the simultaneity issue between demand and price. Accordingly, the estimators show non-intuitive results. Both OLS models have positive estimated demand responses to a price increase. The results confirm that using an instrumental variable or a comparable approach is necessary to obtain unbiased results.

Table 4.5: Comparison of main model results and results for OLS estimation.

	linear		log-log	
	(2a) 2SLS	(5a) OLS	(2b) 2SLS	(5b) OLS
Price [EUR/MWh]	-61.81***	16.14***	-0.0455***	0.0134***
Wind [GW]		133.87***		0.0184***
PV [GW]	-204.0***	-9.533**	-0.0240***	-0.0065***
Gas [EUR/MWh]	86.41***	-46.66***	0.0355***	0.0039**
Coal [EUR/MWh]	61.79	41.60***	0.0006	-0.0089***
EUA [EUR/tCO2]	150.8***	78.66***	0.0400***	0.0243***
Heating degrees [°C]	379.1***	335.8***	0.0279***	0.0233***
Cooling degrees [°C]	176.4***	71.83***	0.0225***	0.0188***
Dummy variables				
Hours	Yes	Yes	Yes	Yes
Weekdays	Yes	Yes	Yes	Yes
Months	Yes	Yes	Yes	Yes
Years	Yes	Yes	Yes	Yes
Fit statistics				
Adjusted R^2	0.868	0.914	0.885	0.914
Observations	65920	65920	65011	65011

95% confidence intervals in brackets. * $p < 0.05$, ** $p < 0.01$, *** $p < 0.001$.

4.8.2 Alternative IV specifications

Figure 4.10 shows the estimators and confidence intervals for the main model specification and two sensitivities. Adding the day-ahead PV generation forecast as IV does not fundamentally change the results. Compared to the main model specification, the estimators of the price effect are slightly lower in all models. This finding is consistent with Hirth et al. (2023). Using the actual wind generation instead of the forecast hardly influences the model's results.

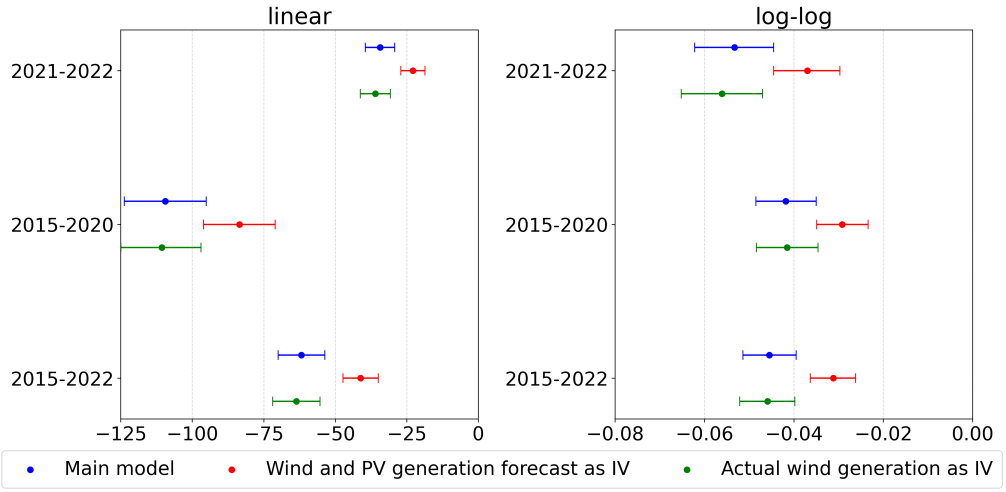

Figure 4.10: Estimators for the price effect on demand for the linear (left) and log-log model specification (right). Results are shown for the main model specification (Table 4.3 and Table 4.4) (blue), a model specification where the day-ahead PV generation forecast was included as additional IV (red) and a model specification where the actual wind generation was used instead of the forecast. Whiskers indicate the 95% confidence interval.

4.8.3 Effect of dummy controls

Table 4.6 shows the main model results of the linear model specification for the years 2015-2022 (2a) compared to the results of model specifications with less dummy control variables (6)-(9). The model without dummy controls (6) does not produce plausible results, e.g. the influence of PV generation on demand is strongly positive due to temporal correlation. Adding dummy controls for the hour of a day (7) can partially correct for this: the sign of the estimator becomes negative. Model (8) further includes dummies for the day of the week. Since there are major differences in the demand structure of weekends and weekdays, the Adjusted R squared and, thus, the model's fit increase significantly. Adding monthly dummies to the adjustment for seasonal effects (8) reduces, in particular, the estimated impact of weather effects (Heating and cooling degrees, PV generation). Finally, the addition of the yearly dummies (main model (2a)) especially affects the estimators of the impact of fuel and emission prices since the influence of changing power plant capacities over time is captured in these dummies.

Table 4.6: Comparison of main linear model results for the years 2015-2022 and results of model specifications with less dummy control variables.

	(6)	(7)	(8)	(9)	(2a)
Price [EUR/MWh]	-123.5***	-72.71***	-73.08***	-58.98***	-61.81***
PV [GW]	472.4***	-307.3***	-289.6***	-212.1***	-204.0***
Gas [EUR/MWh]	228.5***	108.5***	103.8***	80.38***	86.41***
Coal [EUR/MWh]	-172.7***	-2.982	10.84	22.47***	61.79***
EUA [EUR/tCO2]	23.72***	25.12***	26.39***	15.66***	150.8***
Heating degrees [°C]	715.9***	560.2***	567.6***	389.2***	379.1***
Cooling degrees [°C]	296.5***	227.0***	222.7***	190.4***	176.4***
Dummy variables					
Hours	No	Yes	Yes	Yes	Yes
Weekdays	No	No	Yes	Yes	Yes
Months	No	No	No	Yes	Yes
Years	No	No	No	No	Yes
Fit statistics					
Adjusted R^2		0.505	0.836	0.861	0.868
Observations	65920	65920	65920	65920	65920

95% confidence intervals in brackets. * $p < 0.05$, ** $p < 0.01$, *** $p < 0.001$.

4.8.4 Within-variance of the covariates

I exploit the within-variation of the explanatory variables after controlling for time effects when estimating their impacts on the dependent variable. To this end, I include time-related dummy controls in my model. I calculate the variation of the covariates after controlling for time effects by regressing them on the control dummies. Table 4.7 shows the standard deviations of the corresponding residuals, calculated for the linear model specification (2a) and the log-log specification (2b). The within-variation is still considerable after controlling for the time effects. For example, the standard deviation of the main explanatory variable, $Price_t$, is much bigger than the discussed treatments of 1 EUR/MWh. The listed values in Table 4.7 may support the interpretation of the estimated treatment effects of the explanatory variables (Mummolo & Peterson, 2018).

Table 4.7: Within standard deviation of the variables

Model:	(2a)	(2b)
Price [EUR/MWh]	45.44	0.61
Wind [GW]	8.41	0.80
PV [GW]	3.88	0.45
Gas [EUR/MWh]	17.20	0.27
Coal [EUR/MWh]	3.58	0.20
EUA [EUR/tCO2]	4.55	0.15
Heating degrees [°C]	2.89	0.52
Cooling degrees [°C]	2.15	0.52

4.8.5 Estimators for dummy variables

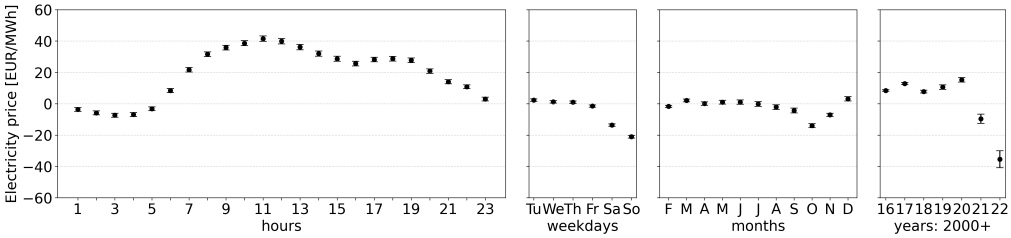

Figure 4.11: Time dummies in the linear first stage (1a)

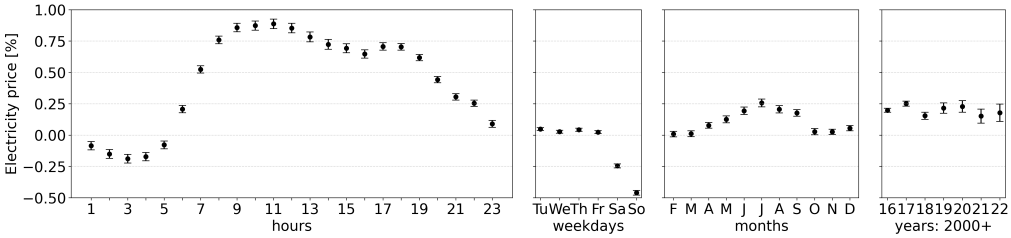

Figure 4.12: Time dummies in the log-log first stage (1b)

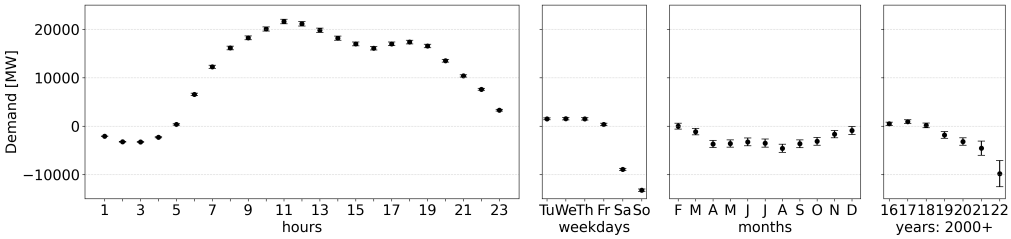

Figure 4.13: Time dummies in the linear second stage 2015-2022 (2a)

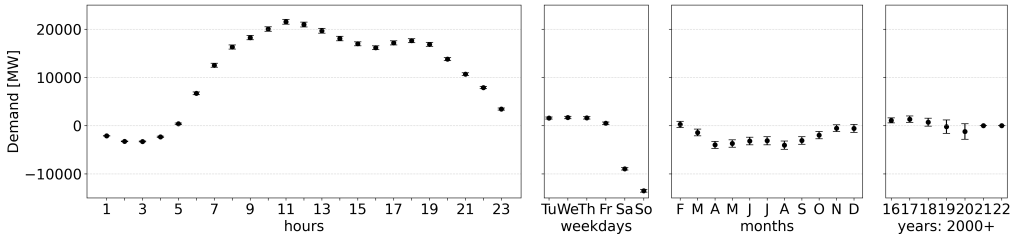

Figure 4.14: Time dummies in the linear second stage 2015-2020 (3a)

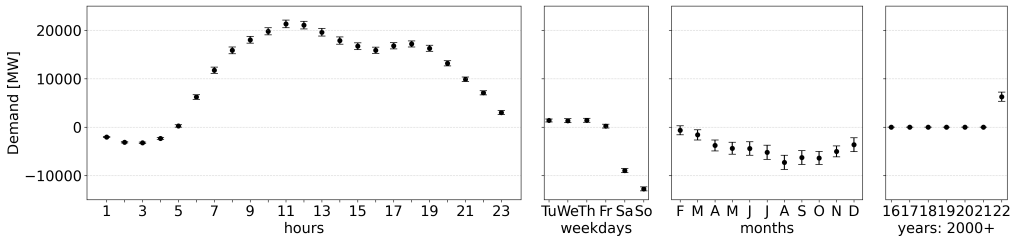

Figure 4.15: Time dummies in the linear second stage 2021-2022 (4a)

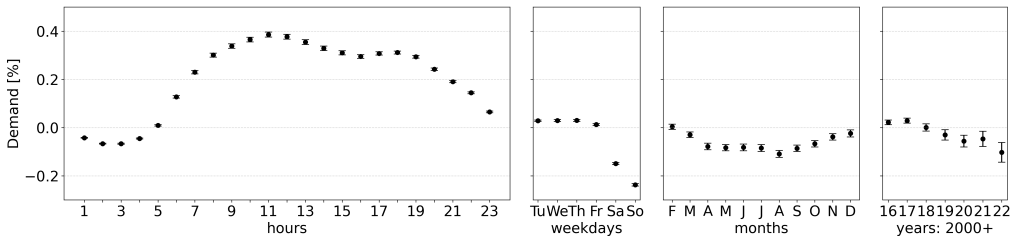

Figure 4.16: Time dummies in the log-log second stage 2015-2022 (2b)

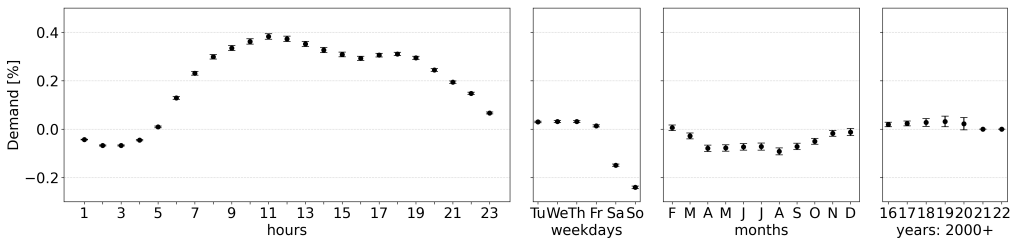

Figure 4.17: Time dummies in the log-log second stage 2015-2020 (3b)

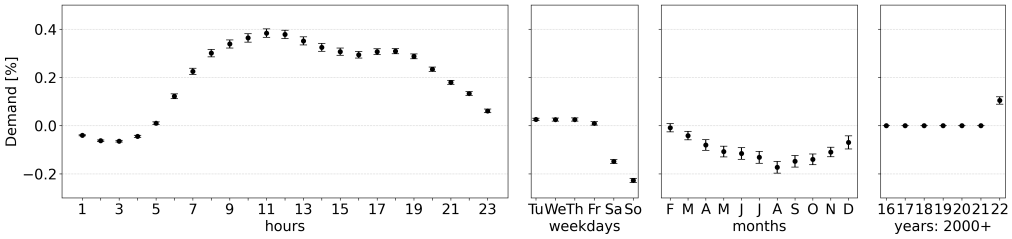

Figure 4.18: Time dummies in the log-log second stage 2021-2022 (4b)

4.8.6 Further estimation results

Models with alternative separation dates

Figure 4.19 shows the estimators and confidence intervals for the main model specification and two alternative models with differing separation dates (X) between the low price time period and high price time period: after the first Quarter of 2021 (red) and after the first half of 2021 (green). The choice of the separation date hardly changes the results. Since the choice of a later date increases the price differences between the subsets, the linear estimates for the subsets diverge even further. In comparison, the estimates for the subsets in the log-log models move closer together. The results thus reinforce the validity of statements made based on the main model specifications.

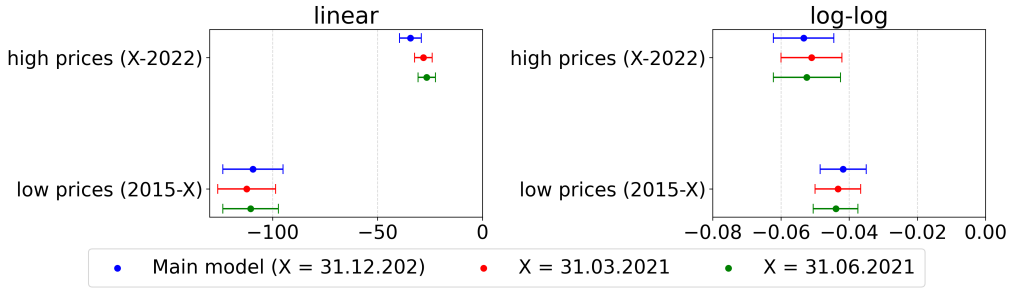

Figure 4.19: Estimators for the price effect on demand for the linear (left) and log-log model specification (right), separately for low and high price time subsets. Results are shown for the main model specification (Table 4.3 and Table 4.4) (blue) and two model specifications with differing separation dates (X) between the low price time period and high price time period. Whiskers indicate the 95% confidence interval.

Models with further supply-side covariates

Figure 4.20 shows the estimators and confidence intervals for the main model specification and an alternative model specification that includes additional supply-side covariates representing German and French available nuclear capacities and German available hydro-power and coal-power capacities. As data on power

plant capacities and availability are unavailable, I use proxies based on the hourly generation data from ENTSO-E (2023). To approximate weekly/monthly available capacities, I use the weekly/monthly generation maxima. I cannot use the hourly or even daily values of generation directly as available capacities, as the generation output of these plants reacts to electricity prices, which would lead to endogeneity issues. I use the weekly maximum for nuclear and hydro generation, as the electricity generation from these plants is less reactive to prices. To approximate the development of available coal-power capacities in Germany, I use the monthly maximum generation values. Including these supply-side covariates hardly changes the results.

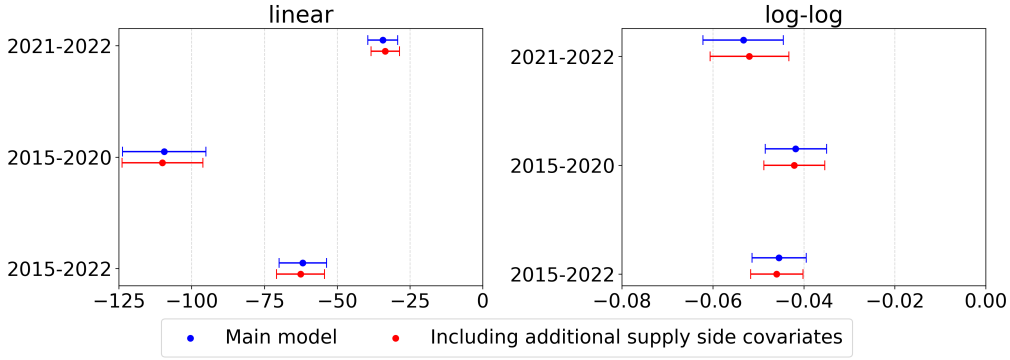

Figure 4.20: Estimators for the price effect on demand for the linear (left) and log-log model specification (right). Results are shown for the main model specification (Table 4.3 and Table 4.4) (blue), and a model specification including additional supply-side covariates (red). Whiskers indicate the 95% confidence interval.

Models without price covariates

Table 4.8 shows the estimators and confidence intervals for the first stage of model specifications without the utilization of gas, coal and EUA prices as covariates. The estimators for the influence of $Wind_t$ on the $Price_t$ are slightly higher than in the main model specifications (Model 1a and 1b). The partial R squared still shows for both models (linear and log-log) that $Wind_t$ explains a relevant part of the variance of the price. The F-statistics of the Montiel-Pflueger robust weak instrument test at 5% confidence level are 9,254 and 7,924, respectively, which is well above the critical value of the test of 37.42. Based on the test result and the significance at the first stage, I conclude that also without the usage of the price covariates $Wind_t$ remains a strong instrument for $Price_t$.

Table 4.8: First stage results of model specifications without price covariates

	(10a) linear		(10b) log-log	
Wind [GW]	-1.978***	[-2.02,-1.94]	-0.319***	[-0.33,-0.31]
PV [GW]	-2.482***	[-2.59,-2.37]	-0.300***	[-0.31,-0.29]
Heating degrees [°C]	0.978***	[0.87,1.09]	0.0897***	[0.08,0.10]
Cooling degrees [°C]	1.734***	[1.54,1.93]	0.0669***	[0.06,0.08]
Dummy variables				
Hours	Yes		Yes	
Weekdays	Yes		Yes	
Months	Yes		Yes	
Years	Yes		Yes	
Fit statistics				
Partial R^2 Wind	0.132		0.174	
Adjusted R^2	0.702		0.643	
Observations	65920		65011	

95% confidence intervals in brackets. * $p < 0.05$, ** $p < 0.01$, *** $p < 0.001$.

The Tables 4.9 and 4.10 show the estimators and confidence intervals for the second stage of model specifications without the utilization of gas, coal and EUA prices as covariates. The estimators of the Models 11 to 13 are of very similar magnitudes to the estimators of the main model specifications (Model 3 to 5). The results thus confirm the analysis results, suggesting that any potential endogeneity issue resulting from the price covariates is inconsequential.

Table 4.9: Second stage results of the linear specification without price covariates

	(11a) 2015-2022	(12a) 2015-2020	(13a) 2021-2022
Price [EUR/MWh]	-56.33***	-109.1***	-34.14***
	[-64.28,-48.39]	[-124.00,-94.26]	[-40.61,-27.68]
PV [GW]	-188.7***	-171.0***	-212.8***
	[-216.16,-161.21]	[-199.52,-142.52]	[-256.20,-169.46]
Heating degrees [°C]	390.9***	362.9***	435.2***
	[339.34,442.53]	[322.40,403.47]	[334.82,535.60]
Cooling degrees [°C]	190.4***	149.5***	274.6***
	[144.50,236.33]	[112.24,186.85]	[179.26,369.97]
Dummy variables			
Hours	Yes	Yes	Yes
Weekdays	Yes	Yes	Yes
Months	Yes	Yes	Yes
Years	Yes	Yes	Yes
Fit statistics			
Adjusted R^2	0.844	0.881	0.836
Observations	65920	49434	16486

95% confidence intervals in brackets. * $p < 0.05$, ** $p < 0.01$, *** $p < 0.001$.
Standard errors are calculated as Newey-West HAC robust standard errors.

Table 4.10: Second stage results of the log-log specification without price covariates

	(11b) 2015-2022	(12b) 2015-2020	(13b) 2021-2022
Price [EUR/MWh] (log)	-0.0454***	-0.0421***	-0.0536***
	[-0.05,-0.04]	[-0.05,-0.03]	[-0.06,-0.04]
PV [GW] (log+1)	-0.0243***	-0.0218***	-0.0286***
	[-0.03,-0.02]	[-0.03,-0.02]	[-0.03,-0.02]
Heating degrees [°C] (log+1)	0.0285***	0.0252***	0.0331***
	[0.02,0.03]	[0.02,0.03]	[0.02,0.04]
Cooling degrees [°C] (log+1)	0.0228***	0.0210***	0.0266***
	[0.02,0.03]	[0.02,0.02]	[0.02,0.03]
Dummy variables			
Hours	Yes	Yes	Yes
Weekdays	Yes	Yes	Yes
Months	Yes	Yes	Yes
Years	Yes	Yes	Yes
Adjusted R^2	0.880	0.890	0.853
Observations	65011	48670	16341

95% confidence intervals in brackets. * $p < 0.05$, ** $p < 0.01$, *** $p < 0.001$.
Standard errors are calculated as Newey-West HAC robust standard errors.

5 Diffusion of electric vehicles and their flexibility potential for smoothing residual demand - A spatio-temporal analysis for Germany

5.1 Introduction

The energy transition towards a decarbonized future brings about fundamental changes in the established power system, including increasing strain on distribution grid components. First, the widespread implementation of decentralized renewable energy systems, such as wind and photovoltaic (PV) systems, which are mostly connected to the low and medium-voltage grid, increases the feed-in of electricity into the distribution grid. Second, new demand applications emerge in the distribution grid, e.g., charging electric vehicles (EV), increasing the load. Both developments increase load and feed-in peaks on the national level as well as place an additional burden on the technical components of local grids, such as low and medium-voltage transformers, which were designed under different conditions and may need to be replaced or expanded to accommodate the changes. The charging of EVs can increase peak load and put a strain on existing distribution grid equipment. However, the flexibility in EV charging offers a solution to mitigate this impact. By charging during periods of high renewable energy generation, load and feed-in peaks can be reduced, thus reducing the strain on the grid.

The availability and necessity of EV charging flexibility depend on various regionally distinct factors, such as the share of the EV load in the total load, the level and structure of the residual load[59], the correlation between flexibility potential and regional load or generation peaks, and the distribution of charging to the different locations (at home, at work, or other places). Thus, to fully comprehend the potential of EV charging flexibility in reducing peaks, a comprehensive regional analysis and quantification of the flexibility potential and its effects are crucial.

Two basic deployment strategies for deploying local EV charging flexibility can be distinguished. On the one hand, flexibility can be used to flatten the national residual load by reducing positive and negative peaks. That is, EV charging flexibility is used to reduce load during peak load situations and to absorb excess renewable generation during times of high generation. Such a deployment strategy

[59]The residual load is the difference between total load and generation by intermittent resources.

aims to reduce system costs by not employing (or even investing in) expensive generation technologies and fully utilizing generated renewable electricity. An incentive scheme for such a deployment strategy would be the incentivization of flexibility deployment based on the uniform pricing signals of the national electricity market. Alternatively, flexibility can be dispatched to smooth the regional residual demand. Such a deployment strategy aims to reduce the load on regional distribution grid components. This approach would reduce costs for the expansion of these grids.[60] Incentive schemes for such a deployment strategy would be, for example, quantity or price signals from distribution system operators according to the expected grid status. The goals of the deployment strategies may be partially opposed, and the question arises of how the two strategies affect the respective objectives.

In this research paper, we therefore first examine the regional evolution of residual load, load and feed-in peaks in Germany until 2045. Our analysis focuses on the spatial and temporal diffusion of EV charging, considering regional sigmoid transition pathways of EV adoption and regional and user-specific driving and load profiles. Our analysis is based on NUTS 3 regional resolution level data.[61] We then develop and implement a spatio-temporal optimization model for EV load flexibility based on the analysis. This model aims to quantify the potential of EV load flexibility of home charging in smoothing residual load time series and reducing load and feed-in peaks. We compare two different deployment scenarios: (1) using flexibility to flatten the national residual load time series, which corresponds to the use of flexibility based on price signals from the national electricity market, and (2) using flexibility on regional residual load and, thus, reduce the strain on regional distribution grid components.

EV charging is considered a major source of demand flexibility, as shifting charging operations can reduce peak loads and thus reduce the need for grid expansion. While some sources also note this at the transmission grid level (Amann et al., 2022; Gunkel et al., 2020), the impact of smart charging is predominantly analyzed at the level of the local distribution grid (e.g. Flataker et al., 2022). Powell et al. (2022) demonstrate that the flexibility of EV charging possesses not just a significant temporal component but also a geographical one, reflecting the propensity of EVs to move between locations over the course of a day. They underscored the necessity for a comprehensive area-wide charging infrastructure to facilitate daytime charging, which could utilize surplus PV generation and avert the late afternoon peak load, as exemplified by workplace charging. Such conditions have direct implications for power system requirements in terms of storage and ramping needs or emissions.

[60] Agora Verkehrswende et al. (2019) quantifies the investment costs in the low and medium voltage grid under the assumption of uncontrolled charging of EVs depending on the charging capacity and the number of electric cars with € 23 to 72 billion between 2020-2030.

[61] The Nomenclature of Territorial Units for Statistics (NUTS) is a hierarchical system for dividing European territory into territorial units. While, for example, NUTS 0 stands for states, NUTS 3 corresponds to smaller units within states, such as districts.

Given the residual load-smoothing potential of flexible end-uses, such as electric vehicle charging, there seems to be a general recognition in the European Union that local flexibility mechanisms are of significant interest for the operation of future distribution networks (CEER, Council of European Energy Regulators, 2020). Regulators have begun to put in place the regulatory framework to incentivize the provision of flexibility and its call-off by distribution system operators, which they are required to do by Article 32 of Directive (2019/944) as part of the clean energy package (Council of European Union & European Parliament, 2019).

However, while there is an elaborated stream of research analyzing the provision of regional flexibility from a market design perspective (Radecke et al., 2019; Rebenaque et al., 2023), to our knowledge, there is no research addressing the concrete added value of local flexibility use in contrast to centralized electricity markets, neither for demand-side flexibility in general nor for EV charging in particular. We attempt to fill this gap with a focus on the German power system at the national and regional levels.

From a system perspective, there are several studies that shed light on the transformation of the German energy and consumption sector until 2045 and beyond (e.g. Burchardt et al., 2021; Consentec et al., 2021; dena, 2021; Kopernikus-Projekt Ariadne, 2021; Prognos et al., 2020). The studies develop individual scenarios for possible pathways to reduce greenhouse gas emissions and to diffuse and use technologies, such as wind turbines, PV systems, or EVs, on the demand and supply side. While the specific numbers on installed capacity and electric vehicles differ, the emerging trends, a significant increase compared to today, are the same (dena, 2022). However, the studies only marginally touch on the regional perspective of the transition and the regional balance of supply and demand.

The regional matching of supply and demand for the German energy system is addressed by Kockel et al. (2022) and Kühnbach et al. (2021). Kockel et al. (2022) analyze the development of regional residual loads in Germany on a spatio-temporal basis, related to an emission reduction of 95% by 2050 based on dena (2018). They note significant potential for demand-side flexibility, but do not specifically model or quantify it. Because the study only considers 2019, with very low EV penetration, and 2050, with penetration near 100%, the EV load is determined by a uniform distribution of regional demand based on regional vehicle counts. However, this approach is not appropriate for modeling EV penetration for the years in between, as it neglects regionally varying penetration rates. For EV charging, the same profiles are used for each region, abstracting from regional characteristics such as longer driving distances in rural areas compared to urban areas.

Kühnbach et al. (2021) focuses primarily on regionalized demand and the potential of demand response. In addition to analyzing regional supply and demand balancing, they examine the residual load-smoothing potential of flexible demand on a regional basis. They compare 2015 and 2030 and define indicators to

measure supply-demand balance. They conclude that demand management is most effective in regions that frequently alternate between demand and supply deficits. However, the study lacks a comparison of regional results with a centralized energy system, and as in Kockel et al. (2022), the chosen scenario does not fit with Germany's recent climate protection goals of climate neutrality by 2045 (Deutscher Bundestag, 2021).

To be compatible with current German climate targets, we develop a scenario based on KN100 from dena (2021). In contrast to existing literature, our analysis focuses on the consistent regional and temporal modeling of EV charging demand and flexibility potentials. To this end, we model EV diffusion for 2019, 2030, and 2045 by utilizing the Bass model (Bass, 1969) that has been applied to EV diffusion in various countries in the literature (Becker et al., 2009; Song, 2013; Won et al., 2009; Zhu et al., 2017). We derive the load and flexibility profiles of EVs from the mobility patterns of the German Mobility Panel (MOP) (KIT - Institut für Verkehrswesen, 2021).

We address two key questions: To what extent can electric vehicle home charging flexibility reduce load and feed-in peaks at the national and regional levels? What are the impacts of the two different deployment strategies on national and regional residual demand curves, as well as load and feed-in peaks? Besides answering these questions, this paper adds to the existing literature in multiple ways:

- Analysis of the spatio-temporal evolution of residual demand under a current scenario for Germany's energy transition pathway until 2045 with a focus on EV diffusion and load.
- Introduction and application of a method for modeling target-consistent regional and temporal diffusion of electric vehicles using sigmoid functions.
- Derivation of user- and region-specific driving, load and flexibility profiles for electric vehicles in Germany until 2045.
- Development and implementation of a model for spatio-temporal deployment of electric vehicle load flexibility under different objectives.

Concerning the development of future residual load, we find that positive and negative peaks in residual load increase over the years on the regional level and aggregated over Germany. The correlation between residual load and EV charging profiles is high in 2019 but decreases until 2045. This implies that the marginal utility of charging flexibility to reduce load peaks decreases over time, although the flexibility potential in absolute terms is increasing with growing EV adoption.

We find that, especially in load- and PV-dominated regions, the nationally incentivized activation of flexibility can result in drastically higher regional demand peaks compared to a scenario without the use of charging flexibility. Our study shows that the two scenarios of flexibility activation can be contradictory in their effects: While the regional incentivization is less efficient in reducing peaks on the national level, the national incentivization leads to increased strain on local

level. Our findings provide valuable insights into the challenges faced by regional grids and the development of strategies to harness EV flexibility to address these challenges.

The paper is structured as follows: In a first step (Section 5.2), regionalized diffusion curves for EV expansion from 2019 to 2045 and regionalized charging profiles for different user types are developed. Then a scenario of electricity demand development and renewable capacity expansion until 2045 is regionalized, and corresponding demand and renewable generation time series are presented (Section 5.3). In Section 5.4, a model for the regionalized optimization of EV charging flexibility is developed. The results (Section 5.5) address the estimation of residual demand time series for the years 2019, 2030, and 2045 on a regional and national level as well as the potential and effects of EV charging flexibility under two different deployment strategies. The paper concludes with a summary of the findings and their implications for the transformation of the power system and usage of EV charging flexibility.

5.2 Spatio-temporal expansion of private electric vehicles

This chapter focuses on the projection of regional expansion paths of electric vehicles and the development of a method to derive individual load and flexibility profiles for each region. Section 5.2.1 describes the applied method to derive regionalized transition pathways for electric vehicles. Each region reflects a NUTS 3 district of Germany. In Section 5.2.2, we develop load profiles for each region, distinguishing between different user types based on their charging locations and times.

5.2.1 Regional diffusion of electric vehicles

In recent years, several studies (e.g. Burchardt et al., 2021; Consentec et al., 2021; dena, 2021; Kopernikus-Projekt Ariadne, 2021; Prognos et al., 2020) presented development pathways for the future energy system and the transition to e-mobility in Germany. The "dena study - towards climate neutrality" projects 14 mil. electric vehicles in 2030 and 36 mil. in 2045 in its climate neutrality scenario "KN100" (dena, 2021). Also, in the summer of 2022, the German Federal Ministry for Economic Affairs and Climate Action announced that 15 mil. electric vehicles should be achieved by 2030 (German Government, 2022). Despite these national projections and targets, there is a lack of scenarios at the regional level. Regions in Germany are very heterogeneous, and it can be assumed that the penetration speeds with electric cars differ among them. Therefore, we aim at decomposing

the national transition scenarios to the local level based on a NUTS 3 resolution, which is, for Germany, equivalent to individual districts.

Forecasting methods for the regional diffusion of technologies can be primarily categorized into agent-based, consumer choice, and diffusion rate and time-series methods (Ayyadi & Maaroufi, 2018). While methods of the first kind are simulation-based, simulating the interactions of agents and how these affect the market, consumer choice models depend on assumptions of consumer decisions about new technology according to certain characteristics (Kumar et al., 2022). Methods of the third kind rely on time series and diffusion rates to study technology diffusion. Existing research utilizing the latter methods primarily focuses on four models: Gompertz (Gompertz, 1825; Muraleedharakurup et al., 2010), Logistic (Berger, 1981; Kumar et al., 2022), Bass, and Generalised Bass (Bass, 1969) diffusion models. The Bass diffusion model fits our problem well because it can account for different speeds in the early and late stages of the diffusion, which is not the case for other models (Bass, 1969; Pavlidou, 2010). It has also been widely applied in the analysis of EV diffusion in other countries and for earlier years (Becker et al., 2009; Song, 2013; Won et al., 2009; Zhu et al., 2017). The Bass diffusion model and its transformation are written in Equations (5.1) and (5.2) as a sigmoid function (Bass, 1969).

$$\frac{f(t)}{1-F(t)} = p + q\frac{A(t)}{m} = p + qF(t) \tag{5.1}$$

$$F(t) = \frac{A(t)}{m} = \int_0^T f(t)dt \quad with\, F(0) = 0 \tag{5.2}$$

The function $f(t)$ describes the likelihood of a purchase at time t with p being the probability of initial purchases at the start of the innovation ($t = 0$). p is referred to as the coefficient for innovators, while q is the coefficient for imitators. The two coefficients define the slope of the sigmoid function at the beginning and at the end. The cumulative diffusion level at time t $F(t)$ equals the cumulative number of adopters $A(t)$, which in our case reflects the number of EV owners divided by the total market size m, the total number of cars.

The diffusion level $F(t)$ in our approach is described as shown in Equation (5.3).[62] The parameter t_0 is included in the function to take the beginning of the diffusion into account and to move the diffusion curve in time. Further, we introduce a scaling factor s. With the scaling factor, we ensure that the diffusion curve meets the maximum penetration rate in 2045. While improving the fit of the sigmoid function to the data points between 2019 and 2045, the scaling factor increases the maximum relative market potential in 2050 above 100%. Since our

[62]The transformation steps are depicted in Appendix 5.7.1.

analysis focuses on the years until 2045, this is not an issue.

$$F(t) = s \cdot \frac{1 - e^{-(p+q)(t-t_0)}}{1 + \frac{q}{p} e^{-(p+q)(t-t_0)}} \tag{5.3}$$

Fitting the curve

We derive our regional scenarios of electric vehicle diffusion by regional decomposition of the national scenario "KN100" of dena (2021), adjusted by the target of 15 million electric vehicles until 2030 defined by the German government (German Government, 2022). The development of regional scenarios using the Bass model is done in a two-step process, visualized in Figure 5.1.

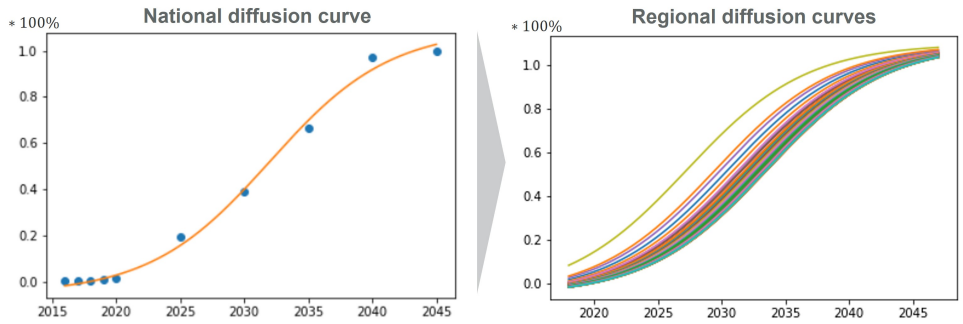

Figure 5.1: Development of regional Diffusion Curves

In the first step, the Bass function is fitted to the national scenario using the non-linear least squares (NLLS) method according to Newville et al. (2016). The left part of Figure 5.1 shows the rate of electric vehicles over time. The blue dots represent the penetration rate in the different years based on historic developments (until 2020) and the national scenario. The penetration rate of 42% in 2030 matches the number of 15 mil. electric vehicles, and a penetration rate of 100% corresponds to 36 mil. electric vehicles. The parameter s, the maximum relative market potential of electric vehicles, is also computed by the fitting method. The computed values for the estimates are: $\hat{s} = 1.096$, $\hat{p} = 0.203$ and $\hat{q} = 0.010$.

While the derived national diffusion curve is fitted to the historic national electric vehicle penetration, historic developments in the specific German regions can drastically differ. In the start year t_0=2020 (the last year regional data is available), every region has its individual position on the curve. Some regions are above the national average and some are below. Therefore, in a second step, we individually shift the national diffusion curve along the time axis for each NUTS 3 region to achieve the specific penetration level, as it is visualized in the right part of Figure 5.1. To calculate the regional EV diffusion levels in 2020 we use historical data of the EV fleet from 2017 to 2020 on postcode level, provided

by the Kraftfahrt-Bundesamt (KBA) in two data sets (Kraftfahrt-Bundesamt, 2018b, 2019b, 2020b, 2021b and Kraftfahrt-Bundesamt, 2018a, 2019a, 2020a, 2021a). TThe EV diffusion levels reached in t_0=2020 for each NUTS 3 region $F^{nuts3}(t = t_0)$ are calculated by dividing a region's total EV fleet $EV_{t_0}^{nuts3}$ by the ratio of the total region fleet $Cars_{t_0}^{nuts3}$ to the total national fleet $Cars_{t_0}^{DE}$ times the total German market size for EVs EV_{2045}^{DE}.

$$F^{nuts3}(t = t_0) = \frac{EV_{t_0}^{nuts3}}{EV_{2045}^{nuts3}} \tag{5.4}$$

$$with \quad EV_{2045}^{nuts3} = \frac{Cars_{t_0}^{nuts3}}{Cars_{t_0}^{DE}} \cdot EV_{2045}^{DE} \tag{5.5}$$

To create diffusion curves for each NUTS 3 region, the derived national diffusion curve is moved along the time axis according to the time difference Δt between t_0 and the time t when the EV diffusion level for t_0 of the respective NUTS 3 region is reached on the national diffusion curves. Equation (5.6) describes the approach. Here, the parameters $\hat{s}$, $\hat{p}$ and $\hat{q}$ reflect the estimates of the national diffusion curve. The derivation of the formula, including Δt, can be found in Appendix 5.7.2.

$$F^{nuts3}(t) = \hat{s} \cdot \frac{1 - e^{-(\hat{p}+\hat{q})(t-t_0+\Delta t)}}{1 + \frac{\hat{q}}{\hat{p}} e^{-(\hat{p}+\hat{q})(t-t_0+\Delta t)}} \tag{5.6}$$

To get the total number of electric vehicles in each NUTS 3 region, the diffusion rates are multiplied by the total estimated market size of EVs for each NUTS 3 region. The latter is derived by multiplying the maximum estimated scenario value for EVs (EV_{2045}^{DE}) with the ratio of the total vehicle fleet of each NUTS 3 region in t_0 to the total national fleet according to equation (5.7). To ensure that the national target of EVs in a specific year is equal to the sum of all regional numbers of EVs, a correction factor σ_t is used for scaling. The scaling factor adjusts the diffusion curves in a single point.

$$EV_t^{nuts3} = F^{nuts3}(t) \cdot \frac{Cars_t^{nuts3}}{Cars_t^{DE}} \cdot EV_{2045}^{DE} \cdot \sigma_t \tag{5.7}$$

The result of the modeled diffusion of EVs is presented in Figure 5.2 for the years 2030 and 2045. In terms of consistency with the following sections, the historic distribution is visualized for the year 2019 instead of 2020. In the figure, the total number of EVs in every NUTS 3 region is normalized by the size of each region. In 2019, around 239 thous. electric vehicles do not lead to high penetration rates per square kilometer. In 2030 mainly bigger cities such as Hamburg, Berlin and Munich, as well as some areas in North-Rhine Westphalia, such as Dusseldorf, do have a significant amount of electric vehicles per square kilometer. Later in 2045, the western part of Germany and the Rhine-Main region are highlighted in red. Also, smaller regions, in terms of area but with a high population per square kilometer, have a high relative amount of electric vehicles.

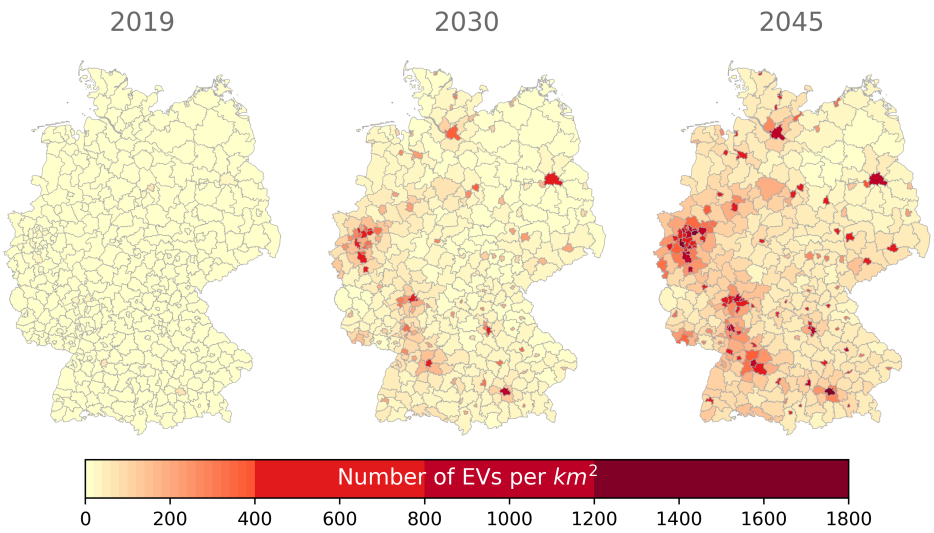

Figure 5.2: Number of electric vehicles in each NUTS 3 region for the years 2030 and 2045

5.2.2 User-specific load and flexibility profiles

The electricity demand of electric passenger vehicles is determined by their underlying driving patterns. For Germany, there are two major panels surveying the mobility behavior of households, *Mobility in Germany (MiD)* (infas et al., 2018) and the *German Mobility Panel (MOP)* (KIT - Institut für Verkehrswesen, 2021). While the MiD is updated every six years, the MOP has been updated annually since 1994. It is a survey-based longitudinal study of the mobility behavior of the German population. Besides household-specific information, it holds data on the households' individual trips, including timestamps, destinations, distances, and modes of travel. The panel categorizes about 14 thousand surveyed households according to ten settlement types, from small villages to metropolises. The dataset and information on the regional settlement structure enable the assignment of households and their respective mobility patterns to different regions. As a common assumption, we assume that the mobility behavior of EVs does not substantially differ from those of conventional passenger cars, and we assume the mobility patterns of vehicles remain constant until 2045. The detailed analysis of 500 thousand individual trips and car-based mobility patterns allows for deriving electric vehicles' energy demand and load profiles and the resulting inherent flexibility of their charging processes by user type, region, charging scenario, and day type for the years 2019, 2030, and 2045.[63]

[63] A brief descriptive analysis of the mobility data is given in Appendix 5.7.3.

Computation of regional differentiated load profiles

By projecting the historical mobility data on the years 2019, 2030, and 2045, average load profiles per vehicle are calculated, which are later scaled by the individual region's total counts of EVs.

The load profiles are calculated for different settlement types, charging scenarios, and day types (weekend and weekday) for each year considered. A total of six settlement types are distinguished, ranging from rural communities to large cities. The charging scenarios represent combinations of three potential charging locations (at home, at work, at other locations). The combinatorial approach results in seven scenarios, e.g., "charging at home and at work, but not at other locations". In this way, a total of 252 profiles are distinguished.

Starting from single trips, consecutive trips within a day are stacked into trip chains to derive the mobility patterns of individual cars in the form of binary time series indicating the standing and driving intervals of the vehicles, including their location. For the trips, the electricity demand is determined based on the distance traveled and the assumed EV fleet's average specific consumption of 0.21 kWh/km in 2019, 0.18 kWh/km in 2030, and 0.15 kWh/km in 2045 (dena, 2021). Assuming a charging power of 11 kW and an immediate start of charging upon arrival at a charging location, the energy demand is translated into profiles. Vehicles charge until the battery is full or a new trip begins. The average load profiles per vehicle are generated by aggregating all profiles and dividing them by the number of vehicles in the respective settlement type, charging scenario, and day type. As an example, the resulting profiles for medium-sized cities for the charging scenarios "charging at home" and "charging at home and work" for the year 2030 are shown in Figure 5.3. When vehicles can only be charged at home, a load peak is observed in the afternoon, while the load is more evenly distributed throughout the day when charging at home and work is possible.

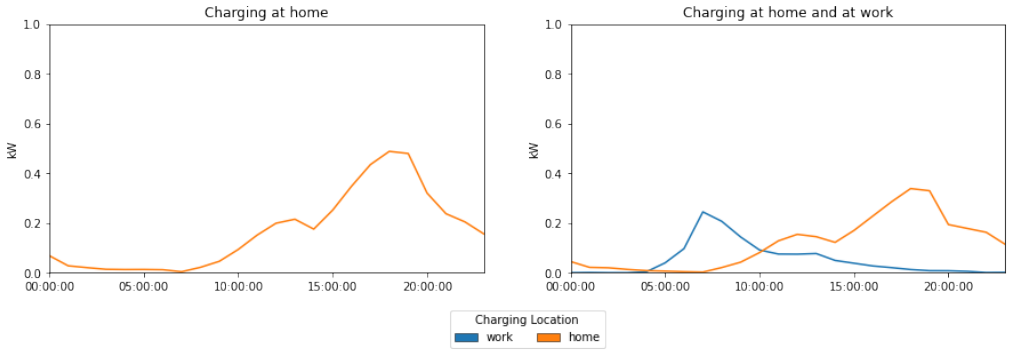

Figure 5.3: Selected load profiles for a medium-sized city in 2045

The final hourly load time series are composed of the standardized profiles and scaled by the respective vehicle counts determined in Section 5.2.1 for each NUTS

3 region. To this end, the regional settlement types are given by BBSR (2022). The proportions of the seven charging scenarios are derived from data on vehicle parking situations at home, distinguished by settlement type based on dena and Prognos (2020)[64]. The scaled load profiles are then used in combination with the results from Section 5.3 to calculate the regional residual load curves in Section 5.5.

Computation of regional differentiated flexibility profiles

To model the home charging flexibility, we derive the flexibility potentials of the charging processes from the mobility patterns and the generated load profiles. The time series of flexibility potential become an input for the flexibility model (Section 5.4), which optimizes the load shifts for charging processes relative to the determined load profiles. Generally, we distinguish between positive and negative charging flexibility while focusing on uni-directional home charging only. Positive flexibility can reduce the load of charging compared to the load profile generated in the previous chapter. Thus, the positive flexibility potential in each hour is equivalent to the determined load profile. Negative flexibility, in turn, means load can potentially be increased in certain intervals. Therefore, the negative flexibility potential is limited upwards by the maximum available capacity. It is calculated as the difference between the generated load profile and the maximum available capacity in each hour if the vehicle is home. For computational reasons, the flexibility model does not model EVs individually, although this would ensure consistency in terms of EV flexibility provision: Car A reduces the load in hour X and increases the load in hour Y. Aggregating all flexibility profiles and centrally optimizing the deployment without restrictions would again lead to inconsistencies and, thus, overestimate the potential for smoothing the residual load: Car A reduces the load in hour X and car B increases the load in hour Y. To address this, we suggest a trade-off between an aggregated centralized, top-down approach and a fully decentralized bottom-up approach using clusters. The mobility patterns are divided into multiple clusters by clustering binary mobility patterns (at home, not at home) using k-medoids to ensure consistency within smaller segments of the observed trip chains. We then consider only the part of each trip chain's flexibility profile that is determined by each cluster centroid's mobility pattern, as conceptually shown in Figure 5.4.

In our analysis, we find eight clusters as a suitable segmentation for the observed mobility patterns for weekdays and weekends. Figure 5.5 shows the resulting eight clusters.

The resulting flexibility profiles for a medium-sized city and the year 2030 are shown in Figure 5.6. Since we only consider flexible charging at home, the positive flexibility is higher when vehicles can only charge at home. In general, the

[64]The shares of the different charging scenarios are depicted in Appendix 5.7.4. We assume equal proportions within the two subgroups of charging scenarios that involve either at least partial home charging or no home charging.

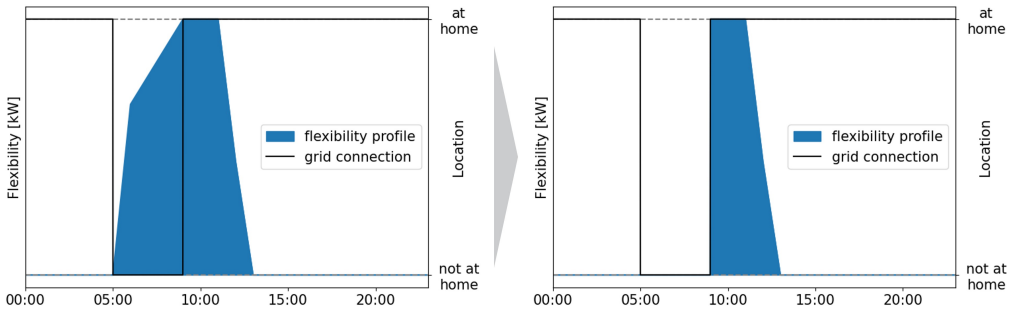

Figure 5.4: Concept for generating flexibility clusters

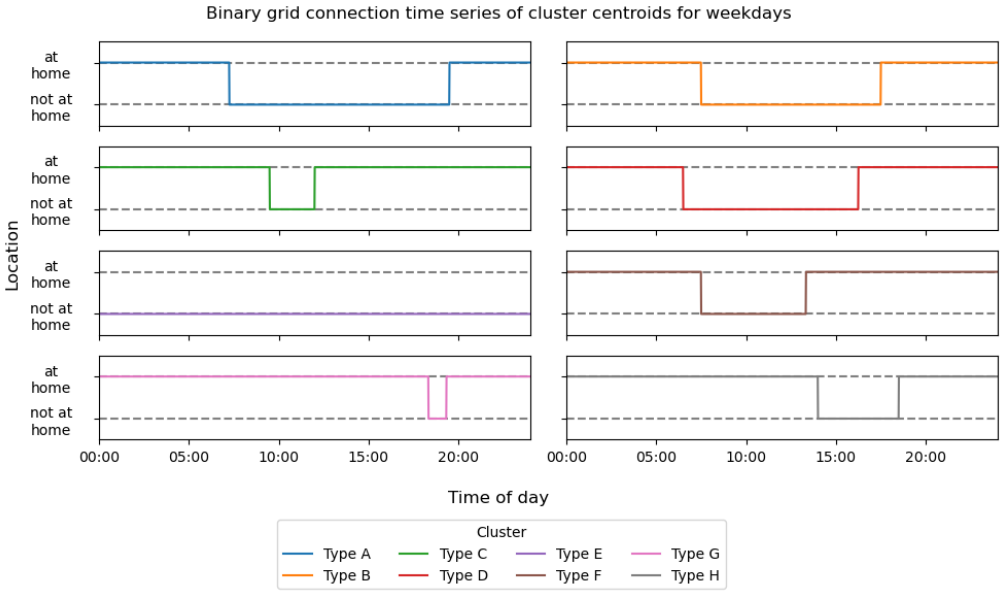

Figure 5.5: Flexibility clusters for weekdays

negative flexibility potential is much higher than the positive flexibility potential, as charging is generally only carried out over short periods in relation to the idle times of the vehicles.

The final flexibility time series for each NUTS 3 region are composed the same way as the load profiles. We assume that all households charging at home are willing to provide flexibility.

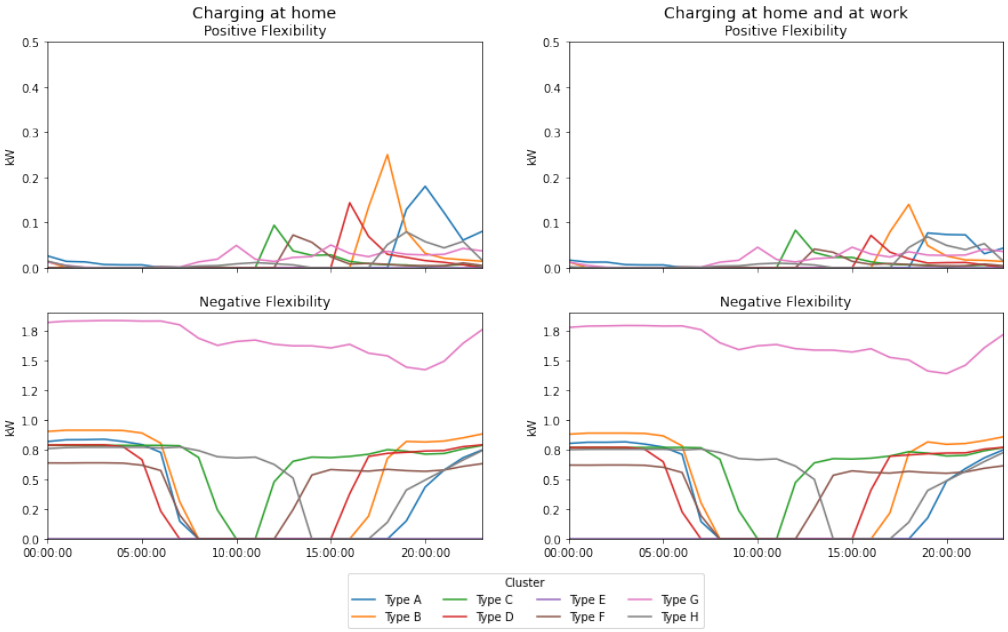

Figure 5.6: Selected flexibility profiles for a medium-sized city in 2045

5.3 Regionalization of demand and supply

In order to examine the potential of using EV home charging flexibility for smoothing national and regional residual demand, we derive regional time series for electricity demand from the other consumption sectors in Section 5.3.1 and electricity generation from renewable energy sources in Section 5.3.2. Both sections focus on the spatial distribution to NUTS 3 regions first and then derive corresponding profiles.

5.3.1 Electricity demand

Spatial distribution of annual demand

Consistent with the EV market development, we adopt the electricity demand development of the remaining consumption sectors until 2045 from the "KN100" scenario from dena (2021). Table 5.1 shows the assumed annual evolution of demand by consumption sector and application.

Table 5.1: Annual electricity demand by sector and application in TWh

Sector	Application	2019	2030	2045
Households	SLP[1] residential	121	119	116
	Heat residential	6	20	29
	Light trucks	0	0	2
Small-scale Industries, Trade and Services	SLP commercial	133	129	118
	Heat commercial	9	21	28
	Base load	4	5	6
	Heavy trucks	0	1	2
	Light trucks	0	2	11
Industry	Heat commercial	4	9	12
	SLP commercial	17	16	19
	Base load	206	241	285
	Heavy trucks	0	5	10
	Light trucks	0	1	3
Rail transport		12	20	24
Conversion sector		8	8	8
Passenger cars[2]		1	34	58
Total		522	625	732

[1] standard load profile
[2] The allocation of the demand from EVs is discussed in Section 5.2. Values deviate from dena (2021) due to updated government targets (15 mil. EVs in 2030).

The spatial allocation of the demand is done in two steps. In the first step, distribution keys, matching the sector-specific demand to the federal states, are derived based on data from Länderarbeitskreis Energiebilanzen (2022).[65] In the second step, sector-specific demand distribution keys to the regions within the federal states are derived. These are based on regional characteristics, such as residents, employees in the tertiary industry, income, and gross value added, taken from VWG (2022a) (2022) and VWG (2022b) (2022). Table 5.2 shows the weighting factors of these characteristics to allocate the demand of the individual sectors from the federal states to regions. The weighting factors are chosen similarly to Bundesnetzagentur (2020).

[65] A detailed discussion of the approach and the derived distribution keys are presented in Appendix 5.7.5.

Table 5.2: Annual electricity demand by sector and application in TWh

Sector	Allocated by	Weighting factor
Households, rail transport	Residents	90%
	Income	10%
Small-scale Industries,	Employed in sector	20%
Trade and Services	Gross value added in sector	80%
Industry, conversion	Gross value added in sector	100%

Temporal distribution of regional demand

To derive the temporal distribution of demand, time series are determined for the individual applications, which are used to distribute the spatially distributed annual demand over the year. Four categories can be distinguished when creating our regional demand time series: Standard load profiles, time series for mobility applications, time series for heat generation, and applications for which we assume a constant power consumption. The standard load profiles (SLP) for household consumption ("H0") and commercial consumption ("G0") are taken from VDEW (1999). The daily profiles are available separately by day of the week (Monday-Friday, Saturday, Sunday/holidays) and by season (Summer, Winter, Transition) and are matched to the calendar year 2015. The profiles for light and heavy electric trucks are taken from ENTSO-E (2022b). The daily profiles are available, separated by Monday-Friday and Saturday-Sunday, and are matched based on this distinction to the calendar year 2015. Due to the temperature dependency of the heat generation profiles, they are calculated for each region separately. To calculate the profiles for households, we use the standardized profiles for heat pump electricity consumption as a function of time of day and outdoor temperature from SWM (2022) as well as regional temperature data for 2015 from Copernicus Climate Change Service (2020). For electricity demand from commercial consumers for heat generation, we use the profile data from Ruhnau and Muessel (2022) and match it with temperature data for 2015. Last, we assume uniform consumption over the year for the base load, rail transport and conversion applications. Figure 5.14 in Appendix 5.7.6 illustrates the different profiles.

5.3.2 Electricity generation

Spatial distribution of annual renewable electricity capacities

As a starting point, existing capacities in 2022 of onshore wind, rooftop PV, large-scale PV and hydropower are spatially distributed according to the Marktstammdatenregister (Bundesnetzagentur, 2022). Offshore wind capacities are located in a separate offshore region and are not spatially distributed. For the

future development of each technology, the methods described in the network development plan 2023 (German TSOs, 2022) are reproduced using regional capacity potentials from Ebner et al. (2019). For 2045, the announced capacity targets within the so-called "Easter package" (Bundesrat, 2022) were assumed: 160 GW onshore wind, 200 GW large-scale and rooftop PV each.

For onshore wind, the distribution to regions is done according to the relative capacity potentials in the federal states compared to the total potential of Germany. As soon as the 2% target for each federal state is reached, the relative distribution factor in this federal state is devalued by 50%. The 2% area target thus represents a threshold value above which less area may be available for wind energy use in a federal state, thus slowing down the expansion. The remaining net expansion is then further distributed to the federal states in an iterative procedure based on the relative distribution of the respective potential. Based on the capacity assigned to each state, the capacity is further distributed to the NUTS 3 regions according to the relative potentials.

For the regional expansion of large-scale PV capacities until 2045, the regional potential areas for each federal state and the NUTS 3 regions are used as well. The target capacities for each federal state according to German TSOs (2022) are distributed by the weighted regional potentials. This is done by using a modification of the potentials. The potential area in the federal state with the highest average yield (Baden-Württemberg) is valued twice as high as the potential area in the federal state with the lowest average yield (Lower Saxony). For rooftop PV installations, the approach is postcode-specific. A constrained growth function is derived for each postcode using the change in existing installations to date and the maximum potential. This function is linear until 50% of potential is reached, and then approaches the potential limit asymptotically. This approach follows the observation that past additions have been largely linear. However, after a certain point, it decreases due to adding less suitable areas and slowly approaching the potential limit.

For hydropower, only existing capacities are regional distributed. No additional expansion is assumed.

Temporal distribution of regional renewable electricity generation

Generation profiles for the spatially distributed renewable capacities are based on the COSMO-REA6 weather data of the year 2015 provided by HErZ, Hans-Ertel Centre for Weather Research (University of Bonn - Germany) and DWD, Deutscher Wetterdienst (2022). The data set contains information regarding wind speed, temperature and solar irradiation. With these data, in-feed profiles for rooftop and large-scale PV are computed by replicating the method described in Huld et al. (2010). For onshore and offshore wind, power curves for standard wind turbines are utilized in combination with wind speed data. Feed-in time series for hydropower equal the historic time series from ENTSO-E (2022a).

5.4 Modelling electric vehicle charging flexibility

By aggregating the results of the previous sections, regionalized residual load time-series are computed. On the national level, positive peaks imply the utilization and steep ramping of (and the necessity of investment in) expensive dispatchable generation units. In contrast, negative peaks imply an excess of renewable energy generation. On the regional level, both positive and negative peaks put strain on distribution grid components such as transformers. Consequently, residual load curves should be smooth and close to zero. Electric vehicle charging represents one source of flexibility potential. We develop an optimization model for the deployment of regional flexibility of electric vehicles. In the model, we distinguish between two deployment strategies. Under the first strategy, the regional flexibility potential is used to flatten the corresponding regional residual load curves by reducing positive and negative peaks. This is our basic model, described in Section 5.4.1. Under the second strategy, the model is adjusted according to Section 5.4.2. Here, the flexibility potential of home charging processes is aggregated to flatten the national residual load curve instead.

5.4.1 Flexibility on regional level

The smoothing of the residual load has two objectives. First, to minimize the absolute distance to zero in every time step, and second, to minimize peaks. The objective functions in Equation (5.8) combines these by minimizing the square absolute value of the residual load. On a regional level, this optimization logic represents the minimization of grid expansion costs, which becomes necessary, especially when large positive or negative peaks occur. On the national level, the generation costs are to be minimized, which become disproportionately more expensive during positive peaks, which serves as a justification for the quadratic optimization approach. The objective function contains the adjusted residual load RL as a variable, which has two dimensions. One temporal $t \in T$ and spatial $n \in N$. The set T contains the 8760 hours of a year, and the set N contains all NUTS 3 regions of Germany.

$$\min z = \sum_{t}^{T} \sum_{n}^{N} |RL_{t,n}|^2 \tag{5.8}$$

The adjusted residual load curve $RL_{t,n}$ equals the residual load curve before load shift $rl_{t,n}$ plus the usage of load shift (LS), as it is shown in Equations (5.9) and (5.10).

$$RL_{t,n} = rl_{t,n} + \sum_{t_1}^{T} \sum_{u}^{User} (LS_{t,t_1,n,u} \cdot ts^{max}_{t,t_1,u}) \quad \forall t \in T \wedge n \in N \tag{5.9}$$

$$with \quad LS_{t,t_1,n,u} = LS^{neg}_{t,t_1,n,u} - LS^{pos}_{t,t_1,n,u} \tag{5.10}$$

The variable LS has two time-dimensions and is defined for every region n and every user type $u \in User$. Furthermore, the variable can be decomposed into a positive part LS^{pos} and a negative part LS^{neg}. Negative flexibility here means that the load increases so that the residual load moves upwards. Positive flexibility reflects load reduction. For every user type u, the binary parameter $ts^{max}_{t,t_1,u}$ defines whether load shifting is possible from time step t_1 to time step t.

With the following two Equations (5.11) and (5.12), it is ensured that the maximum LS potential is not exceeded in every time step t, in every region n and for every user type u. Two equations are necessary to distinguish between a positive and a negative flexibility potential (see Section 5.2.2).

$$\sum_{t}^{T}(LS^{pos}_{t,t_1,n,u} \cdot ts^{max}_{t,t_1,u}) \leq P^{max,pos}_{t_1,n,u} \quad \forall t_1 \in T \wedge n \in N \wedge u \in User \tag{5.11}$$

$$\sum_{t}^{T}(LS^{neg}_{t,t_1,n,u} \cdot ts^{max}_{t,t_1,u}) \leq P^{max,neg}_{t_1,n,u} \quad \forall t_1 \in T \wedge n \in N \wedge u \in User \tag{5.12}$$

The last Equation (5.13) ensures that shifted energy is balanced for every user type and region within a fixed period of 24 hours. For every from-to relationship (amount of energy shifted from t_1 to t), the sum has to equal zero.

$$\sum_{t_1}^{T}(LS_{t,t_1,n,u} \cdot ts^{max}_{t,t_1,u}) = 0 \quad \forall t \in T \wedge n \in N \wedge u \in User \tag{5.13}$$

After the optimization of the use of flexibility, new residual loads are computed.

5.4.2 Flexibility on national level

To use the flexibility potential of home charging processes to flatten the national residual load curve, two equations of the basic model are adjusted. First, the residual load curve in the objective function (Equation (5.8)) has no regional dimension anymore (Equation (5.14)).

$$\min z = \sum_{t}^{T} |RL_t|^2 \tag{5.14}$$

Second, flexibility from all NUTS 3 regions and all user types is aggregated to smooth the national residual load curve. Instead of Equation (5.9), we formulate the following equation to compute the new national residual load curve.

$$RL_t = rl_t + \sum_{t_1}^{T}\sum_{u}^{User}\sum_{n}^{N}(LS_{t,t_1,n,u} \cdot ts^{max}_{t,t_1,u}) \quad \forall t \in T \tag{5.15}$$

All other model equations stay the same as described in the previous section.

5.5 Analysis and results

Based on the methodologies and data presented in previous sections, we conduct a thorough analysis of the characteristics of regional and national residual load curves, and evaluate the impact of two deployment strategies for home charging flexibility. This section is divided into two parts. The first part, Section 5.5.1, focuses on analyzing residual load curves, aiming to answer two primary questions. How do regional residual loads develop over time? And what is the relationship between the load profiles of electric vehicles and regional residual load curves?

In Section 5.5.2, we analyze two deployment strategies for the flexibility provided by electric vehicles. We differentiate between national-oriented and regional-oriented activation of flexibility and use the presented optimization approach to answer the following question: What is the effect of different strategies for activating the flexibility offered by electric vehicles on regional and national residual load curves?

5.5.1 Residual load analysis

We categorize regions into three distinct clusters: Photovoltaic (PV)-dominated, wind-dominated, and load-dominated regions. The clustering is based on two dimensions: the average regional ratios of wind and PV feed-in to the average load, normalized by the maximum ratio across all regions in 2045. The clustering results are presented in Figure 5.7. A region is deemed load-dominated if both dimensions have a normalized value smaller than 0.20. A region is considered wind-dominated if it has a normalized wind-to-load ratio greater than 0.20 and greater than the PV-to-load ratio. The definition for PV-dominated regions follows the same logic.

The wind-dominated regions are primarily situated in the northern part of Germany and consist of 98 NUTS 3 regions, covering an area of 157,753 square kilometers, equivalent to 44% of the total land area of Germany (357,588 square kilometers). The PV-dominated regions are located predominantly in the southern region of Germany, particularly in Bavaria. These 166 NUTS 3 regions have a total area of 140,332 square kilometers, accounting for 39% of Germany's land area. Load-dominated regions are primarily located in Germany's western and southwestern regions and include major urban areas such as Berlin, Hamburg, and Munich. This cluster consists of 137 NUTS 3 regions and has a total area of 59,666 square kilometers, accounting for 17% of Germany's land area. The clusters differ not only in terms of load, wind and PV generation ratios but also, for example, in terms of population density and number of EVs. Both are high in load regions and low in wind regions. A detailed account of the distribution of regional properties for and within each cluster is provided in Appendix 5.7.7.

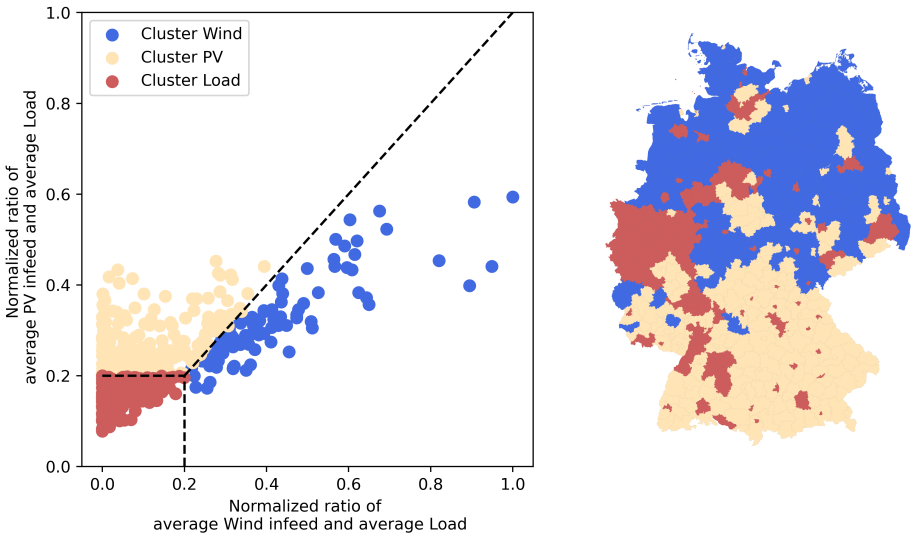

Figure 5.7: Clustering of the NUTS 3 regions

Boxplots are computed for the three clusters and Germany to compare the properties of the residual load curves for the years 2019, 2030, and 2045 without considering flexibility. The results are presented in Figure 5.8.

Regarding the **Cluster Wind**, the majority of residual load curve values show a decrease from 2019 to 2045. The median of the residual load curve decreases from 0.7 *GW* in 2019 to -12.4 *GW* in 2030 and further to -22.2 *GW* in 2045. The increased dependence on the weather for electricity generation leads to an increase in the variance of the residual load curve. The distance between the minimum and maximum values of the boxplot, a measure of dispersion, increases by 178% from 2019 to 2030 and by 338% from 2019 to 2045. This increase is attributed to the significant expansion of wind capacities relative to electrical load growth. The minimum values of the residual load curve increase from -25.0 *GW* in 2019 to -148.6 *GW* in 2045, while the maximum value increases by 41% from 13.1 *GW* in 2019 to 18.5 *GW* in 2045. The **Cluster PV** displays relatively stable properties for the residual load curve, with a slight decrease in the median from 10.1 *GW* in 2019 to 8.2 *GW* in 2045. Similar to the wind-dominated cluster, the variance of the residual load curve increases, albeit to a lesser extent, due to the weather-dependent electricity generation and the limited impact of load. The properties of the residual load curve in **Cluster Load** display a different trend. The median increases from 30.9 *GW* in 2019 to a value of 35.2 *GW* in 2045, an increase of 14%. The maximum value of the residual load increases by around 36%, and the minimum value reduces from 18.5 *GW* in 2019 to -23.2 *GW* in 2045. The addition of new electric loads from electric vehicles and heat pumps in these regions is offset by the effect of rooftop PV expansion. As the peak demand occurs in the evening while the maximum feed-in from rooftop PV occurs at noon, the minimum and maximum values of the residual load curve diverge.

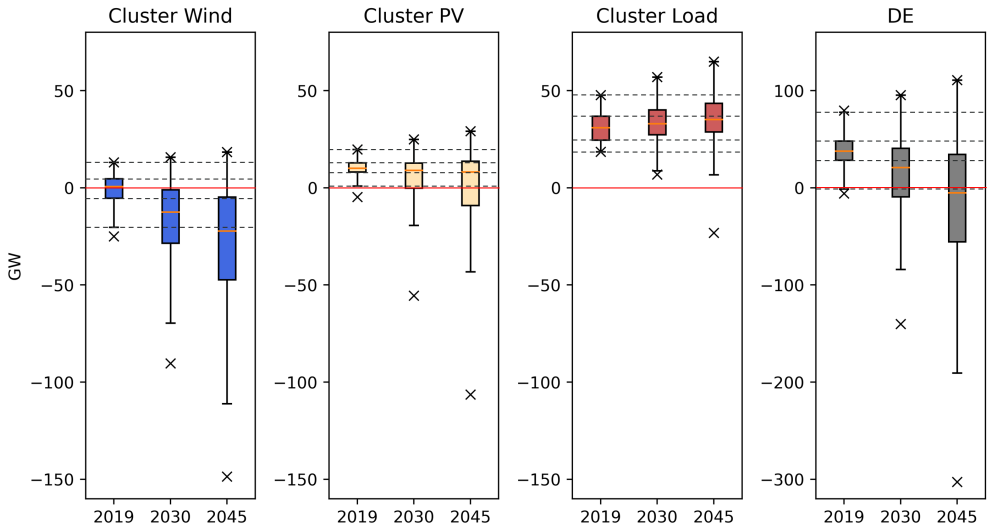

Figure 5.8: Comparison of regional residual load curves prior to the activation of flexibility

Note: The minimum and maximum values are represented by crosses. The median is depicted by the orange line, while the colored box between the lower and upper quantiles represents 50% of all values. The maximum whiskers are equal or lower to 1.5 times the Inter-Quartile Range (range of the colored box)

The residual load curve in Germany (**DE**) displays characteristics similar to those of the renewable-dominated clusters, as they represent a larger share of residual load. Additionally, the German residual load curve includes Offshore Wind feed-in, which is roughly correlated with the wind-dominated cluster.

Correlation between residual load and electric vehicle load curves

Besides the ratios of renewable feed-in and load, the three clusters differ regarding the correlation between residual load and the electric vehicle load curves. Table 5.3 shows the coefficients of correlation for the three clusters and the years 2019, 2030 and 2045.

Table 5.3: Correlation between residual load and electric vehicle load curves

Cluster	**2019**	**2030**	**2045**
Cluster Wind	0.08	-0.19	-0.25
Cluster PV	0.29	-0.21	-0.27
Cluster Load	0.74	0.46	0.11

The coefficients of correlation highlight that the residual load in the load-dominated cluster correlates most with the electric vehicles load profile. However, the correlation almost vanishes until 2045, caused by the penetration of rooftop PV applications and the electrification of further applications like heating or

industrial processes. The residual load becomes less dominated by residential applications in the evening. The increasing weather dependency of electricity generation and a low share of load compared to renewable feed-in is the reason for the lower correlation in 2019 and even negative correlation in 2045 in the other two clusters.

This development is relevant for the use of EV charging flexibility to reduce the residual demand. Today, especially in Cluster PV and Cluster Load, there would be a strong incentive to shift the load of EV charging to counter the high correlation with the residual load peaks. In 2045, however, especially in Cluster Wind and Cluster PV, EVs tend to be charged when the residual load is low (or negative). This development implies that the marginal utility of charging flexibility to reduce load peaks is decreasing over time, although the flexibility potential is increasing in absolute terms with growing EV adoption.

5.5.2 Flexibility of electric vehicles

This section provides a detailed analysis of two deployment strategies for utilizing the flexibility provided by electric vehicles. The objective of the analysis is to understand the impact of these strategies on the residual load curves at both national and regional levels. We distinguish two deployment strategies: First, we use flexibility to flatten the regional and, second, the national residual load curve. In the following, we use the formulations of "nationally incentivized" and "regionally incentivized" flexibility deployment for the use of the two deployment strategies. The optimization model outlined in Section 5.4 is used for the analysis. The properties of the resulting regional and national residual load curves for the years 2030 and 2045 are evaluated and compared.

Characteristics of the activation of flexibility

Figure 5.9 illustrates the model results for a single region with a temporal resolution of 48 hours. The figure highlights the differences in the shape of the residual load and load shifting between the two optimization schemes. For example, the charging process for user type C is shifted to hour 27 in the regional scheme but to hour 10 in the national scheme. The use of flexibility is mainly limited by the positive flexibility potential, as depicted by the dotted lines.

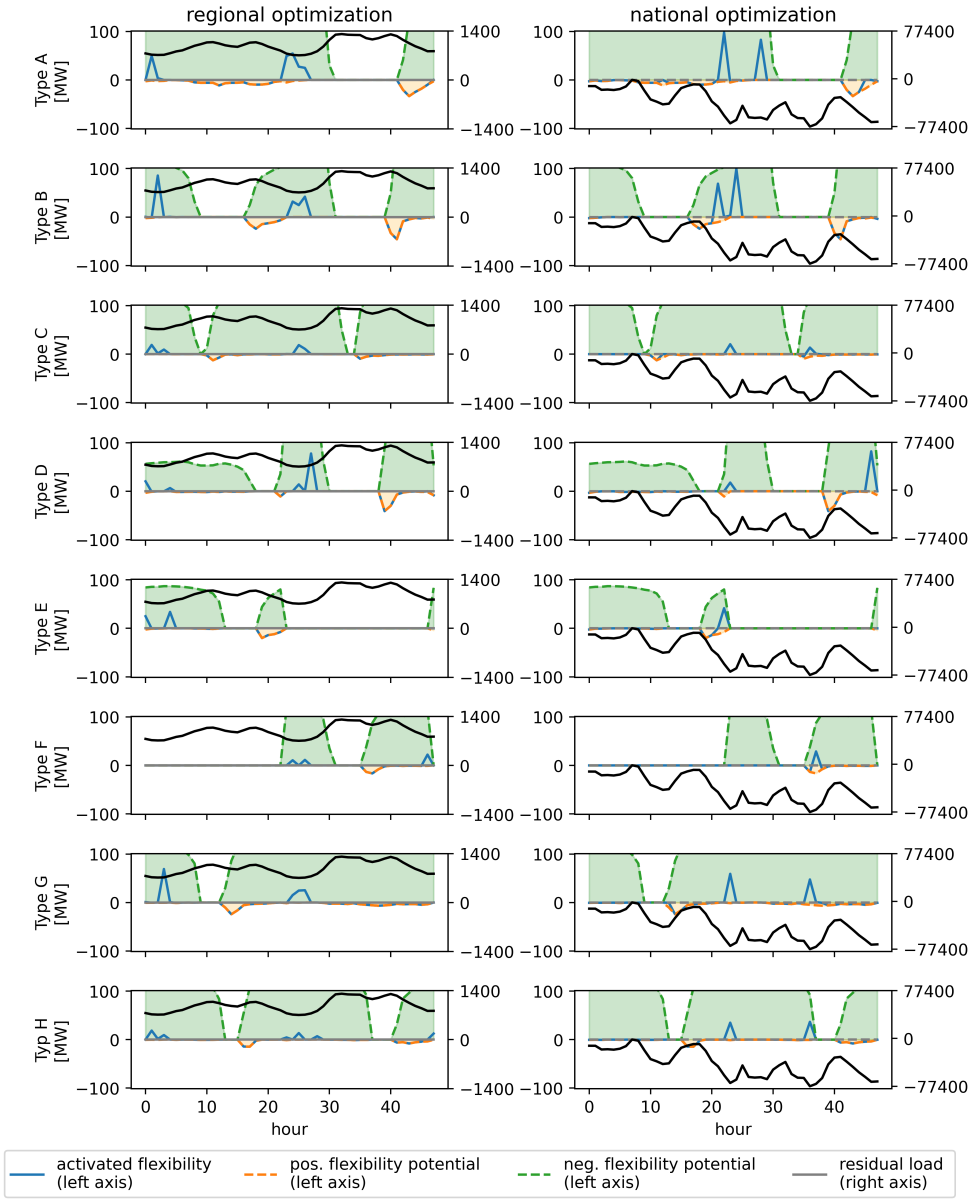

Figure 5.9: Optimal activation of flexibility in region DE111 (Stuttgart)

Note: The left column of the figure shows the results of the regional optimization and the right column shows the results of the national optimization. The residual load before the activation of flexibility (regional on the left and national on the right) is depicted using a black line, and the change of charging processes for user types A to H are shown in blue.

Model results on national level

The mechanisms for activating flexible charging processes impact the properties of the national residual load curve. In Figure 5.10, the residual load curves after

regional and national incentivized activation of flexibility are compared to the residual load curve before the use of flexibility. This is done for the years 2030 and 2045.

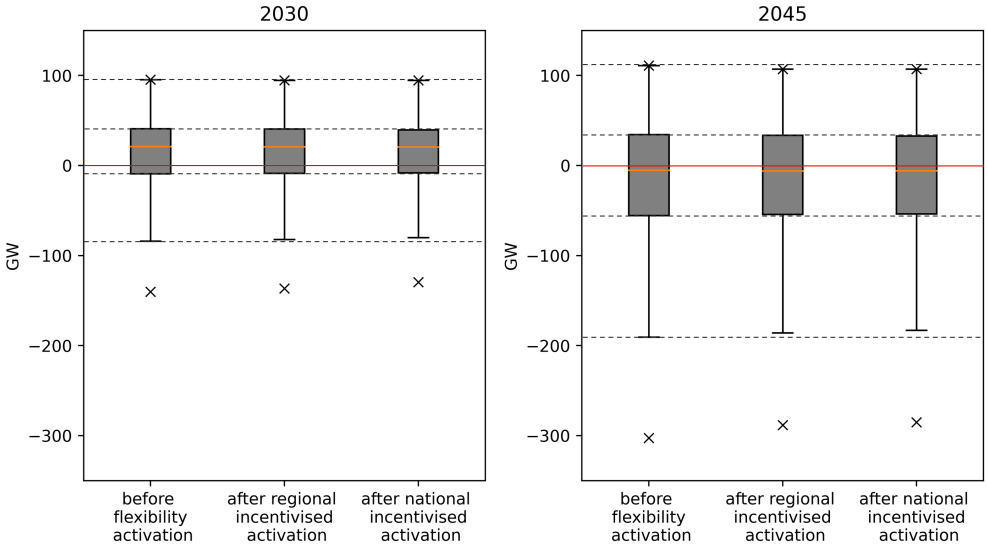

Figure 5.10: Properties of the national residual load curve before and after the use of flexibility

For both years, the range between the minimum and maximum values, as well as the absolute value of the peak change to a small extent through both national and regional incentivization of flexibility. However, national incentivization has a greater impact compared to the regional approach. In 2030, regional incentivization decreases the range between the minimum and maximum values by 1.9%, while national incentivization decreases this range by 4.8%. Before the use of flexibility, the negative peak surpasses the positive one in absolute terms. Regional incentivization reduces the peak by 2.6%, and national incentivization reduces it by 7.5%. These characteristics observed in 2030 can also be seen in 2045, but with higher values and a greater variance of the residual load. The use of flexibility reduces the absolute value of negative peak demand. The minimum changes from -303 GW to -288 GW (-5.0%) with the regional approach and to -285 GW (-5.9%) with the national approach, while the maximum is only reduced by 4 GW (-3.6%) in both cases.

Model results on regional level

We calculate imbalance ratios to analyze the effects of the two flexibility deployment strategies on the regional feed-in and load peaks. These are defined as the positive or negative peaks in each region's residual demand divided by the

respective regional total load and generation over a year.[66] The imbalance ratio can be formulated in a positive (PIR_r), negative (NIR_r) and an absolute (AIR_r) way (see Equation (5.16) to (5.18)). Dividing the maximum amount of power needed in both the positive (RE deficit) and negative (RE surplus) direction in each region by total load and generation allows us to analyze and compare the development of peaks for the heterogeneous regions. Comparing the Imbalance Ratios before and after flexibility activation, we are able to quantify how flexibility changes the altitude of the load and feed-in peaks.

$$PIR_r = \frac{\max\limits_{h \in H}(residualload_{h,r})}{\sum_{h=1}^{8760}(totalload_{h,r} + generation_{h,r})} \cdot 1000 \quad \forall r \in R \tag{5.16}$$

$$NIR_r = \frac{\min\limits_{h \in H}(residualload_{h,r})}{\sum_{h=1}^{8760}(totalload_{h,r} + generation_{h,r})} \cdot 1000 \quad \forall r \in R \tag{5.17}$$

$$AIR_r = \max\left(|PIR_r|, |NIR_r|\right) \cdot 1000 \quad \forall r \in R \tag{5.18}$$

Figure 5.11 visualizes the change of the imbalance ratios after the national and regional incentivized activation of flexibility in each region for the year 2030. Figure 5.12 shows the results for the year 2045. As reference values in both figures, highlighted in gray, the peaks in 2019 are normalized to the load and generation of 2030 and 2045, respectively.

[66] The use of this evaluation variable follows Kühnbach et al. (2021).

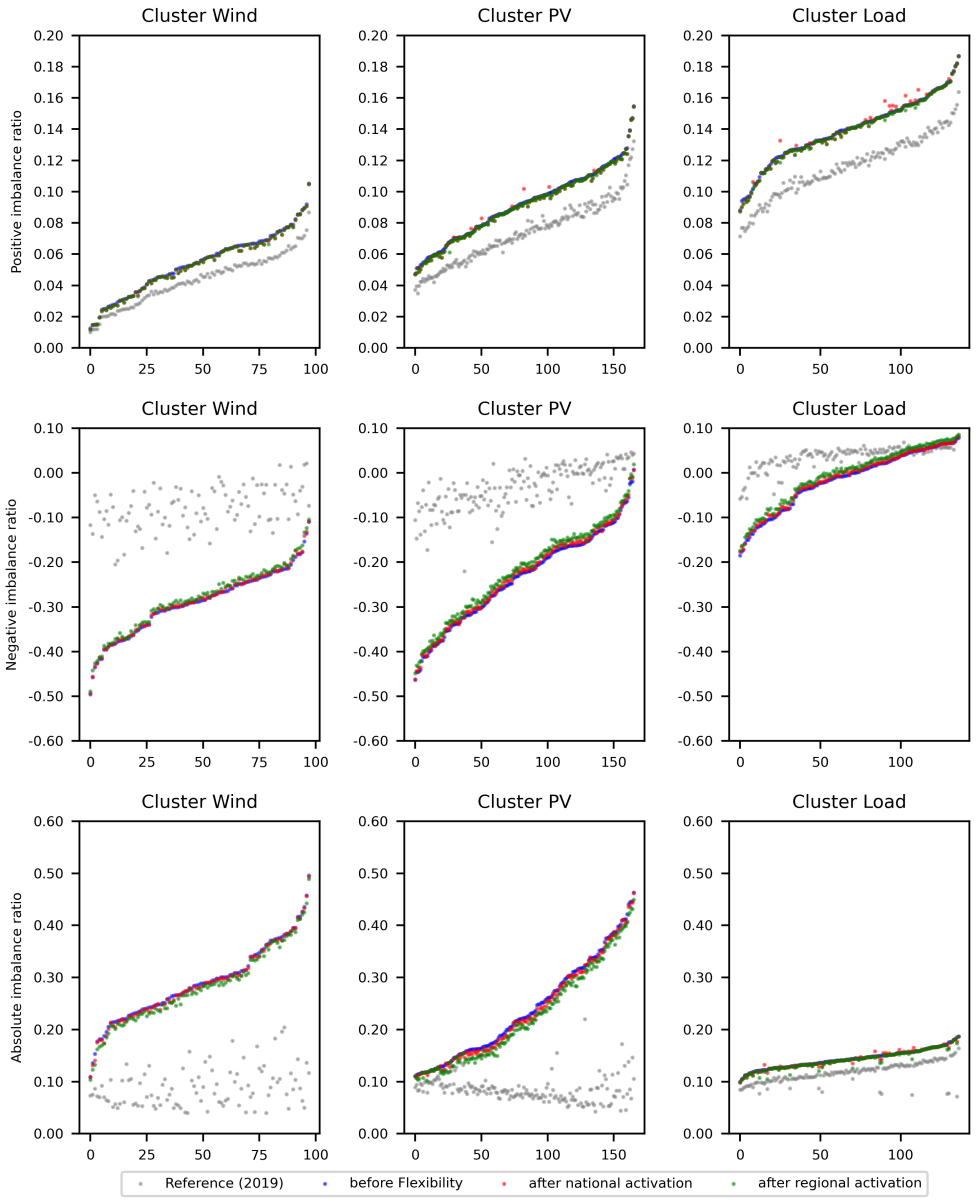

Figure 5.11: Imbalance ratios before and after the use of flexibility in 2030

Note: The x-axis represents the regions in each cluster. In each of the nine sub-figures, the imbalances before flexibility are sorted in ascending order. The imbalance ratios after the activation of flexibility are then matched to the corresponding region.

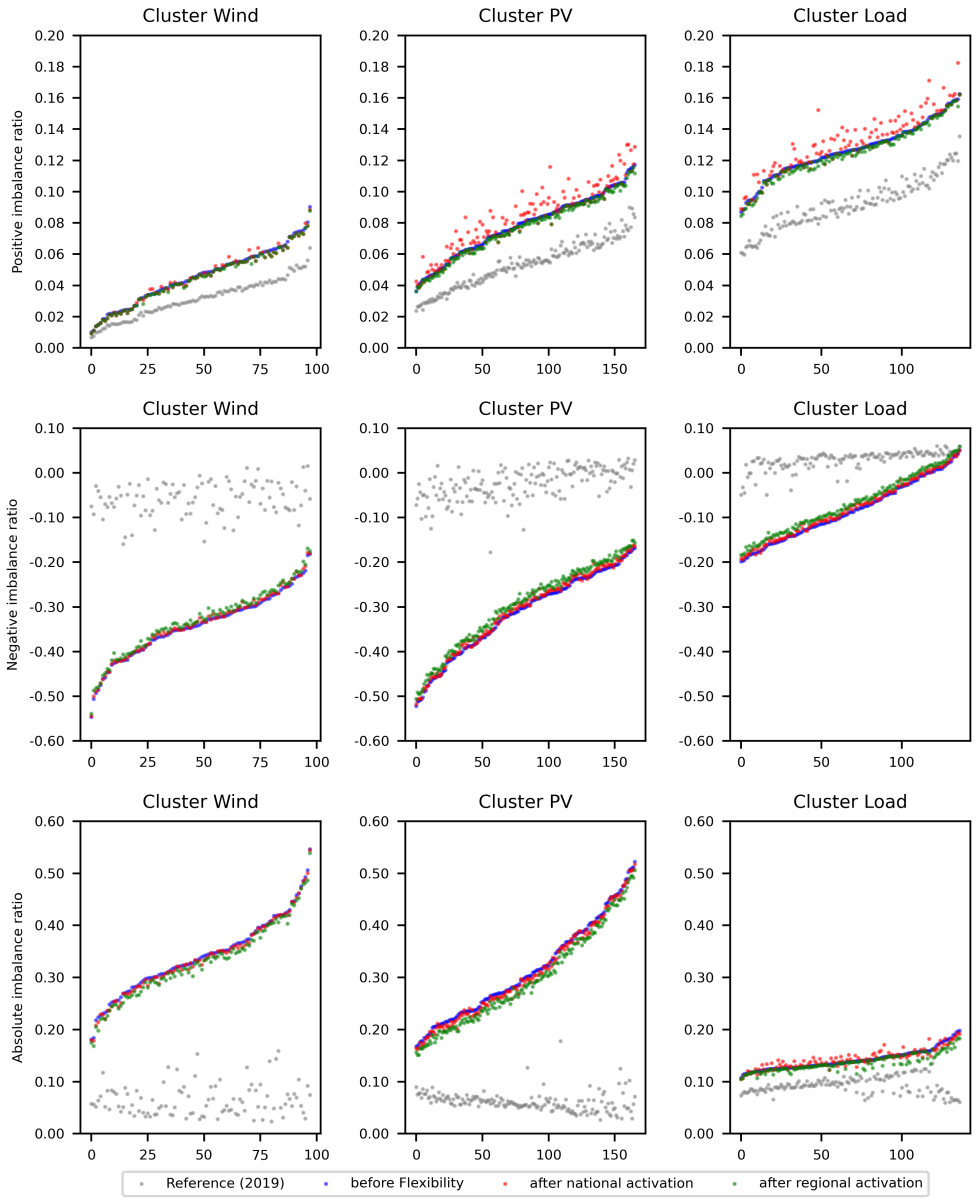

Figure 5.12: Imbalance ratios before and after the use of flexibility in 2045

Note: The x-axis represents the regions in each cluster. In each of the nine sub-figures, the imbalances before flexibility are sorted in ascending order. The imbalance ratios after the activation of flexibility are then matched to the corresponding region.

In renewable-dominated regions in 2045, before the activation of flexibility, the negative imbalance ratio is always greater, in absolute terms, than the positive imbalance ratio. It thus defines the absolute imbalance ratio and the maximum strain on local grid components. In the load-dominated cluster, it is the other way around in about 66% of the regions.

In the **Cluster Wind**, the positive imbalance ratio decreases only slightly when applying both activation mechanisms for flexibility. On average, positive imbalance declines by 1.2% with national incentives and by 2.7% with regional ones. The positive peaks of the residual loads decrease by 0.002 MW/km^2 on average with national incentives and by 0.004 MW/km^2 with the regional approach. The decreasing effect is limited by low positive flexibility potentials and the fact that the charging processes and the situation of the highest residual load do not fall into the same periods, as discussed in Section 5.5.1. The correlation between residual load and charging profile decreases over time, which limits the potential for flexibility in peak load situations. This limitation applies to all three clusters. The negative imbalance ratio in the wind-dominated cluster remains largely unchanged under the national deployment strategy (-1.2% on average in absolute terms[67], corresponding to -0.013 MW/km^2). However, it decreases more when applying the regional strategy (-3.5% in absolute terms, corresponding to -0.037 MW/km^2). As the negative imbalance ratio is greater than the positive one for the regions in this cluster, the absolute imbalance ratio reproduces the negative one in absolute terms.

In the **Cluster PV**, the positive imbalance ratios display a different pattern than the ones in the wind-dominated cluster, with an increase in response to national incentives. The national deployment strategy results in an increase of 5.1% of the positive imbalance ratio on average, which corresponds to an increase of the positive residual peak demand of 0.008 MW/km^2 across all regions within this cluster. But, there are also regions which face distinct greater effects with up to 0.071 MW/km^2. In these cases, peaks can increase by up to 35% following national incentives. This outcome is attributed to more electric vehicles in PV-dominated regions, resulting in a greater potential for positive flexibility. In contrast, positive imbalance ratios are lowered by 2.1% with regional incentives on average, corresponding to a reduction of 0.008 MW/km^2 . The negative imbalance ratio is consistently reduced by regional incentives in absolute terms (-6.3% on average, corresponding to -0.068 MW/km^2). National incentives reduce the absolute value of the negative imbalance ratio, too, but to a less extent (-1.2%; -0.023 MW/km^2). Just as in the wind-dominated cluster, as the negative imbalance ratio is greater than the positive one, the absolute imbalance ratio reproduces the negative one in absolute terms. Last, in the **load-dominated cluster**, we observe that following national incentivized activation of flexibility, positive imbalance ratios are the highest compared to their occurrence in renewable-dominated clusters. On average, the positive imbalance increases by 3.1% (0.043 MW/km^2) with national incentives. But, just like in the PV-dominated cluster, there are also regions with high penetration rates of electric vehicles, which face a distinct greater effect with up to 0.349 MW/km^2. In this case, the peak increases by around

[67] For the positive and absolute imbalance ratio, a reduction corresponds to an improvement: the (positive or negative) residual load peak becomes smaller. For the negative imbalance ratio, a reduction corresponds to a worsening: the negative residual load peaks (the absolute value) become larger. In order to be consistent in terms of the positive/negative impact, all described changes in the negative imbalance ratio refer to the absolute change.

27% following national incentives. Regional incentives instead lower the positive imbalance ratio by 1.4% (-0.018 MW/km^2) on average. The negative imbalance ratio is consistently reduced both by regional and national incentives, but regional incentives have a greater effect (-2.1% compared to -6.3%, corresponding to -0.079 MW/km^2 and -0.208 MW/km^2). In contrast to the separated effects on positive and negative imbalances, the effect of national incentives on the absolute imbalance ratio is region-specific, indicating the regions' heterogeneity in the load-dominated cluster. In some regions, the positive imbalance ratio exceeds the negative imbalance ratio (regions 0 to 90), while the opposite is true in others (regions 91 to 137). In regions with a greater positive imbalance than a negative, the absolute imbalance ratio increases by 3.2% on average with national incentives, corresponding to an increase of absolute residual peak demand by 0.056 MW/km^2 on average. Instead, local incentives lower the absolute imbalance ratio by 1.1% on average, corresponding to a decrease of the absolute peak by 0.019 MW/km^2 on average. In regions with a smaller positive imbalance than a negative, national incentives reduce the absolute imbalance ration by 1.9% on average (-0.036 MW/km^2), whereas local incentives would lower the absolute imbalance ratio even more by 5.9% (-0.104 MW/km^2) on average. Consequently, there are regions in the load-dominated cluster where national incentives are slightly beneficial in lowering the absolute imbalance ratio or do not significantly change it. However, there are also regions where national incentives result in an increase in the absolute imbalance ratio, stemming from the increase in positive peaks. Or, formulated differently, national incentives can significantly increase or slightly reduce the absolute peaks. Regional incentives may either lower the imbalance ratio or have an insignificant impact on the absolute value, depending on the flexibility potential and the correlation between charging profiles and residual load peaks.

Summarizing, national incentives tend to increase the positive imbalance ratio in PV- and load-dominated regions, whereas regional incentives decrease it, albeit to a small extent. However, regional incentives can significantly reduce the negative imbalance ratio.

In the context of the three clusters under consideration, it can be inferred that in regions dominated by wind energy, the national deployment strategy does not exert additional pressure on the distribution grid, but regional incentives can reduce imbalances. In PV-dominated regions, both the national and the regional incentives do lower the absolute imbalance ratio. However, regional incentives have a greater effect. For the regions of both clusters, it can be observed that the flexibility potential is used in particular to absorb excess renewable electricity and has less effect in smoothing load peaks. This is also manifested in the temporal shift patterns in the two clusters: For both the national and the regional incentivization, load shifting takes place primarily from the evening to the times of surplus generation at noon.

In contrast, load-dominated regions are characterized by heterogeneity in terms of positive or negative peak dominance, so the impact of national incentives on

imbalances can be either positive (worsen the situation) or negligible. That is because the national incentivization corresponds to the temporal scheme of the renewable-dominated regions: Load is shifted from the evening into the times of national renewable surplus, only that there is no renewable energy surplus in many load-dominated regions, leaving them worse off. Regional incentives, on the other hand, can reduce absolute imbalances in these regions, as the load is shifted into the night, to address load peaks during the day.

5.6 Conclusion

The expansion of decentralized renewable energy systems and electric vehicles is putting stress on the distribution grids. However, flexible EV charging can help alleviate this impact by reducing peak loads and feed-in by better matching load and supply. The paper conducted a comprehensive regional analysis of Germany to estimate the regional potential of EV charging flexibility for reducing peaks on regional and national levels. This was achieved by modeling regional EV diffusion with sigmoid functions and deriving individual charging and flexibility profiles for each NUTS 3 region in Germany. For both, we presented a detailed method. We further developed a model to optimize the use of EV charging flexibility to either flatten the regional residual loads or the national one.

Our analysis consists of two parts.

In the first part of our analysis, we examined the future development of residual load curves and their correlation with EV charging profiles. Three different clusters were formed: load-dominated, wind-dominated and PV-dominated. We find that the increased dependency on weather-based electricity generation leads to a significant increase in the variance of the residual load curve until 2045. Our results reveal that the regional structure of electricity demand and supply is highly heterogeneous. Moreover, the correlation between residual load and EV charging profiles decreases over time, implying that the marginal utility of charging flexibility to reduce load peaks declines, even if the positive flexibility potential increases in absolute terms.

In the second part, we evaluated the impact of two incentive mechanisms for activating the flexibility of electric vehicles. One aims to flatten the regional residual load curves with local flexibility. The other uses the aggregated flexibility potentials to flatten the national residual load. Results show that both strategies reduce the variance of the residual load and peak demand and feed-in from a national perspective. In 2045, both strategies reduce the positive residual peak load by about 4 GW (3.6%), correspondingly less reserve capacity, storage or imports need to be kept available. The negative residual peak load, i.e. the maximum surplus of renewable capacity, is reduced by 15 GW (5.0%) in case of regional incentivization and even by 18 GW (5.9%) in case of national incentivization. I.e., the use of EV charging flexibility has a significantly greater

potential in absorbing excess renewable generation than in lowering positive peak load. Regional incentivization generally leads to a decline in absolute values of peaks on regional level. Here, as well, the flexibility is particularly useful in absorbing excess renewable generation and thus reducing negative residual load peaks. The local impact of the national incentivized activation varies depending on the region's characteristics. In load- and some PV-dominated regions, national incentivization can result in drastically higher regional demand peaks compared to a scenario without charging flexibility (up to 35%). In wind-dominated regions, this effect is less pronounced. Furthermore, regions with higher shares of EV load than total load and regions with a higher correlation of EV charging profiles with the residual load have higher potential to flatten the residual load and reduce the peak demand.

The two application scenarios of charging flexibility discussed aim at two very different targets: while national incentivization aims at reducing demand in times of low national renewable generation feed-in and thus times of high prices, the regional incentivization aims at reducing the regional strain on grid components. Our study shows that these two targets can be contradictory in their effects: While the regional incentivization is less effective in reaching the smoothing in the national residual demand curve, the national incentivization can even lead to increased strain on local level, especially in load-dominated regions. Policymakers should, thus, consider these regional effects when implementing incentives for flexible EV charging to achieve maximum effectiveness in reducing peaks on regional and/or national levels and avoid unwanted, additional strain on grid components. Furthermore, our results may also provide a justification at the transmission system level for introducing regionally differentiated price signals (e.g. zonal or nodal pricing), as uniform pricing at the national level may result in undesirable effects at the regional level.

While we are able to estimate regional effects of flexibility deployment at the level of NUTS 3 regions with our method, there is a need for further research on its impact on actual distribution grids and grid components. In the course of this, the concrete grid expansion costs and electricity generation costs under different deployment strategies could be quantified and compared. Furthermore, our analysis abstracts from other flexibility options and their interdependencies with the flexible home charging of EVs. Hence, there remains a need for further research, addressing flexibility with workplace charging or charging in public spaces as well. Finally, further research could investigate on the effects of different policy schemes aiming at the implementation of the discussed deployment strategies.

5.7 Appendix

5.7.1 The full Bass model

For the computation of regional transition pathways of electric vehicles, the Bass diffusion model is used. In this section, it is explained how the formula in Equation (5.3) is derived. According to Rogers' concept of the diffusion of innovation (1962), $P(t)$ is "the probability that an initial purchase will be made at time t given that no purchase has yet been made" (Bass, 1969).

$$P(t) = \frac{f(t)}{1 - F(t)} = p + \frac{q}{m}A(t) = p + qF(t) \tag{5.19}$$

The parameter p is the coefficient of innovators meaning the probability of initial purchases at the start of the innovation and q is the coefficient of imitators, signalling the pressure they feel from the increasing number and m is the total market size. $f(t)$ is the likelihood of purchase at time t. $F(t)$ is the cumulative diffusion level at time t, further described in Equation (5.20). $A(t)$ expresses the cumulative number of adopters $a(t)$ in the interval $(0, t)$, presented in Equation (5.21) (Bass, 1969; Van der Kam et al., 2018).

$$F(t) = \frac{A(t)}{m} = \int_0^t f(t)dt \tag{5.20}$$

$$A(t) = \int_0^T a(t)dt = m\int_0^T f(t)dt = mF(t) \tag{5.21}$$

The number of adopters $a(t)$ itself can be calculated according to Equation (5.22)

$$a(t) = mf(t) = P(t)[m - A(t)] = [p + \frac{q\int_0^T a(t)dt}{m}][m - \int_0^T a(t)dt] \tag{5.22}$$

Also, $f(t)$ can be extended as:

$$f(t) = [p + qF(t)][1 - F(t)] = p + (q - p)F(t) - q[F(t)]^2 \tag{5.23}$$

To find $F(t)$, this non-linear differential Equation (5.24) needs to be solved:

$$dt = \frac{dF}{(p + (q - p)F - qF)} \tag{5.24}$$

This equals to:

$$F = \frac{q - pe^{(-t+C)(p+q)}}{q(1 + e^{(-t+C)(p+q)})} \tag{5.25}$$

Since $F(0) = 0$, the integration constant may be evaluated:

$$-C = \frac{1}{p+q} ln(\frac{q}{p}) \tag{5.26}$$

Therefore:

$$F(t) = \frac{1 - e^{-(p+q)t}}{1 + \frac{q}{p} e^{-(p+q)t}} \tag{5.27}$$

or:

$$A(t) = m \frac{1 - e^{-(p+q)t}}{1 + \frac{q}{p} e^{-(p+q)t}} \tag{5.28}$$

To normalize the beginning of the diffusion t_0 at 0, this function can be written as:

$$A(t) = m \frac{1 - e^{-(p+q)(t-t_0)}}{1 + \frac{q}{p} e^{-(p+q)(t-t_0)}} \tag{5.29}$$

which is derived from Van der Kam et al. (2018).

5.7.2 Function transformation of the diffusion curve function

This section displays the transformation of the diffusion curve function given in Equation (5.3) to the diffusion curve function in Equation (5.6). The objective is to calculate t given all other variables and parameters stay constant. Recall Equation (5.3):

$$F(t, \hat{s}, \hat{p}, \hat{q}) = \hat{s} \cdot \frac{1 - e^{-(\hat{p}+\hat{q})(t-t_0)}}{1 + \frac{\hat{q}}{\hat{p}} e^{-(\hat{p}+\hat{q})(t-t_0)}} \qquad | \cdot (1 + \frac{\hat{q}}{\hat{p}} e^{-(\hat{p}+\hat{q})(t-t_0)}) \tag{5.30}$$

For the sake of simplicity, $F(t)$ will be written as F in this function transformation. The transformation steps are shown in Equations (5.31) to (5.38).

$$F(1+\frac{\hat{q}}{\hat{p}}e^{-(\hat{p}+\hat{q})(t-t_0)}) = \hat{s}*(1-e^{-(\hat{p}+\hat{q})(t-t_0)}) \qquad |\text{solving the brackets} \tag{5.31}$$

$$F+F\frac{\hat{q}}{\hat{p}}e^{-(\hat{p}+\hat{q})(t-t_0)} = \hat{s}-\hat{s}e^{-(\hat{p}+\hat{q})(t-t_0)} \qquad |*\hat{p} \tag{5.32}$$

$$\hat{p}F+\hat{q}Fe^{-(\hat{p}+\hat{q})(t-t_0)} = \hat{s}\hat{p}-\hat{s}\hat{p}e^{-(\hat{p}+\hat{q})(t-t_0)} \qquad |-\hat{p}F+\hat{s}\hat{p}e^{-(\hat{p}+\hat{q})(t-t_0)} \tag{5.33}$$

$$\hat{s}\hat{p}e^{-(\hat{p}+\hat{q})(t-t_0)}+\hat{q}Fe^{-(\hat{p}+\hat{q})(t-t_0)} = \hat{s}\hat{p}-\hat{p}F \tag{5.34}$$

$$(\hat{s}\hat{p}+\hat{q}F)e^{-(\hat{p}+\hat{q})(t-t_0)} = \hat{s}\hat{p}-\hat{p}F \qquad |*\frac{1}{\hat{s}\hat{p}+\hat{q}F} \tag{5.35}$$

$$e^{-(\hat{p}+\hat{q})(t-t_0)} = \frac{\hat{s}\hat{p}-\hat{p}F}{\hat{s}\hat{p}+\hat{q}F} \qquad |ln \tag{5.36}$$

$$-(\hat{p}+\hat{q})(t-t_0) = ln(\frac{\hat{s}\hat{p}-\hat{p}F}{\hat{s}\hat{p}+\hat{q}F}) \qquad |*\frac{1}{-(\hat{p}+\hat{q})} \tag{5.37}$$

$$t-t_0 = \frac{ln(\frac{\hat{s}\hat{p}-\hat{p}F}{\hat{s}\hat{p}+\hat{q}F})}{-(\hat{p}+\hat{q})} \qquad |+t_0 \tag{5.38}$$

$$t = \frac{ln(\frac{\hat{s}\hat{p}-\hat{p}F}{\hat{s}\hat{p}+\hat{q}F})}{-(\hat{p}+\hat{q})}+t_0 \tag{5.39}$$

To calculate the time difference Δt between a given time t_{set} when a NUTS 3 region reaches a certain diffusion level $F(t)^{nuts3}$, and the time when the same level is reached on the national diffusion curve, the following Equation (5.40) is the result.

$$\Delta t = t-t_{set} = t-\frac{ln(\frac{\hat{s}\hat{p}-\hat{p}F}{\hat{s}\hat{p}+\hat{q}F})}{-(\hat{p}+\hat{q})}+t_0-t_{set} \tag{5.40}$$

5.7.3 Descriptive analysis of mobility data

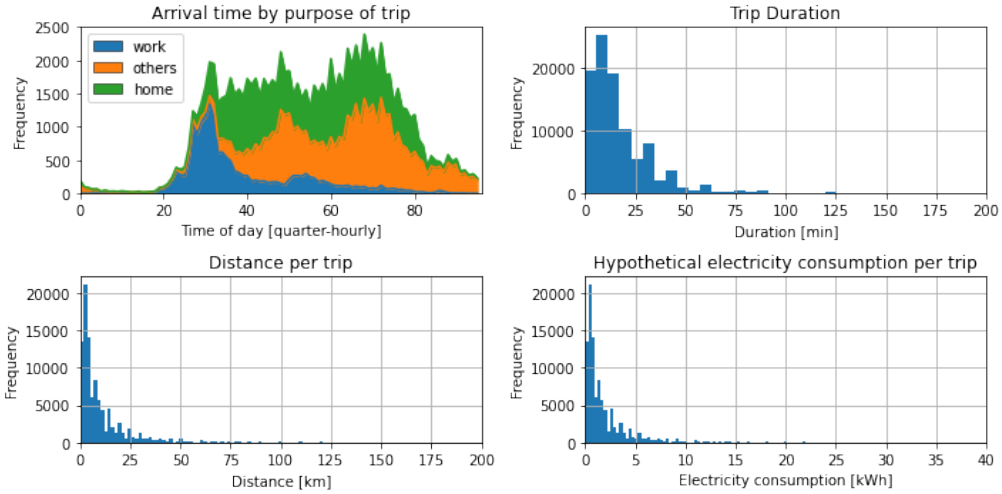

Figure 5.13: Key parameters of the used MOP dataset (KIT - Institut für Verkehrswesen, 2021)

5.7.4 Shares of charging scenarios

Table 5.4: Shares of charging scenarios per settlement type

settlement type	h	h,w	h,o	h,w,o	w	o	w,o	Total
rural community	22%	22%	22%	22%	4%	4%	4%	100%
smaller provincial town	22%	22%	22%	22%	4%	4%	4%	100%
larger provincial town	21%	21%	21%	21%	6%	6%	6%	100%
smaller medium town	18%	18%	18%	18%	9%	9%	9%	100%
larger medium town	20%	20%	20%	20%	7%	7%	7%	100%
smaller metropolis	16%	16%	16%	16%	13%	13%	13%	100%
larger metropolis	10%	10%	10%	10%	19%	19%	19%	100%

Notes: The row total may differ from 100% due to rounding errors. Charging locations: at home (h), at work (w), others (o)

5.7.5 Distribution of demand to federal states

To distribute the national demand of each sector among the federal states, we use data from Länderarbeitskreis Energiebilanzen (2022). The data includes the demand of all federal states separately by sector for the years 1990-2019. We allocate the demand in our model among the federal states based on the distribution of sector-specific demand in 2019. An exception is the state of Saarland, where the most recent data available is from 2016 (Table 5.5). We assume that this distribution does not change fundamentally over time.

Sector	BW	BY	BE	BB	HB	HH	HE	MV
Households	14%	16%	3%	3%	1%	3%	8%	2%
Small-scale industries, trade and services	15%	16%	5%	3%	1%	3%	9%	2%
Industry	12%	15%	1%	3%	1%	2%	5%	1%
Rail transport	11%	19%	8%	5%	1%	3%	11%	2%
Conversion sector	9%	9%	1%	10%	1%	3%	2%	1%

Sector	NI	NW	RP	SL	SN	ST	SH	TH
Households	9%	23%	5%	1%	4%	2%	4%	2%
Small-scale industries, trade and services	9%	20%	4%	1%	4%	3%	3%	3%
Industry	11%	28%	7%	2%	5%	4%	2%	3%
Rail transport	11%	15%	4%	1%	4%	4%	2%	2%
Conversion sector	10%	37%	1%	2%	6%	5%	3%	0%

Table 5.5: Distribution keys of sectoral electricity demand to federal states.

Note: The row total may differ from 100% due to rounding errors.

5.7.6 Demand profiles

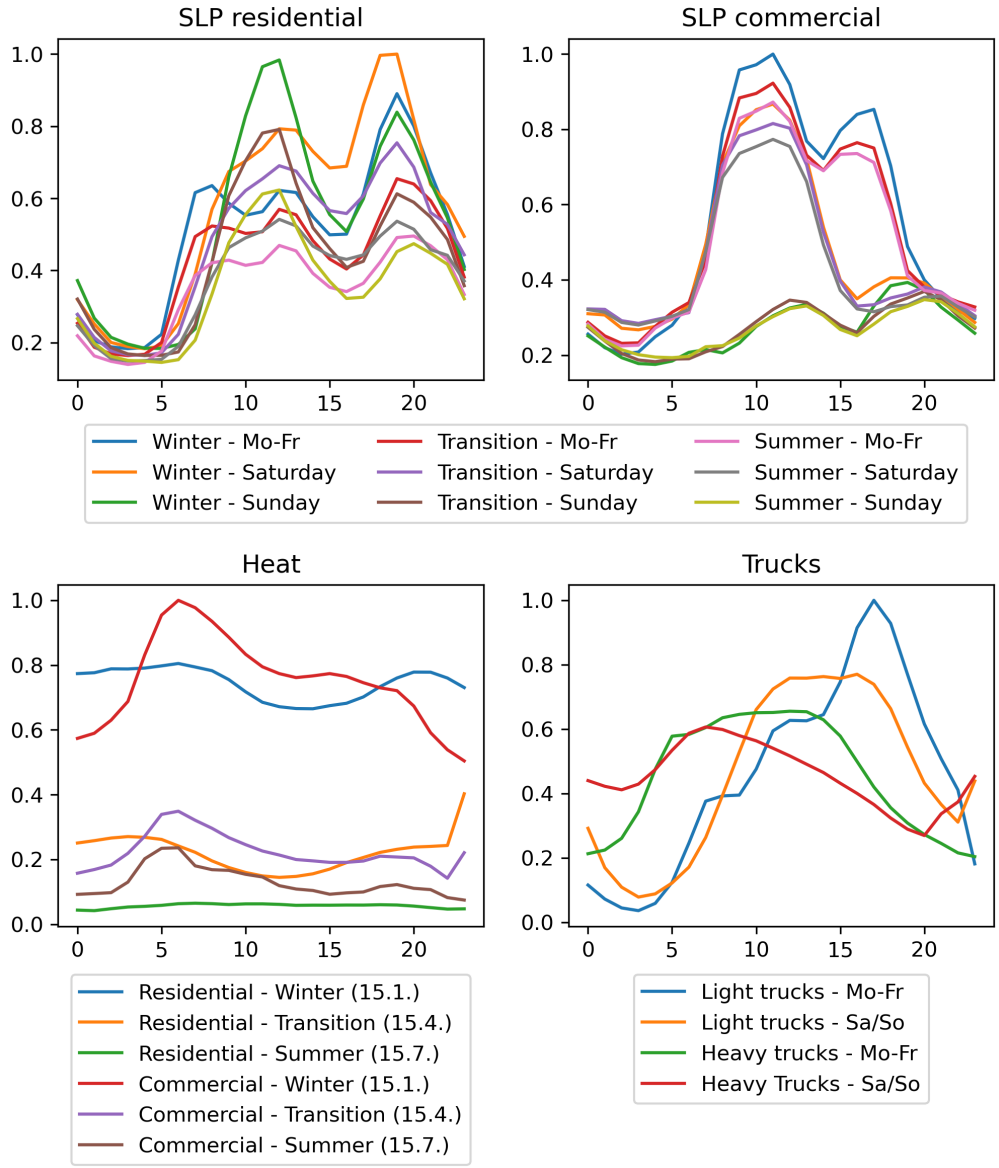

Figure 5.14: Demand profiles per application. Heat profiles are exemplary: shown are the profiles for the region DEA23 (Cologne) on 3 exemplary days of the year.

5.7.7 Cluster properties

Table 5.6: Properties of the regions within the three cluster in 2045

Property	Indicator	Cluster Wind	Cluster PV	Cluster Load
Population density [People per km^2]	Minimum	36	66	125
	Maximum	437	1585	4761
	Mean	117	264	1165
Number of EVs [cars per km^2]	Minimum	14	31	56
	Maximum	167	606	1811
	Mean	55	119	471
Wind Onshore capacity [MW per km^2]	Minimum	0.22	0.00	0.00
	Maximum	1.94	1.26	0.95
	Mean	0.75	0.29	0.15
total PV capacity [MW per km^2]	Minimum	0.19	0.16	0.00
	Maximum	1.59	2.18	2.35
	Mean	0.62	0.69	0.34
large-scale PV capacity [MW per km^2]	Minimum	0.19	0.16	0.00
	Maximum	1.59	2.18	2.34
	Mean	0.62	0.69	0.34
rooftop PV capacity [MW per km^2]	Minimum	0.13	0.15	0.23
	Maximum	2.04	5.41	7.46
	Mean	0.38	0.86	2.20

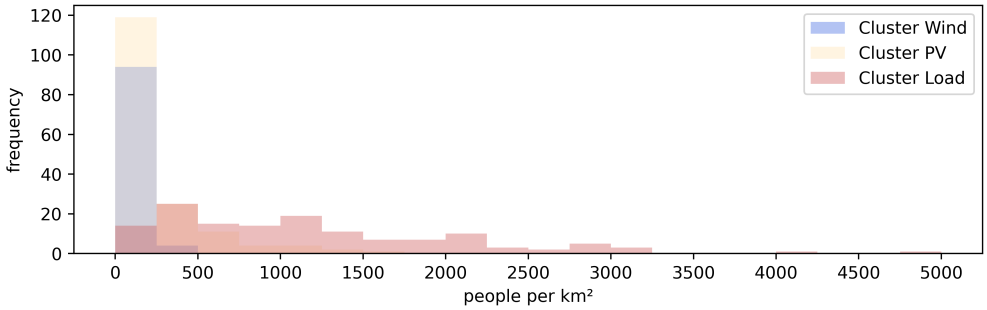

Figure 5.15: Distribution of the population density within each cluster in 2045

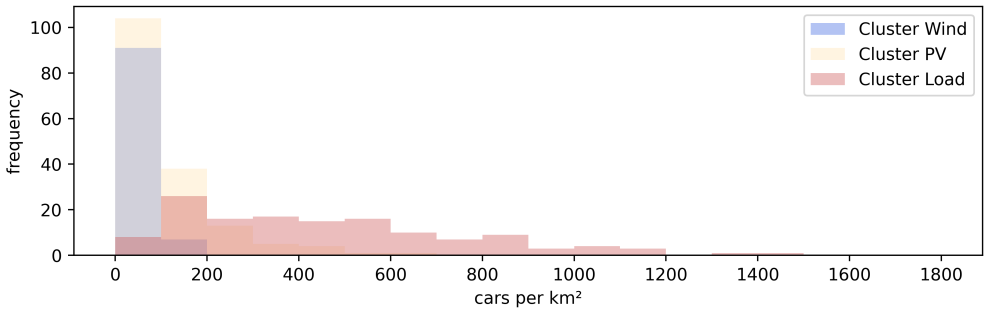

Figure 5.16: Distribution of EVs per km^2 within each cluster in 2045

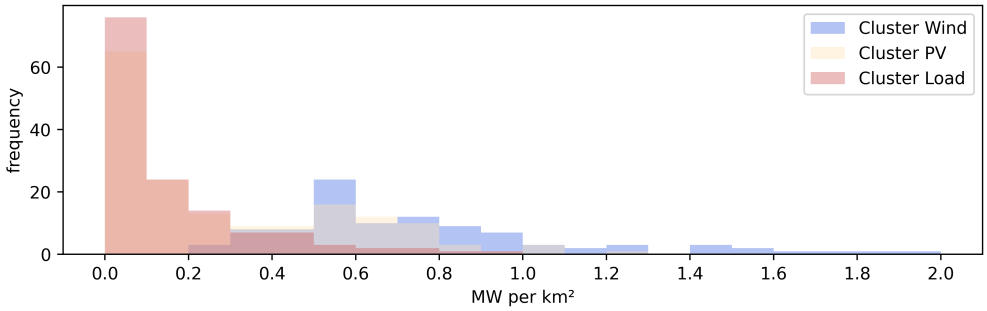

Figure 5.17: Distribution of Wind Onshore capacities per km^2 within each cluster in 2045

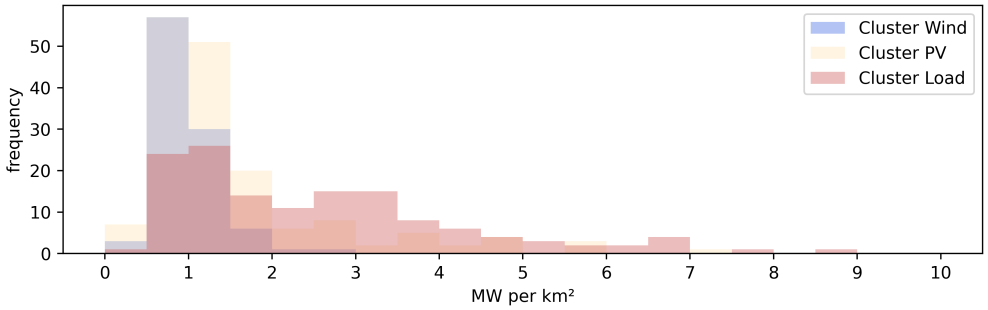

Figure 5.18: Distribution of PV capacities (large-scale PV and rooftop PV) per km^2 within each cluster in 2045

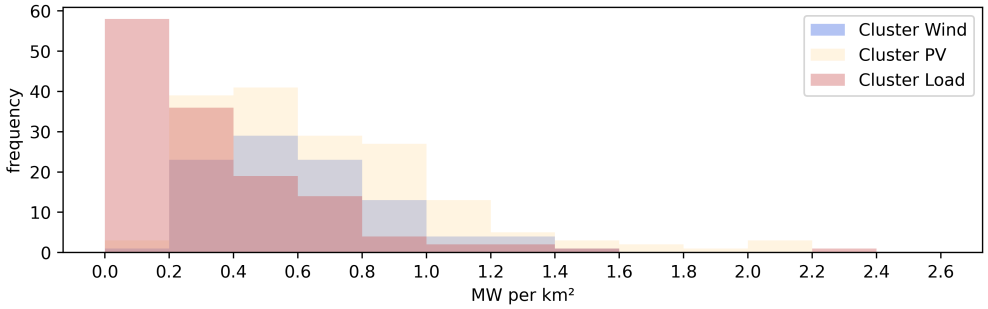

Figure 5.19: Distribution of large-scale PV capacities per km^2 within each cluster in 2045

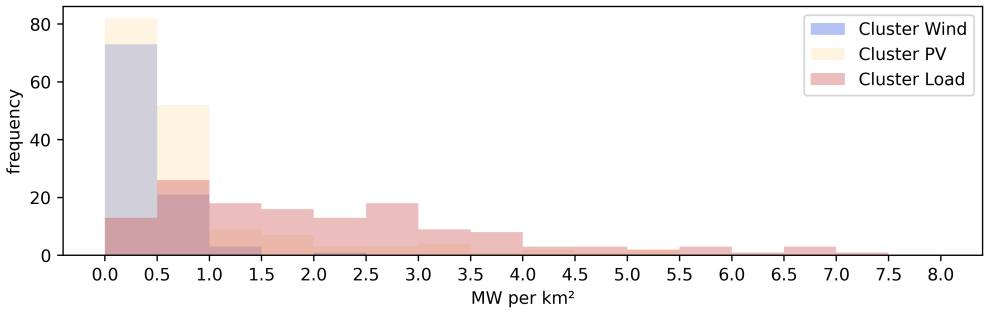

Figure 5.20: Distribution of rooftop PV capacities per km^2 within each cluster in 2045

Bibliography

Agora Verkehrswende, Agora Energiewende, & Regulatory Assistance Project (RAP). (2019). *Verteilnetzausbau für die Energiewende - Elektromobilität im Fokus.* Retrieved 02.03.2023, from https://static.agora-energiewende.de/fileadmin/Projekte/2018/Netzausbau_Elektromobilitaet/AgoraRAP2019_VerteilnetzausbauElektromobilitaet.pdf

Aldy, J. E., Kotchen, M. J., Stavins, R. N., & Stock, J. H. (2021). Keep climate policy focused on the social cost of carbon. *Science (New York, N.Y.)*, *373*(6557), 850–852. doi: 10.1126/science.abi7813

Amann, G., Bermúdez, V., Kovacs, E. B., Gallego, S., Giannelos, S., & Iliceto, A. (2022). *E-Mobility Deployment and Impact on Grids: Impact of EV and Charging Infrastructure on European T&D Grids - Innovation Needs.* Retrieved 02.03.2023, from https://smart-networks-energy-transition.ec.europa.eu/system/files/2022-12/ETIP%20SNET%20E-Mobility%20White%20Paper_pdf.pdf

Andruszkiewicz, J., Lorenc, J., & Weychan, A. (2019). Demand price elasticity of residential electricity consumers with zonal tariff settlement based on their load profiles. *Energies*, *12*(22). doi: 10.3390/en12224317

Angrist, J. D., & Pischke, J.-S. (2008). *Mostly harmless econometrics: An empiricist's companion.* Princeton University Press.

Arnold, F. (2023). On the functional form of short-term electricity demand response - insights from high-price years in Germany. *EWI Working Papers*, *2023-6, Energiewirtschaftliches Institut an der Universitaet zu Koeln (EWI).* Retrieved from https://ideas.repec.org/p/ris/ewikln/2023_006.html

Arnold, F., Ashour Novirdoust, A., & Theile, P. (2023). Environmental policy instruments for investments in backstop technologies under present bias - an application to the building sector. *EWI Working Papers*, *2023-5, Energiewirtschaftliches Institut an der Universitaet zu Koeln (EWI), revised 31 Jul 2023*. Retrieved from https://ideas.repec.org/p/ris/ewikln/2023_005.html

Arnold, F., Jeddi, S., & Sitzmann, A. (2021). How prices guide investment decisions under net purchasing - An empirical analysis on the impact of network tariffs on residential PV. *EWI Working Papers*, *2021-7, Energiewirtschaftliches Institut an der Universitaet zu Koeln (EWI)*. Retrieved from `https://EconPapers.repec.org/RePEc:ris:ewikln:2021_007`

Arnold, F., Jeddi, S., & Sitzmann, A. (2022). How prices guide investment decisions under net purchasing - An empirical analysis on the impact of network tariffs on residential PV. *Energy Economics*, *112*, 106177. doi: 10.1016/j.eneco.2022.106177

Arnold, F., Lilienkamp, A., & Namockel, N. (2023). Diffusion of electric vehicles and their flexibility potential for smoothing residual demand - A spatio-temporal analysis for Germany. *EWI Working Papers*, *2023-4, Energiewirtschaftliches Institut an der Universitaet zu Koeln (EWI)*. Retrieved from `https://ideas.repec.org/p/ris/ewikln/2023_004.html`

Ayyadi, S., & Maaroufi, M. (2018). Diffusion models for predicting electric vehicles market in morocco. In *2018 international conference and exposition on electrical and power engineering (epe)* (p. 0046-0051). doi: 10.1109/ICEPE.2018.8559858

BAFA. (2021). *Informationsblatt CO2-Faktoren: Bundesförderung für Energie- und Ressourceneffizienz in der Wirtschaft - Zuschuss.* Retrieved 01.03.2023, from `https://www.bafa.de/SharedDocs/Downloads/DE/Energie/eew_infoblatt_co2_faktoren_2022.pdf?__blob=publicationFile&v=2`

Baginski, J. P., & Weber, C. (2019). Coherent estimations for residential photovoltaic uptake in germany including spatial spillover effects. *HEMF Working Paper*(No. 02/2019). doi: 10.2139/ssrn.3357359

Balta-Ozkan, N., Yildirim, J., & Connor, P. M. (2015). Regional distribution of photovoltaic deployment in the uk and its determinants: A spatial econometric approach. *Energy Economics*, *51*, 417-429. doi: 10.1016/j.eneco.2015.08.003

Bar-Gill, O., & Hayashi, A. (2021). Present-bias and debt-financed durable goods. *Harvard Law School John M. Olin Center Discussion Paper*(Discussion Paper No. 1055). Retrieved from `https://ssrn.com/abstract=3790736`

Bass, F. M. (1969). A new product growth for model consumer durables. *Management Science*, *15*, 215-227. Retrieved from `https://www.jstor.org/stable/2628128`

BBSR. (2022). *Laufende Raumbeobachtung - Raumabgrenzungen: Siedlungsstrukturelle Gebietstypen.* Bundesinstitut für Bau-, Stadt- und Raumforschung. Retrieved 25.02.2023, from https://www.bbsr.bund.de/BBSR/DE/forschung/raumbeobachtung/Raumabgrenzungen/deutschland/kreisgebietsreformen/SiedlungsstrukturelleGebietstypen_alt/gebietstypen.html

BDEW. (2020). *Erdgas und Sonnenwärme: einfach kombinieren.* Retrieved 18.01.2023, from https://www.bdew.de/static/energie-city-1.56/images/assets/solar/Factsheet_Erdgas_Solar_11-2020.pdf

BDEW. (2021). *BDEW-Strompreisanalyse Januar 2021 .* Retrieved 20.05.2021, from https://www.bdew.de/service/daten-und-grafiken/bdew-strompreisanalyse/

Becker, T. A., Sidhu, I., & Tenderich, B. (2009). Electric vehicles in the US a new model with forecasts to 2030. *Center for Entrepreneuship and technology, University of California, Berkeley*, *2009.1.v.2.0*. Retrieved 02.03.2023, from https://www.globaltrends.thedialogue.org/wp-content/uploads/2014/12/Electric-Vehicles-in-the-United-States-A-New-Model-with-Forecasts-to-2030.pdf

Berger, R. (1981). Comparison of the Gompertz and Logistic Equations to Describe Plant Disease Progress. *Phytopathology*, *71*(7), 716–719. Retrieved 02.03.2023, from https://www.apsnet.org/publications/phytopathology/backissues/Documents/1981Articles/Phyto71n07_716.PDF

Best, R., Burke, P. J., & Nishitateno, S. (2019). Evaluating the effectiveness of australia's small-scale renewable energy scheme for rooftop solar. *Energy Economics*, *84*, 104475. doi: 10.1016/j.eneco.2019.104475

Bhattacharya, J., & Lakdawalla, D. (2004). *Time-inconsistency and welfare* (Working Paper No. 10345). National Bureau of Economic Research. doi: 10.3386/w10345

Bollinger, B., & Gillingham, K. (2012). Peer effects in the diffusion of solar photovoltaic panels. *Marketing Science*, *31*(6), 900–912. doi: 10.1287/mksc.1120.0727

Bönte, W., Nielen, S., Valitov, N., & Engelmeyer, T. (2015). Price elasticity of demand in the EPEX spot market for electricity - New empirical evidence. *Economics Letters*, *135*, 5-8. doi: 10.1016/j.econlet.2015.07.007

Boogen, N., Datta, S., & Filippini, M. (2017). Dynamic models of residential electricity demand: Evidence from Switzerland. *Energy Strategy Reviews*, *18*, 85-92. doi: 10.1016/j.esr.2017.09.010

Bundesnetzagentur. (2020). *Bundesnetzagentur für Elektrizität, Gas, Telekommunikation, Post und Eisenbahnen - Genehmigung des Szenariorahmens 2021-2035.* Retrieved 3.11.2022, from https://www.netzentwicklungsplan.de/sites/default/files/paragraphs-files/Szenariorahmen_2035_Genehmigung_1.pdf

Bundesnetzagentur. (2021a). *EEG-Registerdaten und -Fördersätze.* Retrieved 20.05.2021, from https://www.bundesnetzagentur.de/DE/Sachgebiete/ElektrizitaetundGas/Unternehmen_Institutionen/ErneuerbareEnergien/ZahlenDatenInformationen/EEG_Registerdaten/EEG_Registerdaten_node.html

Bundesnetzagentur. (2021b). *Marktstammdatenregister.* Retrieved 20.05.2021, from https://www.bundesnetzagentur.de/DE/Sachgebiete/ElektrizitaetundGas/Unternehmen_Institutionen/DatenaustauschundMonitoring/Marktstammdatenregister/MaStR_node.html

Bundesnetzagentur. (2022). *Markstammdatenregister.* Retrieved 02.03.2023, from https://www.marktstammdatenregister.de/MaStR

Bundesrat. (2022). *Gesetz zu Sofortmaßnahmen für einen beschleunigten Ausbau der erneuerbaren Energien und weiteren Maßnahmen im Stromsektor.* Retrieved 25.02.2023, from https://www.clearingstelle-eeg-kwkg.de/sites/default/files/2022-07/0315-22.pdf

Burchardt, J., Franke, K., Herhold, P., Hohaus, M., Humpert, H., Päivärinta, J., ... Schröder, J. (2021). *Klimapfade 2.0–Ein Wirtschaftsprogramm für Klima und Zukunft.* Retrieved 02.03.2023, from https://web-assets.bcg.com/f2/de/1fd134914bfaa34c51e07718709b/klimapfade2-gesamtstudie-vorabversion-de.pdf

Bushnell, J. B., & Mansur, E. T. (2005). Consumption under noisy price signals: A study of electricity retail rate deregulation in san diego*. *Journal of Industrial Economics*, *53*(4), 493–513. doi: 10.1111/j.1467-6451.2005.00267.x

Can, B., & Erdem, O. (2013, January). *Present-bias in different income groups* (Research Memorandum No. 008). Maastricht University, Graduate School of Business and Economics (GSBE). doi: 10.26481/umagsb.2013008

Cayla, J.-M., Maizi, N., & Marchand, C. (2011). The role of income in energy consumption behaviour: Evidence from french households data. *Energy Policy*, *39*(12), 7874–7883. doi: 10.1016/j.enpol.2011.09.036

CEER, Council of European Energy Regulators. (2020). *CEER Paper on DSO Procedures of Procurement of Flexibility* (Vol. C19-DS-55-05). Retrieved 15.02.2023, from https://www.ceer.eu/documents/104400/-/-/f65ef568-dd7b-4f8c-d182-b04fc1656e58

Cheung, S. L., Tymula, A., & Wang, X. (2021). *Quasi-Hyperbolic Present Bias: A Meta-Analysis* (No. 15). Retrieved from https://docs.iza.org/dp14625.pdf

Ciarreta, A., Espinosa, M. P., & Pizarro-Irizar, C. (2023). Pricing policies for efficient demand side management in liberalized electricity markets. *Economic Modelling*, *121*, 106215. doi: 10.1016/j.econmod.2023.106215

Coase, R. H. (1960). The problem of social cost. *The Journal of Law and Economics*, *3*, 1–44. Retrieved 02.03.2023, from http://www.jstor.org/stable/724810

Consentec, Fraunhofer ISI, TU Berlin, & ifeu. (2021). *Langfristszenarien für die Transformation des Energiesystems in Deutschland 3.* Retrieved 12.02.2023, from https://www.isi.fraunhofer.de/content/dam/isi/dokumente/cce/2021/LFS_Kurzbericht.pdf

Copernicus Climate Change Service. (2020). *Climate and energy indicators for Europe from 1979 to present derived from reanalysis. Copernicus Climate Change Service (C3S) Climate Data Store (CDS).* (accessed: 28.02.2023) doi: 10.24381/cds.4bd77450

Coria, J., & Sterner, T. (2011). Natural resource management: Challenges and policy options. *Annu. Rev. Resour. Econ.*, *3*(1), 203–230. doi: 10.1146/annurev-resource-083110-120131

Cosmo, V. D., Lyons, S., & Nolan, A. (2014). Estimating the impact of time-of-use pricing on irish electricity demand. *The Energy Journal*, *35*(2), 117–136. Retrieved 23.03.2023, from http://www.jstor.org/stable/24695763

Council of European Union, & European Parliament. (2019). *Directive (EU) 2019/944 of the European Parliament and of the Council.* Retrieved from http:https://eur-lex.europa.eu/legal-content/EN/TXT/PDF/?uri=CELEX:32019L0944&from=EN

Crago, C. L., & Chernyakhovskiy, I. (2017). Are policy incentives for solar power effective? evidence from residential installations in the northeast. *Journal of Environmental Economics and Management*, *81*, 132-151. doi: 10.1016/j.jeem.2016.09.008

Danish Energy Agency. (2021). *Technology data for individual heating plants.* Retrieved 18.01.2023, from `https://ens.dk/en/our-services/projections-and-models/technology-data/technology-data-individual-heating-plants`

Davidson, R., & MacKinnon, J. (1993). Estimation and inference in econometrics. *Oxford University Press*. Retrieved from `https://econpapers.repec.org/repec:oxp:obooks:9780195060119`

De Groote, O., Pepermans, G., & Verboven, F. (2016). Heterogeneity in the adoption of photovoltaic systems in flanders. *Energy Economics*, *59*, 45-57. doi: 10.1016/j.eneco.2016.07.008

de Freitas, B. M. R. (2020). Quantifying the effect of regulated volumetric electriciy tariffs on residential pv adoption under net metering scheme. *Working Papers, CATT - UPPA - Université de Pau et des Pays de l'Adour*. Retrieved from `https://econpapers.repec.org/paper/halwpaper/hal-02976874.htm`

de Groote, O., & Verboven, F. (2019). Subsidies and time discounting in new technology adoption: Evidence from solar photovoltaic systems. *American Economic Review*, *109*(6), 2137–2172. doi: 10.1257/aer.20161343

DellaVigna, S. (2009). Psychology and economics: Evidence from the field. *Journal of Economic Literature*, *47(2)*, 315–72. doi: 10.1257/jel.47.2.315

dena. (2018). *dena-Leitstudie integrierte Energiewende: Impulse für die gestaltung des energiesystems bis 2050. Deutsche Energie-Agentur GmbH (dena), ewi Energy Research & Scenarios gGmbH: Berlin/Köln, Germany.* Retrieved 02.03.2023, from `https://www.dena.de/fileadmin/dena/Dokumente/Pdf/9262_dena-Leitstudie_Integrierte_Energiewende_Ergebnisbericht.pdf`

dena. (2021). *dena Leitstudie - Aufbruch Klimaneutralität.* Retrieved 02.03.2023, from `https://www.dena.de/fileadmin/dena/Publikationen/PDFs/2021/Alle_Gutachten_dena-Leitsudie_Aufbruch_Klimaneutralitaet.pdf`

dena. (2022). *Vergleich der Big 5-Klimaneutralitätsszenarien.* Retrieved 02.03.2023, from `https://www.dena.de/newsroom/publikationsdetailansicht/pub/vergleich-der-big-5-klimaneutralitaetsszenarien/`

dena, & Prognos. (2020). *Privates Ladeinfrastrukturpotenzial in Deutschland.* Deutsche Energie-Agentur GmbH (dena). Retrieved 02.03.2023, from https://www.dena.de/fileadmin/dena/Publikationen/PDFs/2020/dena-STUDIE_Privates_Ladeinfrastrukturpotenzial_in_Deutschland.pdf

Deutscher Bundestag. (2021). *Erstes Gesetz zur Änderung des Bundes-Klimaschutzgesetzes, Bundesgesetzblatt Jahrgang 2021 Teil I Nr. 59, ausgegeben zu Bonn am 30. August 2021.* Retrieved 25.02.2023, from https://www.bgbl.de/xaver/bgbl/start.xav?startbk=Bundesanzeiger_BGBl&start=//*%5B@attr_id=%27bgbl121s3905.pdf%27%5D#__bgbl__%2F%2F*%5B%40attr_id%3D%27bgbl121s3905.pdf%27%5D__1675782713390

Dharshing, S. (2017). Household dynamics of technology adoption: A spatial econometric analysis of residential solar photovoltaic (pv) systems in germany. *Energy Research & Social Science*, *23*, 113–124. doi: 10.1016/j.erss.2016.10.012

Diefenbach, N., Loga, T., & Stein, B. (2015). *Szenarienanalysen und Monitoringkonzepte im Hinblick auf die langfristigen Klimaschutzziele im deutschen Wohngebäudebestand - Bericht im Rahmen des europäischen Projekts EPISCOPE.* Retrieved 20.01.2023, from https://episcope.eu/fileadmin/episcope/public/docs/pilot_actions/DE_EPISCOPE_NationalCase_Study_IWU.pdf

Drugeon, J.-P., & Wigniolle, B. (2021). On Markovian collective choice with heterogeneous quasi-hyperbolic discounting. *Economic Theory*, *72*(4), 1257–1296. doi: 10.1007/s00199-020-01291-z

Ebner, M., Fiedler, C., Jetter, F., & Schmid, T. (2019). Regionalized potential assessment of variable renewable energy sources in europe. In *2019 16th international conference on the european energy market (eem)* (p. 1-5). doi: 10.1109/EEM.2019.8916317

ene't. (2021). *Datenbank Netznutzung Strom Deutschland.* ene't GmbH. (Hückelhoven)

ENTSO-E. (2022a). *ENTSO-E Transparency Platform - Actual Generation per Production Type.* Retrieved 02.03.2023, from https://transparency.entsoe.eu/generation/r2/actualGenerationPerProductionType/show

ENTSO-E. (2022b). *National estimates scenario ERAA 2021 - Hourly demand time-series, Demand Forecasting Methodology.* Retrieved 02.03.2023,

from https://eepublicdownloads.azureedge.net/clean-documents/sdc-documents/ERAA/Demand%20Forecasting%20Methodology%20and%20Insights%20(ERAA%202021).pdf

ENTSO-E. (2023). *ENTSO-E Transparency Platform.* Retrieved 28.02.2023, from https://transparency.entsoe.eu

Espey, J. A., & Espey, M. (2004). Turning on the lights: A meta-analysis of residential electricity demand elasticities. *Journal of Agricultural and Applied Economics*, *36*(1), 65-81. doi: 10.1017/S1074070800021866

Eurostat. (2023). *Population on 1 January by NUTS 2 region. Online data code: TGS00096.* Retrieved 28.02.2023, from https://ec.europa.eu/eurostat/de/home

Fabra, N., Rapson, D., Reguant, M., & Wang, J. (2021). Estimating the elasticity to real-time pricing: Evidence from the spanish electricity market. *AEA Papers and Proceedings*, *111*, 425-29. doi: 10.1257/pandp.20211007

Fett, D., Fraunholz, C., & Keles, D. (2021). Diffusion and system impact of residential battery storage under different regulatory settings. *Working Paper Series in Production and Energy, Karlsruhe Institute of Technology (KIT), Institute for Industrial Production (IIP),*. doi: 10.5445/IR/1000129687

Figgener, J., Stenzel, P., Kairies, K.-P., Linßen, J., Haberschusz, D., Wessels, O., ... Sauer, D. U. (2021). The development of stationary battery storage systems in germany – status 2020. *Journal of Energy Storage*, *33*, 101982. doi: 10.1016/j.est.2020.101982

Filippini, M. (2011). Short- and long-run time-of-use price elasticities in swiss residential electricity demand. *Energy Policy*, *39*(10), 5811-5817. (Sustainability of biofuels) doi: 10.1016/j.enpol.2011.06.002

Filippini, M., Kumar, N., & Srinivasan, S. (2021). Behavioral anomalies and fuel efficiency: Evidence from motorcycles in nepal. *Economics Working Paper Series*, *21*. doi: 10.3929/ethz-b-000487242

Flataker, A., Malmin, O. K. r., Hjelkrem, O. A., Rana, R., Korpå s, M., & Torsæ ter, B. N. (2022). Impact of home- and destination charging on the geographical and temporal distribution of electric vehicle charging load. In *2022 18th international conference on the european energy market (eem)* (p. 1-6). doi: 10.1109/EEM54602.2022.9921062

Frederick, S., Loewenstein, G., & O'Donoghue, T. (2002). Time discounting and time preference: A critical review. *Journal of Economic Literature*, *40*(2), 351–401. doi: 10.1257/002205102320161311

Frondel, M., Kaestner, K., Sommer, S., & Vance, C. (2022). Photovoltaics and the solar rebound: Evidence from germany. *Land Economics*. doi: 10.3368/le.070621-0077R1

Frondel, M., Kussel, G., & Sommer, S. (2019). Heterogeneity in the price response of residential electricity demand: A dynamic approach for germany. *Resource and Energy Economics*, *57*, 119–134. doi: 10.1016/j.reseneeco.2019.03.001

Fuerst, F., & Singh, R. (2018). How present bias forestalls energy efficiency upgrades: A study of household appliance purchases in india. *Journal of Cleaner Production*, *186*, 558–569. doi: 10.1016/j.jclepro.2018.03.100

Gautam, T. K., & Paudel, K. P. (2018). Estimating sectoral demands for electricity using the pooled mean group method. *Applied Energy*, *231*, 54-67. doi: https://doi.org/10.1016/j.apenergy.2018.09.023

Gautier, A., & Jacqmin, J. (2020). Pv adoption: the role of distribution tariffs under net metering. *Journal of Regulatory Economics*, *57*(1), 53–73. doi: 10.1007/s11149-019-09397-6

Gautier, A., Jacqmin, J., & Poudou, J.-C. (2018). The prosumers and the grid. *Journal of Regulatory Economics*, *53*(1), 100–126. doi: 10.1007/s11149-018-9350-5

German Government. (2022). *Nachhaltige Mobilität - Nicht weniger fortbewegen, sondern anders.* Retrieved 25.02.2023, from `https://www.bundesregierung.de/breg-de/themen/klimaschutz/nachhaltige-mobilitaet-2044132#:~:text=Nachhaltige%20Mobilit%C3%A4t%20Nicht%20weniger%20fortbewegen,um%20%C3%BCber%2040%20Prozent%20sinken.`

German TSOs. (2022). *Szenariorahmen zum Netzentwicklungsplan Strom 2037 mit Ausblick 2045, Version 2023, Entwurf der Übertragungsnetzbetreiber.* Retrieved 02.03.2023, from `https://www.netzentwicklungsplan.de/sites/default/files/paragraphs-files/Szenariorahmenentwurf_NEP2037_2023.pdf`

Germeshausen, R. (2018). Effects of attribute-based regulation on technology adoption – the case of feed-in tariffs for solar photovoltaic. *ZEW-Centre for European Economic Research Discussion Paper*, *18-057*.

Gillingham, K., Newell, R. G., & Palmer, K. (2009). Energy Efficiency Economics and Policy. *National Bureau of Economic Research, Working Paper Series*. doi: 10.3386/w15031

Gompertz, B. (1825). Xxiv. on the nature of the function expressive of the law of human mortality, and on a new mode of determining the value of life contingencies. in a letter to francis baily, esq. frs &c. *Philosophical transactions of the Royal Society of London*(115), 513–583.

Greene, W. H. (2003). *Econometric analysis*. Pearson Education India.

Gruber, J., & Köszegi, B. (2004). Tax incidence when individuals are time-inconsistent: the case of cigarette excise taxes. *Journal of Public Economics*, *88*(9), 1959-1987. doi: 10.1016/j.jpubeco.2003.06.001

Gunkel, P. A., Bergaentzlé, C., Græsted Jensen, I., & Scheller, F. (2020). From passive to active: Flexibility from electric vehicles in the context of transmission system development. *Applied Energy*, *277*, 115526. doi: 10.1016/j.apenergy.2020.115526

Günther, C., Schill, W.-P., & Zerrahn, A. (2021). Prosumage of solar electricity: Tariff design, capacity investments, and power sector effects. *Energy Policy*, *152*, 112168. doi: 10.1016/j.enpol.2021.112168

Gutsche, G., Wetzel, H., & Ziegler, A. (2020). How relevant are economic preferences and personality traits for individual sustainable investment behavior? a framed field experiment. *Beiträge zur Jahrestagung des Vereins für Socialpolitik 2020: Gender Economics, ZBW - Leibniz Information Centre for Economics, Kiel, Hamburg*. Retrieved from `https://econpapers.repec.org/paper/zbwvfsc20/224542.htm`

Heiskanen, E., & Matschoss, K. (2017). Understanding the uneven diffusion of building-scale renewable energy systems: A review of household, local and country level factors in diverse european countries. *Renewable and Sustainable Energy Reviews*, *75*, 580–591. doi: 10.1016/j.rser.2016.11.027

HErZ, Hans-Ertel Centre for Weather Research (University of Bonn - Germany), & DWD, Deutscher Wetterdienst. (2022). *COSMO-REA6*. Retrieved 02.03.2023, from `https://reanalysis.meteo.uni-bonn.de/?Download_Data___COSMO-REA6`

Heutel, G. (2015). Optimal policy instruments for externality-producing durable goods under present bias. *Journal of Environmental Economics and Management*, *72*, 54–70. doi: 10.1016/j.jeem.2015.04.002

Hinz, F., Schmidt, M., & Möst, D. (2018). Regional distribution effects of different electricity network tariff designs with a distributed generation structure: The case of germany. *Energy Policy*, *113*, 97–111. doi: 10.1016/j.enpol.2017.10.055

Hirth, L., Khanna, T., & Ruhnau, O. (2023). How aggregate electricity demand responds to hourly wholesale price fluctuations. *ZBW - Leibniz Information Centre for Economics, Kiel, Hamburg*. Retrieved 22.06.2023, from `https://ideas.repec.org/p/zbw/esprep/272048.html`

Hughes, J. E., & Podolefsky, M. (2015). Getting green with solar subsidies: evidence from the california solar initiative. *Journal of the Association of Environmental and Resource Economists*, *2*(2), 235–275. doi: 10.1086/681131

Huld, T., Gottschalg, R., Beyer, H. G., & Topič, M. (2010). Mapping the performance of PV modules, effects of module type and data averaging. *Solar Energy*, *84*(2), 324-338. doi: 10.1016/j.solener.2009.12.002

ICAP. (2023). *International carbon Action Partnership - ICAP Allowance Price Explorer.* Retrieved 03.03.2023, from `https://icapcarbonaction.com/en/ets-prices`

IEA. (2020). *World energy outlook 2020.* Author. doi: 10.1787/557a761b-en

IEA. (2022). *Buildings.* Paris. Retrieved 15.02.2023, from `https://www.iea.org/reports/buildings`

Imai, T., Rutter, T. A., & Camerer, C. F. (2021). Meta-analysis of present-bias estimation using convex time budgets. *The Economic Journal*, *131*(636), 1788–1814. doi: 10.1093/ej/ueaa115

infas, DLR, IVT, & infas 360. (2018). *Mobilität in Deutschland (im Auftrag des BMVI).* Retrieved 02.03.2023, from `www.mobilitaet-in-deutschland.de`

Ito, K. (2014). Do consumers respond to marginal or average price? evidence from nonlinear electricity pricing. *American Economic Review*, *104*(2), 537–563. doi: 10.1257/aer.104.2.537

Ito, K., & Zhang, S. (2020). Reforming inefficient energy pricing: Evidence from china. *National Bureau of Economic Research*, *No. w26853*. doi: 10.3386/w26853

IWU. (2016). *IEE Project TABULA - TABULA.xls.* Retrieved 20.01.2023, from `https://www.building-typology.eu/`

Jacksohn, A., Grösche, P., Rehdanz, K., & Schröder, C. (2019). Drivers of renewable technology adoption in the household sector. *Energy Economics*, *81*, 216–226. doi: 10.1016/j.eneco.2019.04.001

Jägemann, C., Hagspiel, S., & Lindenberger, D. (2013). The economic inefficiency of grid parity: The case of german photovoltaics. *EWI Working Paper*(13/19). Retrieved from `https://www.econstor.eu/handle/10419/92970`

Jeddi, S., & Sitzmann, A. (2019). Netzentgeltsystematik in deutschland–status-quo, alternativen und europäische erfahrungen. *Zeitschrift für Energiewirtschaft*, *43*(4), 245–267.

Just, L., & Wetzel, H. (2020). Distributed generation and cost efficiency of german electricity distribution network operators. *EWI Working Paper*, *No. 20/09*. Retrieved from `https://econpapers.repec.org/paper/risewikln/2020_5f009.htm`

Kang, M. (2015). Welfare criteria for quasi-hyperbolic time preferences. *Economics Bulletin*, *Volume 35*(Issue 4), 2506–2511. Retrieved 21.12.2022, from `http://www.accessecon.com/Pubs/EB/2015/Volume35/EB-15-V35-I4-P251.pdf`

Kang, M. (2022). The positive impact of investment subsidies on the economy with present-biased consumers. *The Quarterly Review of Economics and Finance*, *85*, 229–235. doi: 10.1016/j.qref.2022.03.006

Kaschub, T., Jochem, P., & Fichtner, W. (2016). Solar energy storage in german households: profitability, load changes and flexibility. *Energy Policy*, *98*, 520–532. doi: 10.1016/j.enpol.2016.09.017

KIT - Institut für Verkehrswesen. (2021). *Deutsches Mobilitätspanel (MOP) - Wissenschaftliche Begleitung und Auswertungen Bericht 2020/2021: Alltagsmobilität und Fahrleistung.* Retrieved 15.02.23, from `https://mobilitaetspanel.ifv.kit.edu/downloads/Bericht_MOP_20_21.pdf`

Klein, M., & Deissenroth, M. (2017). When do households invest in solar photovoltaics? an application of prospect theory. *Energy Policy*, *109*, 270–278. doi: 10.1016/j.enpol.2017.06.067

Knaut, A., & Paulus, S. (2016). When are consumers responding to electricity prices? An hourly pattern of demand elasticity. *EWI Working Paper, No 16/07*. Retrieved 07.03.2023, from `http://hdl.handle.net/10419/144865`

Kockel, C., Nolting, L., Priesmann, J., & Praktiknjo, A. (2022). Does renewable electricity supply match with energy demand? A spatio-temporal analysis for the German case. *Applied Energy*, *308*, 118226. doi: 10.1016/j.apenergy.2021.118226

Kopernikus-Projekt Ariadne. (2021). *Ariadne-Report: Deutschland auf dem Weg zur Klimaneutralität 2045 - Szenarien und Pfade im Modellvergleich.* doi: 0.48485/pik.2021.006

Kotsogiannis, C., & Schwager, R. (2022). Present bias and externalities: Can government intervention raise welfare? *Canadian Journal of Economics/Revue canadienne d'économique*, *55*(3), 1480–1506. doi: 10.1111/caje.12572

Kraftfahrt-Bundesamt. (2018a). *Bestand an Kraftfahrzeugen und Kraftfahrzeuganhängern nach Gemeinden, 1. Januar 2018 (FZ 3).* `https://www.kba.de/DE/Statistik/Produktkatalog/produkte/Fahrzeuge/fz3_b_uebersicht.html?nn=3514348`.

Kraftfahrt-Bundesamt. (2018b). *Bestand an Kraftfahrzeugen und Kraftfahrzeuganhängern nach Zulassungsbezirken, 1. Januar 2018 (FZ 1).* Retrieved from `https://www.kba.de/DE/Statistik/Produktkatalog/produkte/Fahrzeuge/fz1_b_uebersicht.html?nn=3514348`

Kraftfahrt-Bundesamt. (2019a). *Bestand an Kraftfahrzeugen und Kraftfahrzeuganhängern nach Gemeinden, 1. Januar 2019 (FZ 3).* Retrieved from `https://www.kba.de/DE/Statistik/Produktkatalog/produkte/Fahrzeuge/fz3_b_uebersicht.html?nn=3514348`

Kraftfahrt-Bundesamt. (2019b). *Bestand an Kraftfahrzeugen und Kraftfahrzeuganhängern nach Zulassungsbezirken, 1. Januar 2019 (FZ 1).* Retrieved from `https://www.kba.de/DE/Statistik/Produktkatalog/produkte/Fahrzeuge/fz1_b_uebersicht.html?nn=3514348`

Kraftfahrt-Bundesamt. (2020a). *Bestand an Kraftfahrzeugen und Kraftfahrzeuganhängern nach Gemeinden, 1. Januar 2020 (FZ 3).* Retrieved from `https://www.kba.de/DE/Statistik/Produktkatalog/produkte/Fahrzeuge/fz3_b_uebersicht.html?nn=3514348`

Kraftfahrt-Bundesamt. (2020b). *Bestand an Kraftfahrzeugen und Kraftfahrzeuganhängern nach Zulassungsbezirken, 1. Januar 2020 (FZ 1).* Retrieved from `https://www.kba.de/DE/Statistik/Produktkatalog/produkte/Fahrzeuge/fz1_b_uebersicht.html?nn=3514348`

Kraftfahrt-Bundesamt. (2021a). *Bestand an Kraftfahrzeugen und Kraftfahrzeuganhängern nach Gemeinden, 1. Januar 2021 (FZ 3).*

Retrieved from https://www.kba.de/DE/Statistik/Produktkatalog/produkte/Fahrzeuge/fz3_b_uebersicht.html?nn=3514348

Kraftfahrt-Bundesamt. (2021b). *Bestand an Kraftfahrzeugen und Kraftfahrzeuganhängern nach Zulassungsbezirken, 1. Januar 2021 (FZ 1).* Retrieved from https://www.kba.de/DE/Statistik/Produktkatalog/produkte/Fahrzeuge/fz1_b_uebersicht.html?nn=3514348

Krusell, P., Kuruscu, B., & Smith, A. A. (2002). Equilibrium welfare and government policy with quasi-geometric discounting. *Journal of Economic Theory*, *105*(1), 42–72. doi: 10.1006/jeth.2001.2888

Kühnbach, M., Bekk, A., & Weidlich, A. (2021). Prepared for regional self-supply? On the regional fit of electricity demand and supply in Germany. *Energy Strategy Reviews*, *34*, 100609. doi: 10.1016/j.esr.2020.100609

Kumar, R. R., Guha, P., & Chakraborty, A. (2022). Comparative assessment and selection of electric vehicle diffusion models: A global outlook. *Energy*, *238*, 121932. doi: 10.1016/j.energy.2021.121932

Labandeira, X., Labeaga, J. M., & López-Otero, X. (2017). A meta-analysis on the price elasticity of energy demand. *Energy Policy*, *102*, 549–568. doi: 10.1016/j.enpol.2017.01.002

Lades, L. K., Peter Clinch, J., & Kelly, J. A. (2021). Maybe tomorrow: How burdens and biases impede energy-efficiency investments. *Energy Research & Social Science*, *78*. doi: 10.1016/j.erss.2021.102154

Laibson, D. (1997). Golden Eggs and Hyperbolic Discounting. *The Quarterly Journal of Economics*, *112*(2), 443–478. doi: 10.1162/003355397555253

Länderarbeitskreis Energiebilanzen. (2022). *Vollständige Energiebilanz.* Retrieved 3.11.2022, from https://www.lak-energiebilanzen.de/eingabe-dynamisch/?a=e900

Lijesen, M. G. (2007). The real-time price elasticity of electricity. *Energy Economics*, *29*(2), 249-258. Retrieved from https://www.sciencedirect.com/science/article/pii/S0140988306001010 doi: https://doi.org/10.1016/j.eneco.2006.08.008

Loga, T., Diefenbach, N., Stein, B., & Born, R. (2012). *TABULA - Scientific Report Germany - Further Development of the National Residential Building Typology.* Retrieved 20.01.2023, from https://episcope.eu/fileadmin/tabula/public/docs/scientific/DE_TABULA_ScientificReport_IWU.pdf

Meier, S., & Sprenger, C. (2010). Present-biased preferences and credit card borrowing. *American Economic Journal: Applied Economics*, *2*(1), 193–210. doi: 10.1257/app.2.1.193

Mertesacker, S. (2021). *Essays on the Empirical Analysis of Residential Energy Demand* (Doctoral dissertation, University of Cologne). Retrieved from `http://kups.ub.uni-koeln.de/id/eprint/52689`

Mummolo, J., & Peterson, E. (2018). Improving the interpretation of fixed effects regression results. *Political Science Research and Methods*, *6*(4), 829–835. Retrieved from `https://www.cambridge.org/core/journals/political-science-research-and-methods/article/improving-the-interpretation-of-fixed-effects-regression-results/4145615389057E25D4B46D44AC9CB89C` doi: 10.1017/psrm.2017.44

Muraleedharakurup, G., McGordon, A., Poxon, J., & Jennings, P. (2010). Building a better business case: the use of non-linear growth models for predicting the market for hybrid vehicles in the uk. *Ecological Vehicles and Renewable Energies. Monaco*.

Newville, M., Stensitzki, T., Allen, D. B., Rawlik, M., Ingargiola, A., & Nelson, A. (2016, June). *Lmfit: Non-Linear Least-Square Minimization and Curve-Fitting for Python.* Astrophysics Source Code Library, record ascl:1606.014.

O'Donoghue, T., & Rabin, M. (1999). Doing it now or later. *American Economic Review*, *89*(1), 103–124. doi: 10.1257/aer.89.1.103

O'Donoghue, T., & Rabin, M. (2015). Present Bias: Lessons Learned and To Be Learned. *American Economic Review*, *105*(5), 273–279. doi: 10.1257/aer.p20151085

Ossenbrink, J. (2017). How feed-in remuneration design shapes residential pv prosumer paradigms. *Energy Policy*, *108*, 239–255. doi: 10.1016/j.enpol.2017.05.030

Palm, A. (2020). Early adopters and their motives: Differences between earlier and later adopters of residential solar photovoltaics. *Renewable and Sustainable Energy Reviews*, *133*, 110142. doi: 10.1016/j.rser.2020.110142

Pavlidou, A. (2010). Diffusion of the diffusion curve: A research on the SS-curvescurves in relation to technological clusters. *Utrecht University, Faculuty of Geoscience, Utrecht*.

Phelps, E. S., & Pollak, R. A. (1968). On second-best national saving and game-equilibrium growth. *The Review of Economic Studies*, *35*(2), 185. doi: 10.2307/2296547

Pickert, L., Gierkink, M., Ashour Novirdoust, A., Willers, P., & Langerhans, L. (2022). *Wirtschaftlichkeit von energetischen Sanierungsmaßnahmen: Eine Analyse anhand exemplarischer Einfamilienhäuser.* Retrieved 15.01.23, from `https://www.ewi.uni-koeln.de/cms/wp-content/uploads/2022/10/20221007_EWI_Analyse_Wirtschaftlichkeit_von_Sanierungsmassnahmen_Endbericht.pdf`

Pigou, A. C. (1920). *The Economics Of Welfare.*

Powell, S., Cezar, G. V., Min, L., Azevedo, I. M. L., & Rajagopal, R. (2022). Charging infrastructure access and operation to reduce the grid impacts of deep electric vehicle adoption. *Nature Energy*, *7*(10), 932–945. doi: 10.1038/s41560-022-01105-7

Prognos, Öko-Institut, & Wuppertal-Institut. (2020). *Klimaneutrales Deutschland. Studie im Auftrag von Agora Energiewende, Agora Verkehrswende und Stiftung Klimaneutralität.* Retrieved 15.01.23, from `https://static.agora-energiewende.de/fileadmin/Projekte/2021/2021_04_KNDE45/A-EW_209_KNDE2045_Zusammenfassung_DE_WEB.pdf`

Radecke, J., Hefele, J., & Hirth, L. (2019). Markets for Local Flexibility in Distribution Networks A Review of European Proposals for Market-based Congestion Management in Smart Grids. *ZBW - Leibniz Information Centre for Economics, Kiel, Hamburg*. Retrieved from `https://www.econstor.eu/handle/10419/204559`

Rebenaque, O., Schmitt, C., Schumann, K., Dronne, T., & Roques, F. (2023). Success of local flexibility market implementation: A review of current projects. *Utilities Policy*, *80*, 101491. doi: https://doi.org/10.1016/j.jup.2023.101491

Rode, J., & Müller, S. (2020). I spot, i adopt! peer effects and visibility in solar photovoltaic system adoption of households. *Beiträge zur Jahrestagung des Vereins für Socialpolitik 2020, ZBW - Leibniz Information Centre for Economics, Kiel, Hamburg*.

Rode, J., & Weber, A. (2016). Does localized imitation drive technology adoption? a case study on rooftop photovoltaic systems in germany. *Journal of Environmental Economics and Management*, *78*, 38–48. doi: 10.1016/j.jeem.2016.02.001

Ruhnau, O., & Muessel, J. (2022). *When2heat heating profiles. open power system data.* doi: 10.25832/when2heat/2022-02-22

RWI, & Microm. (2020). *RWI-GEO-GRID: Socio-economic data on grid level - Scientific Use File(wave 9).* RWI – Leibniz Institute for Economic Research. doi: 10.7807/microm:vuf:v9

Sahari, A. (2019). Electricity prices and consumers' long-term technology choices: Evidence from heating investments. *European Economic Review*, *114*, 19–53. doi: 10.1016/j.euroecorev.2019.02.002

Saint-Paul, G. (2011). *The Tyranny of Utility - Behavioral Social Science and the Rise of Paternalism.* Princeton: Princeton University Press. doi: 10.1515/9781400838899

Schaffer, A. J., & Brun, S. (2015). Beyond the sun—socioeconomic drivers of the adoption of small-scale photovoltaic installations in germany. *Energy Research & Social Science*, *10*, 220–227. doi: 10.1016/j.erss.2015.06.010

Schleich, J., Gassmann, X., Meissner, T., & Faure, C. (2019). A large-scale test of the effects of time discounting, risk aversion, loss aversion, and present bias on household adoption of energy-efficient technologies. *Energy economics*, *80*, 377–393. doi: 10.1016/j.eneco.2018.12.018

Schlesewsky, L., & Winter, S. (2018). Inequalities in energy transition: The case of network charges in germany. *International Journal of Energy Economics and Policy*, *8*(6), 102–113. doi: 10.32479/ijeep.6917

Selvakkumaran, S., & Ahlgren, E. O. (2019). Determining the factors of household energy transitions: A multi-domain study. *Technology in Society*, *57*, 54–75. doi: 10.1016/j.techsoc.2018.12.003

Shaffer, B. (2020). Misunderstanding nonlinear prices: Evidence from a natural experiment on residential electricity demand. *American Economic Journal: Economic Policy*, *12*(3), 433–461. doi: 10.1257/pol.20180061

Song, X. (2013). Forecast of electric vehicles in china based on bass model. *Electric Power*. Retrieved from `https://api.semanticscholar.org/CorpusID:112646378`

StataCorp. (2021). *Stata statistical software: Release 17.*

Statistisches Bundesamt (Destatis). (2023). *Genesis-Online - 61111-0002: Consumer price index: Germany, months.* Retrieved 15.06.2023, from `https://www-genesis.destatis.de/genesis/online`

Strotz, R. H. (1955). Myopia and inconsistency in dynamic utility maximization. *The Review of Economic Studies*, *23*(3), 165. doi: 10.2307/2295722

SWM. (2022). *Lastprofil Wärmepumpe.* Retrieved 2022-11-03, from `https://www.swm-infrastruktur.de/strom/netzzugang/bedingungen/waermepumpe`

Taylor, T. N., Schwarz, P. M., & Cochell, J. E. (2005). 24/7 hourly response to electricity real-time pricing with up to eight summers of experience. *Journal of Regulatory Economics*, *27*, 235–262. doi: 10.1007/s11149-005-6623-6

United Nations. (2023). *Net zero coalition.* Retrieved 2023-05-03, from `https://www.un.org/en/climatechange/net-zero-coalition`

Van der Kam, M., Meelen, A., van Sark, W., & Alkemade, F. (2018). Diffusion of solar photovoltaic systems and electric vehicles among dutch consumers: Implications for the energy transition. *Energy Research & Social Science*, *46*, 68-85. doi: 10.1016/j.erss.2018.06.003

VDEW. (1999). *Repräsentative VDEW-Lastprofile.* Retrieved 03.11.2022, from `https://www.bdew.de/energie/standardlastprofile-strom/`

VWG. (2022). *Arbeitnehmerentgelt, Bruttolöhne und -gehälter in den kreisfreien Städten und Landkreisen der Bundesrepublik Deutschland 2000 bis 2020, Reihe 2, Kreisergebnisse Band 2, Berechnungsstand: November 2021.* Arbeitskreis "Volkswirtschaftliche Gesamtrechnungen der Länder".

VWG. (2022). *Bruttoinlandsprodukt, Bruttowertschöpfung in den kreisfreien Städten und Landkreisen der Bundesrepublik Deutschland 1992 und 1994 bis 2020, Reihe 2, Kreisergebnisse Band 1, Berechnungsstand: November 2021.* Arbeitskreis "Volkswirtschaftliche Gesamtrechnungen der Länder".

Werthschulte, M., & Löschel, A. (2021). On the role of present bias and biased price beliefs in household energy consumption. *Journal of Environmental Economics and Management*, *109*, 102500. doi: 10.1016/j.jeem.2021.102500

Whitman, G. (2006). Against the New Paternalism: Internalities and the Economics of Self-Control. *Policy Analysis*, *2006*(563). Retrieved from `https://www.cato.org/sites/cato.org/files/pubs/pdf/pa563.pdf`

Wolak, F. A. (2011, May). Do residential customers respond to hourly prices? evidence from a dynamic pricing experiment. *American Economic Review*, *101*(3), 83-87. doi: 10.1257/aer.101.3.83

Wolff, G., & Feuerriegel, S. (2017). Short-term dynamics of day-ahead and intraday electricity prices. *International Journal of Energy Sector Management*, *11*, 557–573. doi: 10.1108/IJESM-05-2016-0009

Won, J.-R., Yoon, Y.-B., & Lee, K.-J. (2009). Prediction of electricity demand due to phevs(plug-in hybrid electric vehicles) distribution in korea by using diffusion model. In *2009 transmission & distribution conference & exposition: Asia and pacific* (p. 1-4). doi: 10.1109/TD-ASIA.2009.5356888

Woo, C., Liu, Y., Zarnikau, J., Shiu, A., Luo, X., & Kahrl, F. (2018). Price elasticities of retail energy demands in the united states: New evidence from a panel of monthly data for 2001-2016. *Applied Energy*, *222*, 460-474. doi: 10.1016/j.apenergy.2018.03.113

Wooldridge, J. M. (2010). *Econometric analysis of cross section and panel data, second edition.* MIT Press.

Wooldridge, J. M. (2013). *Introductory econometrics: A modern approach, 5th edition.* Cengage learning.

Zhu, Y., Tokimatsu, K., & Matsumoto, M. (2017). Study on the diffusion of ngvs in japan and other nations using the bass model. In *Sustainability through innovation in product life cycle design* (p. 765-778). Singapore: Springer Singapore. doi: 10.1007/978-981-10-0471-1_52

CURRICULUM VITAE

Fabian Arnold

PERSONAL DATA

Date of Birth	2nd March 1992
Place of Birth	Aachen
Nationality	German

EDUCATION

Since 01/2018	**Institute of Energy Economics (EWI)** and **Department of Economics, University of Cologne** Doctoral Candidate in Economics
10/2015 - 09/2017	**RWTH Aachen University** Master of Science (M.Sc.), Business Administration and Engineering: Electrical Power Engineering
09/2015 - 01/2016	**National Taiwan University of Science and Technology, Taiwan** Semester abroad
10/2011 - 09/2015	**RWTH Aachen University** Bachelor of Science (B.Sc.), Business Administration and Engineering: Electrical Power Engineering
06/2011	**Bischöfliches Pius Gymnasium, Aachen** Abitur

WORKING EXPERIENCE

Since 01/2018	**Institute of Energy Economics at the University of Cologne (EWI)** Research Associate
09/2021 - 11/2021	**International Energy Agency (IEA)** Consultant; Gas, Coal & Power Markets Division
07/2020 - 12/2020	**International Energy Agency (IEA)** Consultant; Gas, Coal & Power Markets Division
11/2016 - 04/2017	**Institute of High Voltage Technology (IFHT)** **at RWTH Aachen University** Graduate Student Research Assistant
04/2016 - 09/2016	**Institute for Power Electronics and Electrical Drives (ISEA)** **at RWTH Aachen University** Student Research Assistant
04/2015 - 09/2015	**Institute of High Voltage Technology (IFHT)** **at RWTH Aachen University** Student Research Assistant
05/2014 - 10/2014	**EnBW Energie Baden-Württemberg AG, Stuttgart** Internship
05/2013 - 03/2014	**FGH-Certification GmbH, Aachen** Student Assistant

LANGUAGES

German	Mother tongue
English	Proficient

PUBLICATIONS

Articles in Peer-Reviewed Journals:

- F. Arnold, S. Jeddi, A. Sitzmann (2022). How prices guide investment decisions under net purchasing – An empirical analysis on the impact of network tariffs on residential PV. *Energy Economics*, Vol. 112, August 2022, 106177. DOI: 10.1016/j .eneco.2022.106177.
- H. Scharf, F. Arnold, D. Lencz, (2021). Future natural gas consumption in the context of decarbonization - A meta-analysis of scenarios modeling the German energy system *Energy Strategy Reviews*, Vol. 33, 100591, January 2021. DOI: 10.1016/j .esr.2020.100591.

Working Papers:

- F. Arnold (2023). On the functional form of short-term electricity demand response – insights from high-price years. *EWI Working Paper* 23/06.
- F. Arnold, A. Ashour Novirdoust, P. Theile (2023). Environmental policy instruments for investments in backstop technologies under present bias – an application to the building sector. *EWI Working Paper* 23/05.
- F. Arnold, A. Lilienkamp, N. Namockel (2023). Diffusion of electric vehicles and their flexibility potential for smoothing residual demand – A spatio-temporal analysis for Germany. *EWI Working Paper* 23/04.
- F. Arnold, S. Jeddi, A. Sitzmann (2021). How prices guide investment decisions under net purchasing – An empirical analysis on the impact of network tariffs on residential PV. *EWI Working Paper* 21/07.

Selected Further Publications:

- F. Arnold, K. Gruber, E. Çam (2022). Strompreise im Rekordjahr 2021 - Analyse der Entwicklung der Strompreise und zugrundeliegender Treiber. *et - Energiewirtschaftliche Tagesfragen*, Vol. 72 (3), pp. 19-21, March 2022.
- J. Zinke, F. Arnold, C. Fernandez Alvarez (2021). Coal 2021 - Analysis and forecast to 2024. *International Energy Agency (IEA)/OECD.*
- P. Hauser, D. Lencz, S. Schulte, F. Arnold, E. Çam, H. Scharf, D. Möst (2021). Erdgas langfristig im Spannungsfeld von Versorgungssicherheit und Dekarbonisierung. *et - Energiewirtschaftliche Tagesfragen*, Vol. 71 (3), pp. 51-54, March 2021.
- F. Arnold, S. Jeddi, C. Fernandez Alvarez (2020). Coal 2020 - Analysis and forecast to 2025. *International Energy Agency (IEA)/OECD.*
- S. Schulte, F. Arnold, D. Schlund (2020). Kohle vs. Gas – Veränderungen der Merit-Order 2018 und 2019. *et - Energiewirtschaftliche Tagesfragen*, Vol. 70 (3), pp. 62-63, March 2020.
- M. Gierking, D. Lencz, F. Arnold (2019). Auswirkungen einer Beendigung der Kohleverstromung bis 2038 auf den Strommarkt, CO2-Emissionen und ausgewählte Industrien - Eine Analyse des Abschlussberichts der WSB-Kommission. *EWI study on behalf of the Ministry of Economic Affairs, Innovation, Digitalisation and Energy of the State of North Rhine-Westphalia.*

PRESENTATIONS AND TALKS

- Kohle: Globale Trends, europäische Klimaziele und der deutsche Strommarkt. *EWI Insights.* March 2021. Cologne.
- Bottom-up modelling of heating investment in Germany. *13th Enerday 2019.* April 2019. Dresden.
- Myopia and Uncertainty in Energy System Planning. *30th European Conference on Operational Research, EURO 2019.* June 2019. Dublin, Ireland.